الجـــــــــــــــــــمـهـوريـــــة الجـــــــــــــزائـريـة الديمـــــــقـراطيـة الـشـــــــــعبيـة

REPUBLIQUE ALGERIENNE DEMOCRATIQUE ET POPULAIRE

وزارة التـــــــــــــــــــــــــــعـليـم العـــــــالي و البـــــــــحث العـــــلـمـــي

Ministère de l'Enseignement Supérieur et de la Recherche Scientifique

جـــــــــــــــامعة أبي بكـــر بـلـقـايـد – تـلمســـــــــــــان –

Université Aboubakr Belkaïd – Tlemcen –
Faculté de TECHNOLOGIE

MEMOIRE

Présenté pour l'obtention du **diplôme** de **MASTER**

En : Automatique

Spécialité : Automatique et informatique industrielle

Par : BOUABDALLAH AHMED ADEL

Sujet

Development of a simulator for flexible wastewater bioprocesses for automatic control

Soutenu publiquement, le 26/09/2024, devant le jury composé de :

M. Bensalah Choukri	MCB	Université de Tlemcen	Président
Mme. Khedim Zeyneb	MCB	ESSA-Tlemcen	Examinateur
M. Benyahia Boumediene	Professeur	Université de Tlemcen	Encadreur
M. Harmand Jérôme	Directeur de recherche	LBE-INRAE-NARBONNE	Co-Encadreur

Année universitaire : 2023 /2024

Acknowledgments

First and foremost, I would like to express my profound gratitude to Allah the Almighty for granting me the courage and patience necessary to complete this work.

I am deeply thankful to my parents for their unwavering encouragement and support throughout every stage of this journey. Your love and guidance have been instrumental in my achievements. May God always bless and protect you.

I would particularly like to thank my supervisor, **Mr. BENYAHIA Boumediene**, for his expert assistance, patience, and encouragement. His critical insight has been invaluable in structuring the work and enhancing the quality of the various sections.

My heartfelt thanks also go to **Mr. Jérôme Harmand**, our co-supervisor, for the six months we spent working under your supervision. I greatly appreciate your insightful feedback, steadfast support, and invaluable help in overcoming the challenges we faced. Your positive energy and motivation were truly inspiring and greatly contributed to my progres

I am grateful to both of you for providing this opportunity and experience, which have profoundly changed and matured me in countless ways.

I also wish to extend my gratitude to everyone at **LBE-INRAE-NARBONNE** for their warm welcome and exceptional guidance. While I cannot name everyone individually, I deeply appreciate the support from all, including the permanent staff, interns, and doctoral candidates.

Special thanks go to my cousin, **Mr. MEDJAHDI Karam**, for his unwavering support from the very beginning to the present. I am truly grateful for his encouragement, guidance, and assistance, and for being an extraordinary person throughout this journey.

I would also like to thank my brother, roommate, and partner in crime, **BOUDALIA Rayene**, for sharing this remarkable journey with me through all the ups and downs. I wish you all the best for the future, my friend.

I want to acknowledge my friends, especially **Djassim**, **Zakari**, and **Wail**, for always cheering me on and being there whenever I needed support. You are the best. I also extend my gratitude to all my family members. Thank you all.

Finally, I wish to thank everyone who contributed, directly or indirectly, to the completion of this work. I hope the members of the jury will find here the expression of my sincere thanks for the honor of taking the time to read and evaluate this work.

Contents

List of Figures

List of Tables

List of Nomenclature

- **WWTP**: Wastewater Treatment Plant
- **ASM1**: Activated Sludge Model No. 1
- **ASM1-2ND**: Activated Sludge Model No. 1 with two stages of nitrification and denitrification
- **BOD**: Biological Oxygen Demand
- **COD**: Chemical Oxygen Demand
- **KLA**: Gas-Liquid (oxygen) Mass Transfer Coefficient
- **SNO_3**: Nitrate Concentration
- **SNO_2**: Nitrite Concentration
- **SNH_4^+**: Ammonium Concentration
- **QRext**: Returned Activated Sludge Flow
- **QRint**: Internal Recirculation Flow
- **Qwast**: Waste Activated Sludge Flow
- **SRT**: Solids Retention Time
- **XAOB**: Ammonia Oxidizing Bacteria
- **XNOB**: Nitrite Oxidizing Bacteria
- **XBH**: Heterotrophic Biomass
- **SN_2**: Nitrogen Gas
- **SO**: Dissolved Oxygen
- **SS**: Soluble Substrate
- **SNH**: Ammonium Concentration
- **SALK**: Alkalinity
- **XP**: Particulate Inert from Biomass Decay
- **XS**: Particulate Slowly Biodegradable Matter
- **XI**: Particulate Inert Matter
- **SND**: Soluble Organic Nitrogen
- **XND**: Particulate Organic Nitrogen

- **XBA**: Autotrophic Biomass
- **SNH_3**: Ammonia Concentration
- **SN_2**: Nitrogen Gas Concentration
- **SNO**: Nitrate/Nitrite Concentration
- **Qin**: Inflow rate
- **Qout**: Outflow Rate

Chapter 1

General Introduction

Contents

1 Introduction

Water scarcity is a pressing issue that can result from a variety of causes, such as demand outstripping supply, inadequate water infrastructure, or institutional failures to address needs. This growing problem affects all continents, with poorer communities being the hardest hit. To effectively address this challenge and support a growing global population, according to World Health Organization (2023), over 2 billion individuals live in water-stressed nations, and this is expected to worsen in some places as a result of climate change and population development. Water scarcity makes farming much more difficult, threatening a community's access to food. Food-insecure communities can experience both acute and chronic hunger. Children in these communities are particularly at risk of malnutrition-related conditions, such as stunting and wasting, as well as chronic diseases related to poor nutrition, such as diabetes. By 2025, two-thirds of the world's population may face water shortages, and ecosystems around the world will suffer even more World Wildlife Fund (2024). Despite efforts to conserve water resources - an important commitment in the face of impending scarcity - agriculture will continue to expand globally. Over the past 50 years, agricultural production has increased by a factor of 2.5 to 3, while the area under cultivation has increased by only 12%. In particular, more than 40% of the increase in food production has come from irrigated land, which has doubled in size. Over the same period, the amount of land used per person has gradually decreased to less than 0.25 ha. As shown in Figure 1.1, on the other hand, 72% of all water withdrawals are used by agriculture, 16% by municipalities for households and services, and 12% by industries UN-Water (2021).

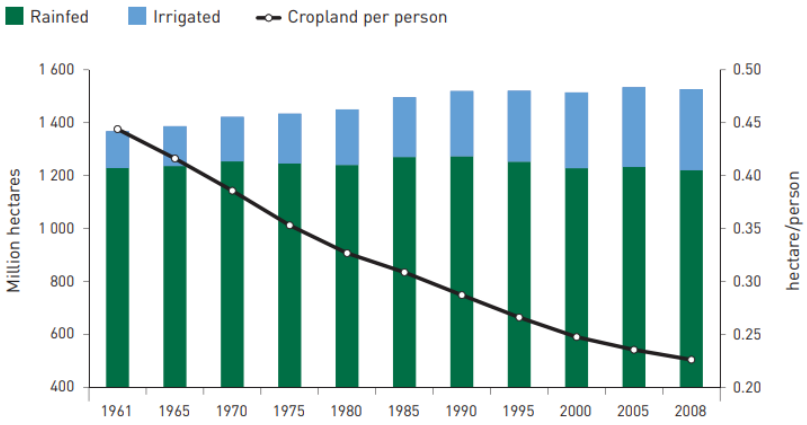

Figure 1.1: Evolution of irrigated and non-irrigated cultivated areas (1961-2008) OpenWA (2023).

The factors contributing to water stress and the need to protect the environment underline the importance of promoting the reuse of treated wastewater and conserving water resources. Wastewater reuse involves the use of untreated, partially treated, or treated wastewater for various resources, including potable and non-potable water, irrigation water, nutrients, energy, and heat value. From an environmental point of view, the reuse of treated wastewater has many advantages. In the case of sensitive natural areas, the benefit is that the amount of wastewater released into the environment is reduced and better controlled, helping to limit the loss of biodiversity. In the latter case, recharging or maintaining the quality of water supplies (both surface and groundwater) for drinking water is often a key concern. Treated wastewater is an economically beneficial resource because its supply is constant and, with quality control, it allows better management in times of water scarcity, ensuring stable agricultural and industrial production. However, if treated wastewater is reused in agriculture, it does not replenish rivers, which can

cause significant problems in closed systems such as the Mediterranean, especially given its numerous desalination plants. However, the reuse of treated wastewater is still in its infancy and is limited worldwide by a number of constraints. Some of these challenges are environmental, in particular the risk of salinisation and the potential spread of heavy metals and micropollutants, while others are sanitary and economic, such as ensuring the health of users and gaining public acceptance for the use of treated wastewater in agriculture.

My work in this Master's thesis is to investigate how modelling and control techniques can be used to optimise treatment plants for water reuse, in particular how the quality of treated effluent can be adapted to crop needs. Agricultural water demand varies over time and does not match the consistent availability of treated wastewater, which is produced regularly throughout the year. Agricultural cycles and seasons modulate water demand. It is therefore necessary either to store treated wastewater produced during periods of low demand (ensuring that the quantity matches crop requirements, but not necessarily the quality), or to develop a system that allows flexible operation of wastewater treatment plants. This would adapt both the quantity and quality of treated wastewater to crop needs, leading to the concept of a Water Resource Recovery Facility (WRRF).

In this Master's thesis, 'flexibility' in a treatment process refers to the ability of a system to be dynamically controlled so that the quality of the treated water can be adjusted to meet the requirements for its effective reuse. Therefore, the reuse of treated wastewater involves a transition between two modes of operation, referred to as degraded mode and full mode.

In this thesis, most of the associated risks are either neglected or addressed through technological considerations until the final chapter. One major risk - the sanitary risk associated with the spread of pathogens into the environment - is considered negligible when using membrane bioreactors, as they involve membrane filtration. Membrane bioreactors are increasingly used as advanced treatment systems, combining biological treatment with activated sludge and liquid/solid separation by membranes.

2 How to improve the reuse of treated wastewater?

Existing wastewater treatment plants (shown in Figure 1.2) are designed to treat wastewater to meet regulatory standards for discharge into the environment. The resulting sludge is, at best, used as a fertiliser for agricultural or industrial purposes. These processes do not focus on tailoring the quality of treated wastewater for specific uses. They are energy-intensive and produce CO2 and potentially nitrous oxide, which are potent greenhouse gases.

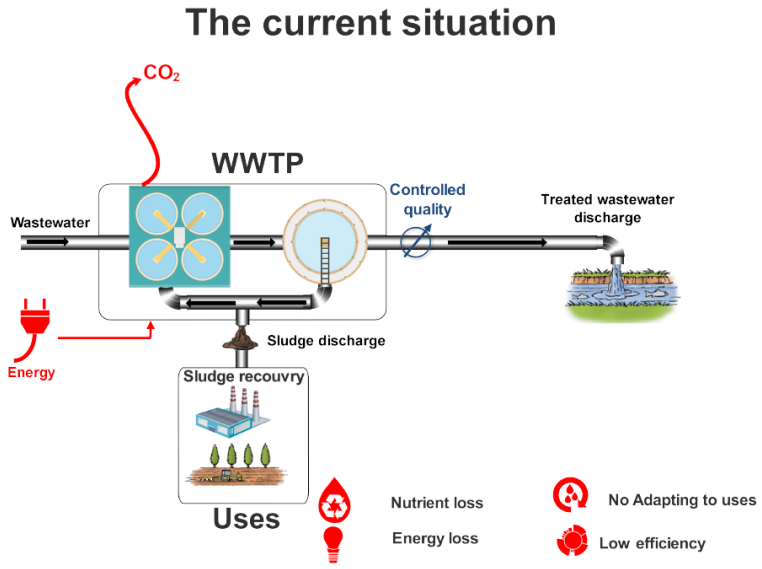

Figure 1.2: The current situation of the WWTP Aichouche (2021)

The perspective of this system needs to shift towards a resource recovery approach, as advocated by the circular economy paradigm Sfez et al. (2019). In this 'vision for the future,' less energy is introduced into the system through energy recovery, while a 'flexible system' can be optimized to precisely produce energy and water characteristics tailored to new and existing uses (shown in Figure 1.3).

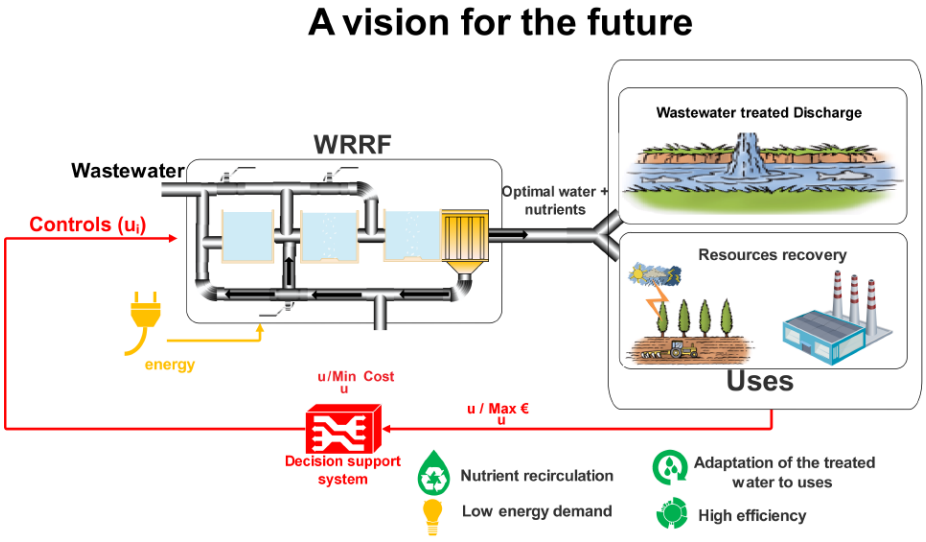

Figure 1.3: A vision for the future of the WRRF Aichouche (2021)

In an ideal scenario (see Figure 1.4), the control diagram shows an 'integrated system' that includes the entire treatment chain - from the resource to the soil and the plants. The input to this system is the input characteristics of the wastewater, while the output is the production and state of the biomass of interest (or various potential uses). The challenge is to design a decision support/control system capable of optimally calculating the control inputs from the available measurements, taking into account practical constraints and external disturbances. Achieving this requires the coupling of different types of models, including those of WWTP/WRRF, water transport/storage, soil, and plants. This coupling is very challenging because some models, such as plant models, are not as advanced as those used for biological treatment of wastewater. Therefore, instead of pursuing this ideal vision, the next section describes a slightly different approach proposed by Fraouck Aichouche Aichouche (2021).

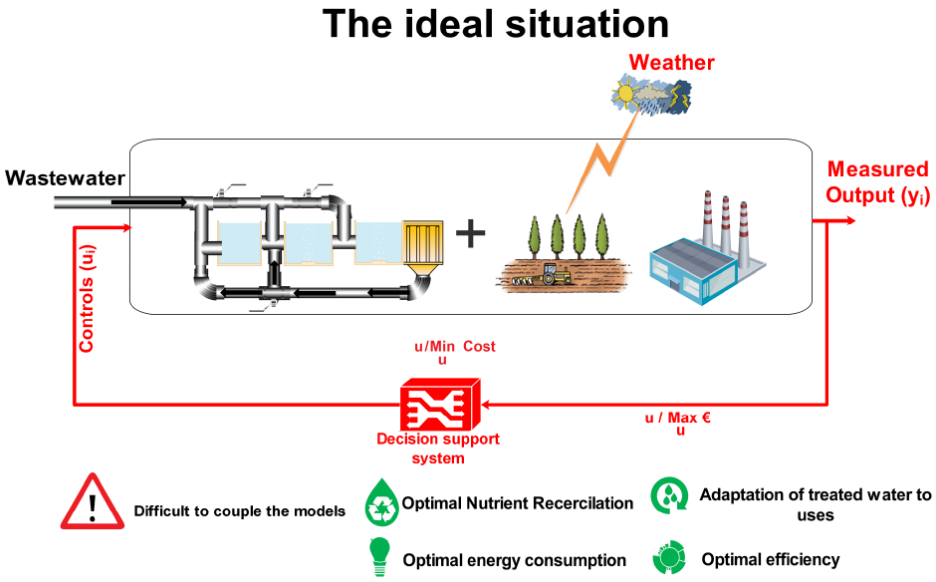

Figure 1.4: The ideal situation of the WRRF Aichouche (2021)

2.1 Health risks of water reuse

The source and composition of wastewater, its treatment, storage, and distribution, as well as irrigation techniques, agricultural practices, and local climate, soil, and groundwater conditions, all contribute significantly to the specific chemical risks associated with water reuse Helmecke et al. (2020). These risks include micropollutants, a group of mineral or organic substances that can be toxic even at very low concentrations in the micro- or nanogram per litre range Shakir et al. (2017). They are used in industrial processes or are components of many agricultural and household products. These molecules can be divided into several groups, including pesticides, pharmaceutical or veterinary residues, and organic compounds derived from plastics. In addition, reclaimed wastewater contains pathogens (viruses, fungi, bacteria, etc.) and emerging contaminants such as antibiotic resistance genes that can make bacteria resistant. Consequently, the transmission of infections by these contaminants is a major concern in the reuse of treated wastewater.

2.2 Reuse limitations

The challenge of reusing treated wastewater in agriculture has two main aspects: conserving water resources and recovering nutrients, especially nitrogen and phosphorus, for crops or industrial use. However, there are a number of constraints to this reuse, including:

- Various research studies have found that nitrogen levels - such as nitrate (N-NO3), ammonium (NH4-N) or total nitrogen - increase after wastewater irrigation for

  periods ranging from one to 20 years. Although this increase in nitrogen and phosphorus from wastewater can increase agricultural production and reduce the need for chemical fertilisers, it can also affect soil microbial communities, in particular the processes involved in the cycling of these nutrients Jaramillo and Restrepo (2017).

- The nutrients in treated wastewater can serve as valuable fertilisers for crop production. However, sometimes these nutrients are in forms that can easily leach into the soil, potentially affecting groundwater quality Candela et al. (2007).

- Another study investigated the effects of salinity on the structure, activity, and community of soil microorganisms. Their results suggest that higher salinity levels metabolically stress soil microbiota. In addition, the carbon-nitrogen ratio of the biomass tends to be lower in higher salinity soils, reflecting the predominance of bacteria in the microbial biomass of saline soils Candela et al. (2007).

2.3 Limitations of the proposed approach

The innovative approach outlined in Aichouche (2021) has several limitations. In particular, while there are numerous models that take into account plant water requirements, there are very few models that take into account nitrogen, phosphorus, or other essential compounds. In addition, it is challenging to define a universal optimisation criterion for the proposed approach: what specific objectives should the innovation aim to optimise? In the absence of clear indicators and criteria for performance evaluation, it becomes difficult to evaluate the reuse of treated water in terms of cost, effectiveness, and environmental impact. Finally, the concept of flexibility remains unclear in the context of this study.

3 Aims and Objectives

The aim of this work is to investigate strategies for operating a wastewater treatment system that produces adaptable water quality for agricultural reuse. This will involve the creation of a simulator based on an innovative approach using a flexible wastewater treatment system. The system is dynamically controlled to operate on demand. As shown in Figure 1.5, the approach uses an initial model to identify or estimate the water and nitrogen needs of crops/plants. These needs are used as setpoints for the flexible wastewater resource recovery facility (WRRF). In a closed loop, the flexible system is dynamically controlled to meet the needs specified by the crop/plant model. The optimum crop nitrogen requirements are used to adjust the treatment process in the flexible system to ensure that water quality supports optimum crop growth.

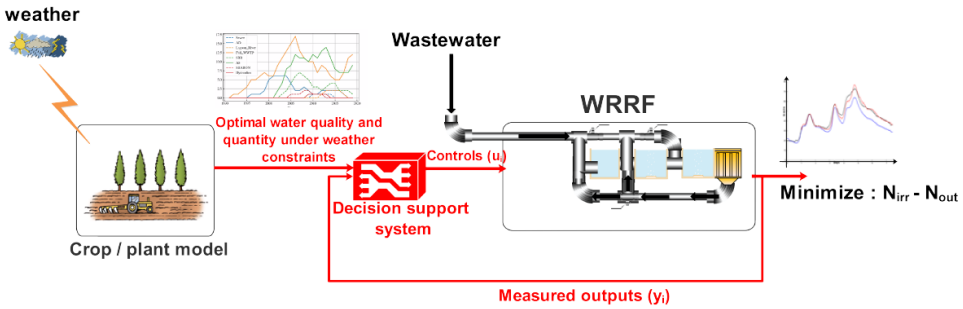

Figure 1.5: Strategy for closing the loop between the WRRF model and the crop/plant model

This flexible system must be able to provide different qualities of treated effluent to meet irrigation needs during periods of water stress (ensuring nutrient recovery in the treated water for reuse) while meeting discharge requirements during non-irrigation periods.

Chapter 2

Modeling of a «WRRF» for water Reuse

Contents

1 wastewater treatment process

1.1 Introduction

A wastewater treatment plant (WWTP) typically uses a combination of mechanical, physical, chemical and biological processes to remove pollutants from incoming wastewater. The most widely used of these is the activated sludge process. In the biological treatment stage, microorganisms play a key role in removing significant amounts of organic matter - such as carbon, nitrogen and phosphorus - from the wastewater. Here we focus on carbon and nitrogen removal, where microorganisms oxidise the biodegradable organic matter, resulting in the production of carbon dioxide. Biological nitrogen removal takes place in two stages nitrification and denitrification. During this process, the activated sludge (flocculated biomass) is separated from the treated effluent in the final clarifier by gravitational settling. Most of the separated sludge is then returned to the biological process via a recirculation circuit. Several configurations are available for these processes.

1.2 Conventional activated sludge processes

Activated sludge systems are among the most commonly used biological treatment methods in wastewater treatment plants. These systems use microorganisms to effectively break down organic pollutants in wastewater.

The characteristics of an activated sludge process are influenced by factors such as:

- the flow regime within the reactor
- the size and number of reactors
- the configuration of these reactors
- and the recycle flows and the influent parameters.

These parameters include environmental conditions and system constraints that dictate how the biological processes operate. Among the many nitrification/denitrification activated sludge processes, three basic configurations are most commonly used in practice

1.2.1 Pre-denitrification process

Pre-denitrification is a method used in activated sludge systems. In this approach, two separate continuous flow stirred tank reactors (CSTRs) are used to achieve the required anoxic and aerobic conditions, with microorganisms circulating between the reactorsHajaya (2019). Process summary:

- **Anoxic Reactor:** Receives effluent containing organic carbon and ammonia, together with a nitrate-rich biomass recycle from the aerobic reactor. Here organic carbon is partially mineralised and nitrate is reduced to nitrogen gas.
- **Aerobic Reactor:** The effluent from the anoxic reactor is sent here where air is introduced to ensure high oxygen levels and effective mixing. In this reactor the remaining organic carbon is completely mineralised and ammonia is converted to nitrate.

- **Settler:** Separates the biomass from the treated liquid, with the biomass being recycled to maintain control of the solids residence time of the system, independent of the hydraulic residence time.

This process scheme is shown in Figure 2.1.

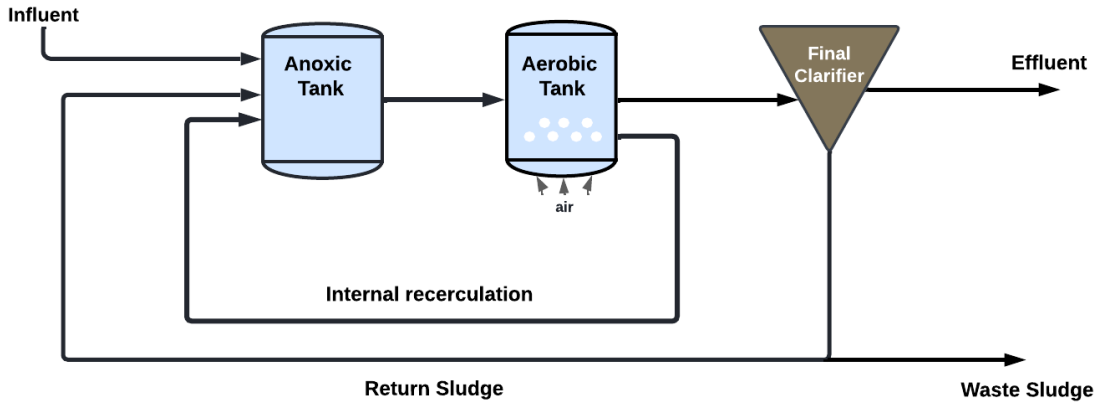

Figure 2.1: Pre-denitrification process

1.2.2 Post-denitrification process

Activated Sludge Model 1 (ASM1) post-denitrification (figure 2.2),refers to a process configuration where denitrification occurs after the main aerobic treatment stage. In this configuration, an anoxic reactor is positioned after the aerobic reactor. This arrangement often requires the addition of an external carbon source to act as an electron donor for denitrification, as most of the readily biodegradable organic matter has already been consumed in the preceding aerobic stage. The denitrification rate in post-denitrification can be modelled using ASM1 parameters, with particular emphasis on the anoxic growth rate of heterotrophs and the half saturation coefficients for both nitrate and organic substrate. One of the main advantages of post-denitrification is its ability to achieve very low effluent nitrate concentrations, making it particularly beneficial where stringent nitrogen limits must be met. However, there are challenges associated with this approach, most notably the cost of adding an external carbon source and the potential for excess carbon to be carried over into the effluent.

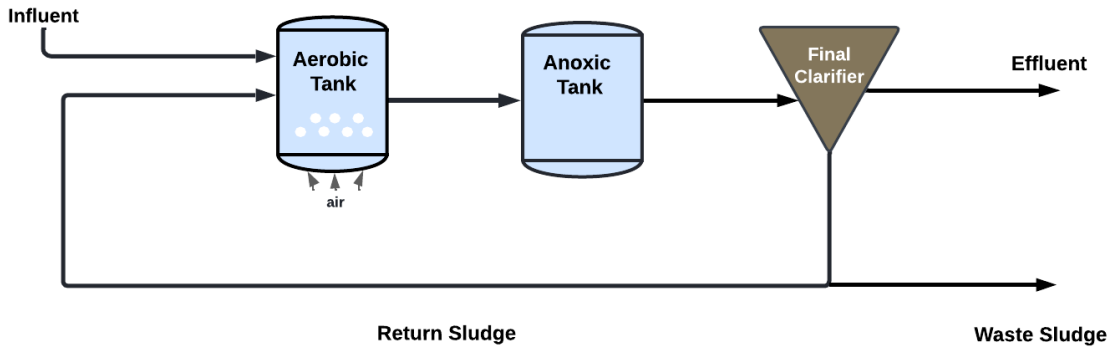

Figure 2.2: Post-denitrification processs

1.2.3 Step feed process

In the step-feed process shown in Figure 2.3 , the effluent is evenly distributed to each denitrification compartment. The effluent then flows by gravity through the nitrification and denitrification compartments in turn. Mixed liquor from the last nitrification compartment (the last tank) and sludge from the settling tank are returned to the first denitrification compartment. This arrangement allows repeated denitrification and nitrification reactions in each compartment. As a result, almost complete removal of nitrogen components is expected after passing through the first denitrification compartment, provided that the BOD (Biochemical Oxygen Demand) of the effluent is sufficiently high relative to the nitrogen content.

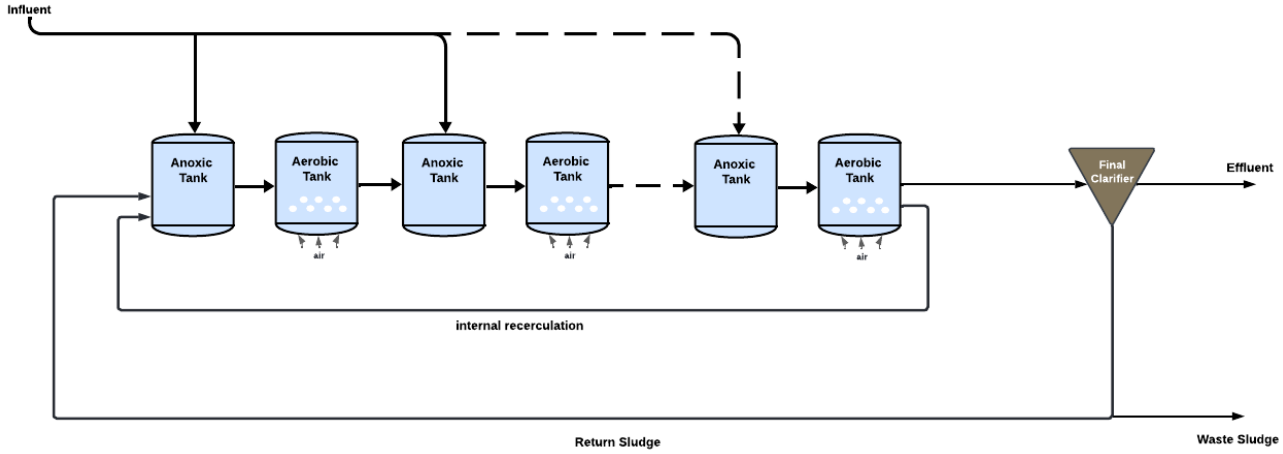

Figure 2.3: Step-feed process

1.3 Wastewater with a new perspective

In the circular economy, wastewater is seen as a valuable resource for energy, nutrients and water, rather than just a source of pollution. This paradigm shift from traditional wastewater treatment plants to water resource recovery facilities (WRRFs), as discussed in the introduction, presents new challenges in the design, modelling and control of these facilities. The shift changes the treatment objectives, emphasising nutrient recovery, water reuse, energy recovery and overall performance.

The selection of the appropriate system design is critical, as WRRF effluent requirements directly influence the choice of processes needed to achieve specific treated water quality, energy and sustainability goals. Conventional technologies typically focus on increasing treatment efficiency by improving nitrogen and carbon removal processes to meet stringent effluent standards, while also aligning with broader sustainability goals.

1.4 Activated sludge bioreactors

Activated sludge bioreactors are complicated systems due to the complex water flow, chemical reactions and changes in the influent wastewater. This makes them difficult to model and requires many simplifications to develop a workable model. These bioreactors come in different shapes, sizes and designs. This work focuses on only a small part of these systems, namely activated sludge reactors and continuously fed submerged membrane reactors, without considering membrane fouling in the design.

1.5 Bioreactor hydraulics

Bioreactor hydraulics refers to the movement and flow of fluids within a bioreactor, which is critical to ensuring proper mixing, nutrient distribution and interaction between microorganisms and substrates.

In activated sludge systems, An understanding of the hydraulics is essential to optimise the treatment process, as it affects how efficiently the bioreactor operates and how well it can handle variations in wastewater input. Proper hydraulic design helps to achieve uniform conditions throughout the reactor, preventing problems such as dead zones or short circuits, and ensuring that the biochemical reactions necessary for treatment are carried out effectively.

Large-scale bioreactors typically do not exhibit perfect mixing or ideal plug flow behaviour; instead, their internal flow patterns usually fall «somewhere in between» these two extremes. These intermediate conditions are often modelled using a series of reactors in a cascade arrangement(figure 2.4).As the number of reactors in the cascade increases, the residence time distribution begins to resemble plug flow, eventually approaching ideal plug flow behaviour when the number of reactors (N) becomes very large. The cascade bioreactor configuration can be fine-tuned by adjusting the number, volume and arrangement of completely stirred tank reactors (CSTRs), changing the recycling rate, adding sidestream tanks to represent dead zones or introducing bypasses to simulate short circuits.

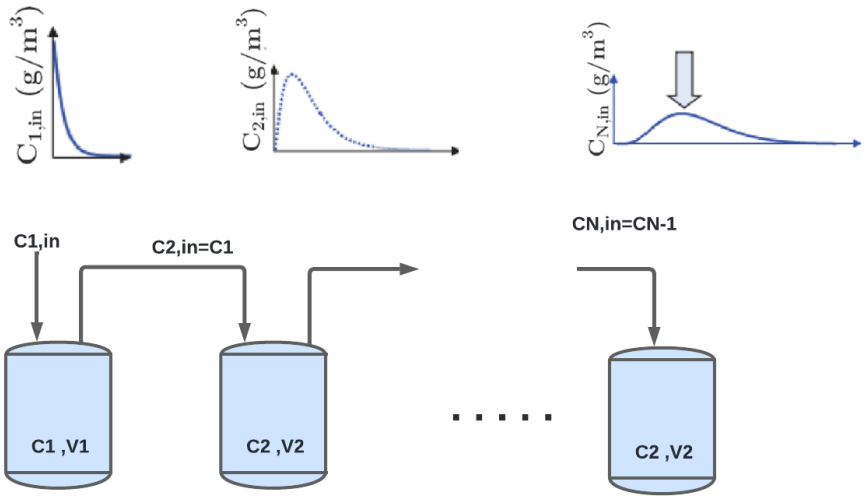

Figure 2.4: Graphical representation of a cascade of N CSTR

Depending on the treatment objectives and the characteristics of the influent, different scenarios can arise. Literature suggests that under typical WWTP conditions, plug flow reactors are generally the most efficient (de Gooijer et al. (1996); Scuras et al. (2001)). In addition, a series of well-mixed reactors with volumes designed based on the influent and a hydraulic retention time (HRT) that matches the desired treatment performance can effectively approximate the behaviour of a plug flow reactor.

Each bioreactor in figure 2.4 is described by the general mass balance equation

$$\frac{d}{dt}(CV) = \sum \text{Sources} - \sum \text{Sinks} \tag{1.1}$$

where **C** is the vector of the concentrations of various components in the bioreactor,**V** is the liquid phase volume, which is constant in a CSTR.The concentration **C** of each component in the bioreactor is reduced by the **sinks** and increased by the **sources**. In the bioreactors described in this thesis, the sinks and sources are attributed to:

- Mass flow of liquid, including the main outflow and inflow,
- Mass flow of air, such as aeration,
- Secondary outflow, such as waste activated sludge (WAS).

The mass balance equation for any CSTR, ignoring aeration and chemical dosing, can be expressed as follows:

$$\frac{d}{dt}(CV) = Q_{\text{in}}C_{\text{in}} - Q_{\text{out}}C_{\text{out}} \pm rV \tag{1.2}$$

where:

- $C, C_{\text{in}}, andC\text{out}$ is the vectors of concentrations of all considered wastewater constituents in the influent, in the reactor and in the effluent
- r represents the reaction rate with dim(r) = dim(C),
- Q_{in} is the inflow rate,
- Q_{out} is the outflow rate,
- V is the volume of the bioreactor.

In a completely stirred tank reactor (CSTR), where $C_{\text{out}} = C$ and $Q_{\text{in}} = Q_{\text{out}}$, the mass balance can be expressed using the following ordinary differential equation (ODE):

$$\frac{dC}{dt} = Q_{\text{in}}\,(C_{\text{in}} - C) \pm r \tag{1.3}$$

The ratio $\frac{Q_{\text{in}}}{V}$ defines the dilution rate D, which is the reciprocal of the hydraulic retention time (HRT):

$$D = \frac{Q_{\text{in}}}{V} = \frac{1}{\text{HRT}} \tag{1.4}$$

The reaction term r in Equation 1.3 can be calculated using various models and approaches.

1.6 Modeling of biochemical reactions

The kinetics of biochemical processes describe the rate at which biomass grows as a function of state variables, in particular substrate concentrations. These models assume that substrates are converted directly into products and biomass in a single step, without considering the complex reactions at the cellular level. These macroscopic models do not account for variations in the composition and activity of individual cells, and often group different bacterial species into a single biomass category. Biomass is characterised by its concentration X (g m^{-3}), maximum growth rate $\hat{\mu}$ (d^{-1}), decay rate k_D (d^{-1}), and yield coefficient Y (-). Depending on the growth model used, additional kinetic and stoichiometric parameters such as Monod constants K for different substrates may also be included.

2 Activated Sludge Models (ASMs)

ASMs (Activated Sludge Models) are reliable and widely used dynamic models for understanding, designing, optimising and controlling activated sludge wastewater treatment processes. There are different versions of ASMs and the choice of which to use depends on factors such as modelling objectives, desired accuracy, calibration effort, ease of use and the specific type of process being modelled.

The first phase of the development of activated sludge models took place between 1950 and 1960. During this period,Jr and Porges (1957) introduced simple empirical equations to estimate the amount of excess sludge produced and the oxygen demand in the treatment tank.

In 1982, the International Water Quality Association (IWAQ) established an international working group to accelerate the development of dynamic models for wastewater treatment plants. The aim was to develop a single starting model and to reach consensus. The group's initial work involved cataloguing existing models and identifying barriers to their development. They found that although many dynamic models existed, their complexity, disorganised presentation and limitations of computer technology hindered their widespread use. The group's findings were published in 1987 and introduced the ASM1 model Henze et al. (1987).

Over the past two decades, several versions of dynamic models, including ASM1, ASM2, ASM2d, and ASM3 Henze et al. (2000), have been developed. These models have evolved since the introduction of the first version ASM1 , by incorporating advancements in the understanding of wastewater treatment processes.The ASM1 model describes the degradation processes of organic matter, both aerobic and anoxic, as well as nitrification and denitrification in activated sludge systems. It remains a reliable and widely used foundation in dynamic simulation software. Subsequently, models were developed to include phosphorus removal processes, aiming to predict phosphorus behavior.In 1995, the work of the study group was expanded to publish the ASM2 model.In 1999, two further modifications led to the introduction of ASM2d, a modified version of ASM2Henze et al. (1999).Finally, ASM3 has been developed to address the limitations of ASM1, in particular its inability to simulate certain phenomena such as substrate storage during periods of substrate absence.

These models are designed to predict the performance of single-reactor activated sludge systems and to assist engineers in the design and optimisation of activated sludge wastewater treatment plants (WWTPs). While the above models are the best known in the technical and scientific community, several other activated sludge models have been published and successfully tested in various studies.

2.1 Structure Activated Sludge Models (ASMs)

Activated sludge models (ASMs) use a matrix structure to simulate biological and chemical processes in wastewater treatment. The reaction rate vector $r \in \mathbb{R}^n$ is defined as:

$$r = \begin{pmatrix} r_1(\hat{C}_1 \subseteq C, u) \\ \vdots \\ r_n(\hat{C}_n \subseteq C, u) \end{pmatrix} \tag{1.5}$$

- r_j Rate of change of concentration C_j due to reactions.
- C Vector of all component concentrations, including soluble and particulate matter.
- $\hat{C}_i$ Subset of concentrations relevant to the j-th reaction.
- u Vector capturing external inputs.

Each reaction rate r_j results from one or more biological or chemical processes, represented by the process rate vector $p \in \mathbb{R}^m$:

$$p = \begin{pmatrix} p_1(\hat{C}_1 \subseteq C, u) \\ \vdots \\ p_m(\hat{C}_n \subseteq C, u) \end{pmatrix} \tag{1.6}$$

Each process $p_i \in p$ (where $i = 1, \ldots, m$) follows two basic rules from chemistry:

- **Mass Stays the Same**: This means that during any chemical reaction, the total weight of everything stays the same. The weight of what you start with (reactants) will always be equal to what you end up with (products).
- **Energy Stays the Same**: This rule says that energy cannot be made or destroyed—it can only change forms. For example, energy from motion can change into heat, or electricity can turn into heat.

The reaction rates are linear combinations of these processes:

$$r = A^T p \tag{1.7}$$

where $A \in \mathbb{R}^{m \times n}$ is the stoichiometric matrix (Petersen or Gujer matrix):

$$A = \begin{pmatrix} a_{1,1} & \cdots & a_{1,n} \\ \vdots & \ddots & \vdots \\ a_{m,1} & \cdots & a_{m,n} \end{pmatrix} \tag{1.8}$$

This matrix efficiently maps process rates to reaction rates, ensuring mass conservation and governing the dynamic behaviour of the system.

Each stoichiometric parameter $a_{i,j}$ in matrix A represents the relationship between the rate of the i-th process p_i and the rate of change of the concentration of the j-th component C_j due to that process. Specifically:

- If $a_{i,j} > 0$, C_j is a product of the process.
- If $a_{i,j} < 0$, C_j is a substrate for the process.
- If $a_{i,j} = 0$, C_j is not involved in the process.

In simulations of a Continuous Stirred Tank Reactor (CSTR), the vector of state variables $x \in \mathbb{R}^n$ is equivalent to the vector of concentrations C. Thus, by substituting C with x, we get $\dot{x} = r$, and Equation 1.7 can be rewritten as:

$$\dot{x} = A^T p$$

In the context of Activated Sludge Models (ASMs), these conservation laws imply that each process p must conserve carbon (C), nitrogen (N), phosphorus (P), and net electrical charge. The quantities of C, N, P, and electrical charge in all components are represented in a mass and charge conservation matrix:

$$I_{4\times n} = \begin{pmatrix} I_{1,1} & \cdots & I_{1,n} \\ \vdots & \ddots & \vdots \\ I_{4,1} & \cdots & I_{4,n} \end{pmatrix} \tag{1.9}$$

where $I_{i,j}$ represents the quantities of C, N, P, and electrical charge for $i = 1, 2, 3$, and 4, respectively, for the j-th component. Each reaction $r \in r$ must satisfy all four balance equations, imposing restrictions on the stoichiometric parameters $a_{i,j} \in A_{m\times n}$.

To satisfy these balance equations, the following matrix equation must hold:

$$A_{m\times n}(I_{4\times n})^T \geq 0_{m\times 4} \tag{1.10}$$

To meet this requirement, among k non-zero stoichiometric parameters in matrix A, $k - 4m$ parameters are selected manually, and the remaining $4m$ parameters are computed by solving the above matrix equation to ensure mass and charge conservation.

2.2 Reaction kinetics

The processes $p \in p$ described in Equation 1.6 correspond to different biochemical enzymatic reactions carried out by different types of bacteria within the activated sludge process. These reactions involve substrate consumption, product formation, energy consumption or release, and biomass growth or degradation. In general, the rate of a process involving a single substrate and a single bacterial biomass, without taking into account temperature variations, can be expressed as follows:

$$p(X, S) = m\mu(X, S) \tag{1.11}$$

- $p(X, S)$ (g m^{-3} d^{-1}): The process rate.
- m (d^{-1}): The maximum growth rate.
- $\mu(X, S)$: The process rate dependency function, which depends on substrate S and biomass X concentrations.

In biotechnology and the Activated Sludge Models (ASMs), the process rates $p(X, S)$ are proportional to the biomass concentration X (g m^{-3}). Thus, the process rate dependency function $\mu(X, S)$ can be expressed as:

$$\mu(X, S) = \mu(S)X$$

As a result, Equation 1.11 can be rewritten as:

$$K(X, S) = m\mu(S)X \tag{1.12}$$

The value of $p(X, S)$ is less than the maximum process rate m due to factors such as substrate limitation, diffusion, inhibition, and competition between bacteria for the same substrate. These factors are represented by a non-dimensional function $\mu(S) < 1$, which can take different forms as shown in the table 2.1.

Model	Kinetics expression $\mu(S)$
1st order kinetics	$\mu(S) = k \cdot S$
Monod	$\mu(S) = \frac{\mu_{\max} S}{K_s + S}$
Moser	$\mu(S) = \frac{\mu_{\max} S}{K_S + S^n}$
Haldane	$\mu(S) = \frac{\mu_{\max} S}{K_s + S + \frac{S^2}{K_I}}$

Table 2.1: Reaction kinetics dependent on single substrate concentration Bastin and Dochain (1990)

- K_S, K_0, and K_H represent the half-saturation constants for the Monod, Moser, and Haldane equations, respectively.
- K_i is the inhibition constant.
- Monod kinetics is a special case of Moser kinetics where $n = 1$.

The figure 2.5 compares the Monod, Moser, and Haldane kinetic models, showing how the process rate varies with substrate concentration for each model

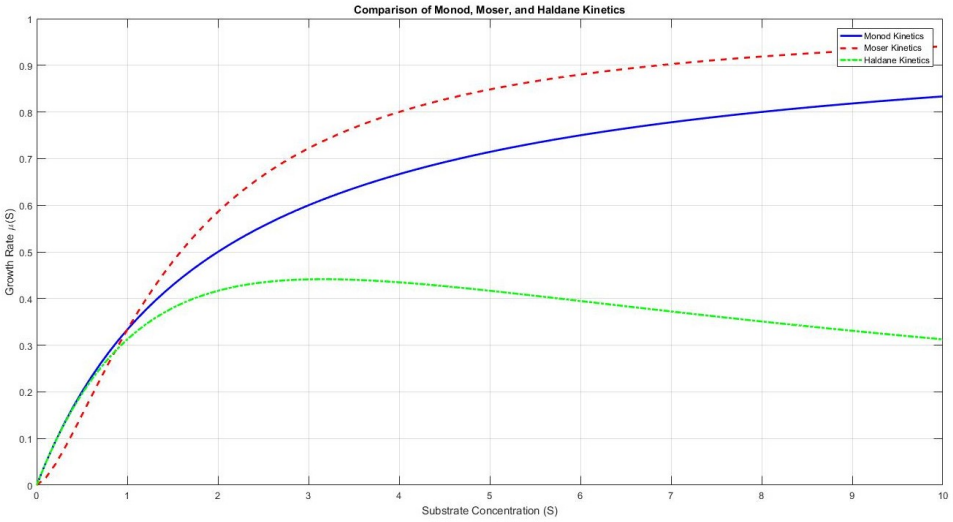

Figure 2.5: Comparison of Monod, Moser, and Haldane Kinetics

In ASM models, the population dynamics of bacterial species involve two opposing processes: growth and decay. The net growth of a bacterial species, taking into account biomass growth, maintenance, decay, and lysis, is expressed as the difference between these two opposing mechanisms, as shown in Equation (1.13):

$$p(X, S) = m\mu(S)X - k_D X \tag{1.13}$$

where k_D (in units of d^{-1}) is the bacterial decay coefficient

2.3 Activated Sludge Model No. 1 (ASM1)

The Activated Sludge Model No. 1 (ASM1), developed by Henze et al. (1987), is a widely recognised standard for modelling activated sludge systems. This model accurately represents the dynamics of nitrogen and chemical oxygen demand in suspended solids treatment processes, incorporating mechanisms for both nitrification and denitrification. ASM1 has proven effective in describing activated sludge processes where the wastewater is well characterised and from domestic or municipal sources, but is less suitable for industrial wastewater The model does not include phosphorus removal.

The Activated Sludge Model No. 1 (ASM1) is based on eight fundamental biological processes and considers two types of bacteria: heterotrophic and autotrophic. These processes include the microbial growth and decay dynamics of both types of bacteria, as well as nutrient removal mechanisms such as nitrification and denitrification.These biological processes are represented in Table(2.2)

Process Rate	Mathematical Expression
1–Heterotrophs, aerobic growth	$\mu_H \left(\frac{S_S}{K_{XS}+S_S}\right)\left(\frac{S_O}{K_{OH}+S_O}\right) X_H$
2–Heterotrophs, anaerobic growth	$\mu_H \left(\frac{S_S}{K_{XS}+S_S}\right)\left(\frac{K_{OH}}{K_{OH}+S_O}\right)\left(\frac{S_{NO}}{K_{NO}+S_{NO}}\right) X_H$
3–Autotrophs, aerobic growth	$\mu_A \left(\frac{S_{NH}}{K_{NH}+S_{NH}}\right)\left(\frac{S_O}{K_{OA}+S_O}\right) X_A$
4–Heterotrophs, decay	$b_H X_H$
5–Autotrophs, decay	$b_A X_A$
6–Organic nitrogen, ammonification	$k_a S_{ND} X_I$
7–Hydrolysis of particulate organic matter	$k_h \left(\frac{X_S}{X_I}\right)\left(\frac{S_O}{K_H+S_O}\right)\left(\frac{K_{OH}}{K_{OH}+S_O}\right)\left(\frac{S_{NO}}{K_{NO}+S_{NO}}\right) X_I$
8–Hydrolysis of particulate organic nitrogen	$k_h \left(\frac{X_S}{X_I}\right)\left(\frac{S_O}{K_H+S_O}\right)\left(\frac{K_{OH}}{K_{OH}+S_O}\right)\left(\frac{S_{NO}}{K_{NO}+S_{NO}}\right)\left(\frac{X_{ND}}{X_I}\right) X_I$

Table 2.2: Expression of the process rates for ASM1 Henze et al. (2000)

In this model, chemical oxygen demand (COD) and total nitrogen (TN) are divided into several state variables based on physico-chemical properties (such as particulate and soluble forms) and biodegradability (inert, rapidly biodegradable or slowly biodegradable), as shown in the table (2.3).

COD Fractions	**TN Fractions**
Soluble readily biodegradable matter (SS)	Soluble organic (SND)
Soluble inert (SI)	Ammoniacal nitrogen (SNH)
Particulate slowly biodegradable matter (XS)	Particulate organics (XND)
Particulate inert (XI)	Nitrates and nitrites (SNO)
Particulate inert from biomass decay (XP)	Oxygen (SO)
Heterotrophic biomass (XBH)	Alkalinity (SALK)
Autotrophic biomass (XBA)	

Table 2.3: Summary of Fractions and Parameters

ASM1 (Activated Sludge Model No. 1) models various biological and chemical processes to simulate wastewater treatment. The key processes include microbial growth of heterotrophic and autotrophic bacteria, breakdown of organic matter (COD) and nitrogen compounds, nitrification (conversion of ammonia to nitrates), denitrification (conversion of nitrates to nitrogen gas) and decay of microorganisms. These processes work together to remove organic pollutants and nitrogen from wastewater, and their interactions are illustrated in the figure below(2.6).

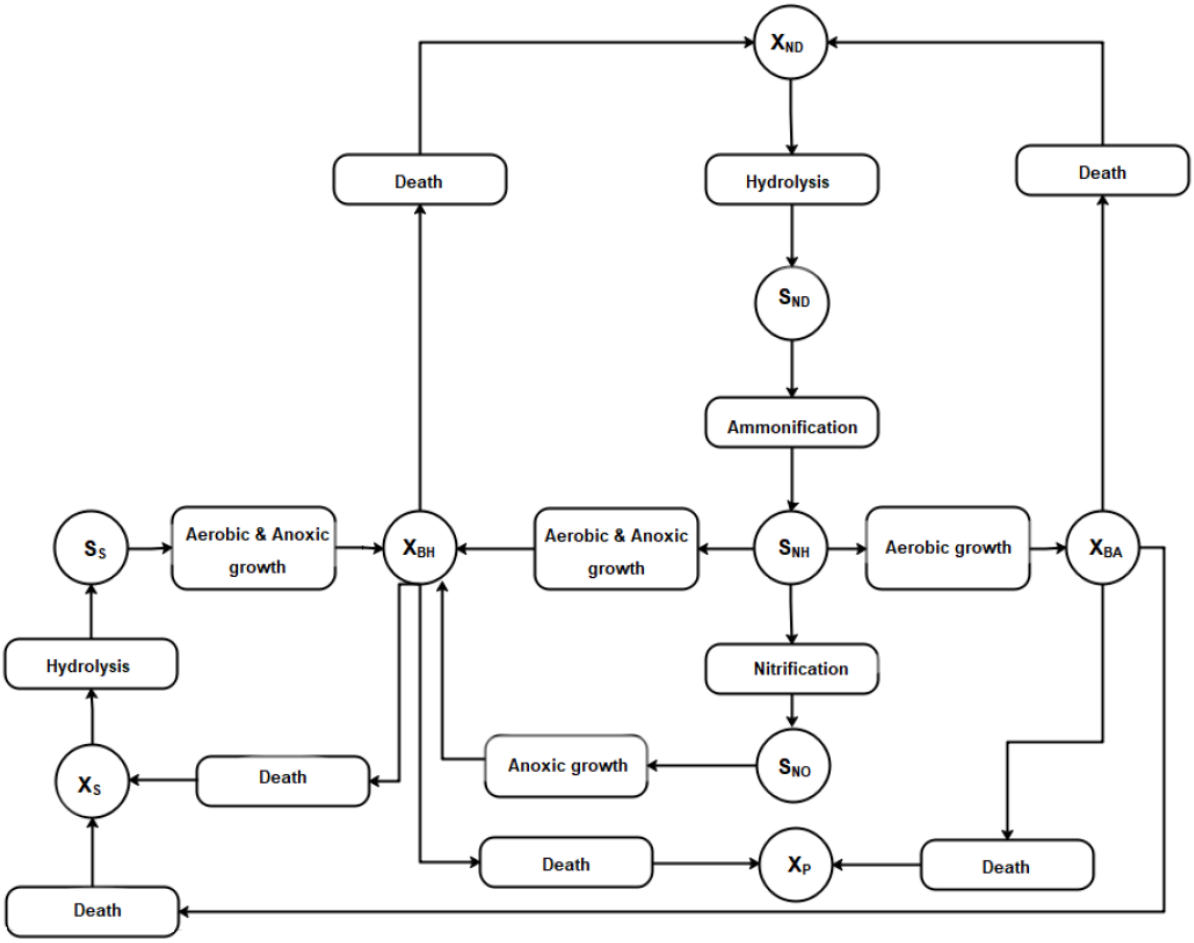

Figure 2.6: Overview of ASM1 processes

Although ASM1 has been successfully applied in a wide range of scenarios for its original purposes, such as predicting sludge production, oxygen demand and effluent quality, the model has certain limitations:

- It does not take into account the limiting effects of alkalinity, nitrogen, phosphorus and other inorganic nutrients on biomass growth. - The model separates particulate organic matter into two compartments: influent derived (XI) and biomass decomposition (XP). In practice, however, these two COD fractions cannot be clearly separated. - Processes such as death, predation, biomass lysis and endogenous respiration are grouped under lysis, hydrolysis and growth mechanisms, but are not modelled individually.

2.4 A modified Activated Sludge Model ASM1-2ND

Most activated sludge models, including ASM1 (Model 2.7), treat nitrification as a single step process. This simplification is generally acceptable for modelling conventional treatment systems. However, problems such as nitrite accumulation can occur due to design flaws or operational inefficiencies. Therefore, it may be valuable to consider nitrification and denitrification as distinct two-step processes, particularly in the context of water reuse. Consideration of the different forms of nitrogen, including nitrite, which can be readily oxidised to nitrate, may be important for accurate modelling and effective treatment.

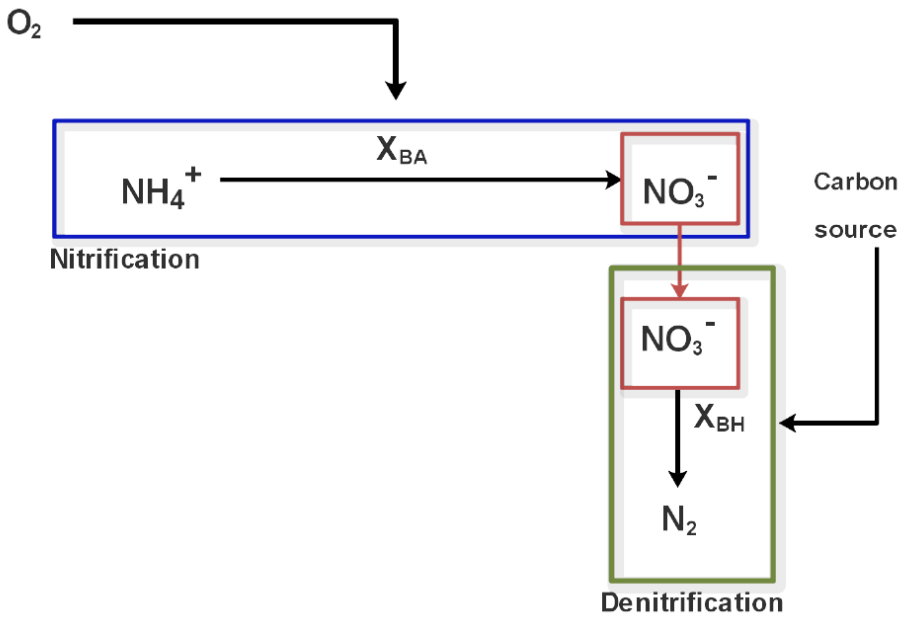

Figure 2.7: Scheme of nitrification and denitrification processes in the ASM1 Model

The ASM1-2ND model developed by Ostace et al. (2011) is an advanced version of ASM1 that incorporates a two-step nitrification and denitrification process (figure 2.8). The modified ASM1-2ND model maintains the main components of the original ASM1 model, including the division of total chemical oxygen demand (COD) into three categories: biodegradable COD, non-biodegradable COD and active biomass. However, the treatment of nitrogen components has been updated. In ASM1-2ND, nitrification is represented as a two-step process, with nitrate and nitrite concentrations modelled as separate state variables (SNO2 and SNO3) rather than as a single variable (SNO) as in ASM1. The SNO2 component acts as an intermediate between the nitrification and denitrification processes. In addition, the autotrophic bacteria in ASM1 (XBA) are divided into two types: Nitrosomonas bacteria (XAOB), which oxidise ammonium to nitrite, and Nitrobacter bacteria (XNOB), which oxidise nitrite to nitrate.

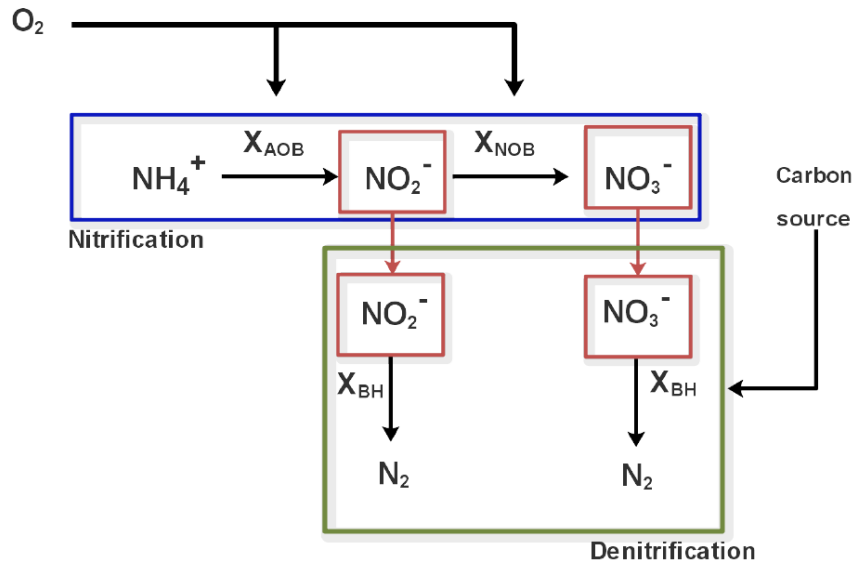

Figure 2.8: Scheme of nitrification and denitrification processes in the ASM1-2ND Model

The ASM1-2N model describes eleven dynamic processes (table 2.4) that describe the growth and decay of biomass in an activated sludge system. The model uses Monod kinetics to characterise the growth of heterotrophic bacteria through three aerobic and two anoxic processes. As noted above, this model differs from the original ASM1 [Henze et al. (2000)] in that it incorporates a two-step nitrification process. This is achieved through the involvement of two distinct groups of autotrophic bacteria: Ammonia oxidising bacteria (AOB) and Nitrite oxidising bacteria (NOB). In the model these bacteria are represented as XAOB and XNOB respectively.

The aerobic growth rates of the AOB and NOB (denoted as μ_{AOB} and μ_{NOB} in Table 2.4) are given by:

$$\mu_{AOB} = \frac{\mu_{AOB} \cdot S_{NH}}{K_{NH} + S_{NH}} \cdot \frac{S_O}{K_{OA} + S_O} \cdot X_{AOB} \tag{1.14}$$

$$\mu_{NOB} = \frac{\mu_{NOB} \cdot S_{NO_2}}{K_{NO_2} + S_{NO_2}} \cdot \frac{S_O}{K_{OA} + S_O} \cdot \frac{K_{NH}}{S_{NH} + K_{NH}} \cdot X_{NOB} \tag{1.15}$$

Equation (1.13) represents the first step of the nitrification process, known as partial nitrification, in which ammonium is oxidised to nitrite. In this step, both the ammonium concentration (S_{NH}) and the dissolved oxygen concentration (S_O) act as limiting factors. In contrast, equation (2.2) introduces a 'switching function' that models the role of ammonium (S_{NH}) as an inhibitor in the second step, where nitrite (S_{NO_2}) is further oxidised to nitrate (S_{NO_3}).

For the denitrification process, facultative heterotrophic biomass utilises organic carbon by anoxic respiration. In the absence of dissolved oxygen, nitrite or nitrate act as electron acceptors, facilitating the conversion of these compounds to dinitrogen.

For the denitrification process, the reaction rates (denoted as μ_{HNO_2} and μ_{HNO_3} in Table (2.4) are given by the following expressions:

$$\mu_{BHNO_2} = \frac{\mu_{HNO_2} \cdot S_s}{K_s + S_s} \cdot \frac{K_{OH}}{K_{OH} + S_O} \cdot \frac{S_{NO_2}}{K_{NO} + S_{NO_2}} \cdot \frac{S_{NH}}{K_{NH} + S_{NH}} \cdot X_{BH} \tag{1.16}$$

$$\mu_{BHNO_3} = \frac{\mu_{HNO_3} \cdot S_s}{K_s + S_s} \cdot \frac{K_{OH}}{K_{OH} + S_O} \cdot \frac{S_{NO_3}}{K_{NO} + S_{NO_3}} \cdot \frac{S_{NH}}{K_{NH} + S_{NH}} \cdot X_{BH} \tag{1.17}$$

In order to accurately model the evolution of the concentration of each component in the ASM1-2ND activated sludge model, we need to use the stoichiometric matrix(tabel 2.5), which defines the relationships and reactions between the different components. This matrix is crucial in setting up the reactions implemented in our simulations. The stoichiometric matrix, as detailed in the table below, outlines the coefficients associated with each component for the various processes modelled in the simulation.

Finally, The ASM1-2ND model is the most effective for simulation in this work. However, to fully understand its capabilities, it is essential to first explore the ASM1 model. Therefore, we first performed simulations using the original ASM1 model to understand the basic concepts. While these simulations are not detailed in this thesis, they were critical to understanding the development and modelling of the ASM1-2ND. Moving forward, our focus will be on the use of the ASM1-2ND model.

Processes	**Processes rate equation** ρ_i
1 Aerobic growth of heterotrophs	$\mu_H \left(\frac{S_S}{K_{XS}+S_S}\right)\left(\frac{S_O}{K_{OH}+S_O}\right) X_{BH}$
2 Anoxic growth of heterotrophs on S_{NO2}	$\mu_H \eta_{NO2} \left(\frac{S_S}{K_{XS}+S_S}\right)\left(\frac{K_{OH}}{K_{OH}+S_O}\right)\left(\frac{S_{NO2}}{K_{NO2}+S_{NO2}}\right) X_{BH}$
3 Anoxic growth of heterotrophs on S_{NO3}	$\mu_H \eta_{NO3} \left(\frac{S_S}{K_{XS}+S_S}\right)\left(\frac{K_{OH}}{K_{OH}+S_O}\right)\left(\frac{S_{NO3}}{K_{NO3}+S_{NO3}}\right) X_{BH}$
4 Decay of heterotrophs	$b_H X_{BH}$
5 Aerobic growth of Nitrosomonas	$\mu_{AOB} \left(\frac{S_{NH}}{K_{NH}+S_{NH}}\right)\left(\frac{S_O}{K_{OA}+S_O}\right) X_{AOB}$
6 Aerobic growth of Nitrobacter	$\mu_{NOB} \left(\frac{S_{NO2}}{K_{NO2}+S_{NO2}}\right)\left(\frac{S_O}{K_{OA}+S_O}\right) X_{NOB}$
7 Decay of Nitrosomonas	$b_{AOB} X_{AOB}$
8 Decay of Nitrobacter	$b_{NOB} X_{NOB}$
9 Ammonification of soluble organic nitrogen	$k_a S_{ND} X_{BH}$
10 Hydrolysis of entrapped organics	$k_h \left(\frac{X_S/X_{BH}}{K_X+X_S/X_{BH}}\right)\left(\frac{S_O}{K_{OH}+S_O} + \eta_g \frac{K_{OH}}{K_{OH}+S_O}\frac{S_{NO3}+S_{NO2}}{K_{NO}+S_{NO3}+S_{NO2}}\right) X_{BH}$
11 Hydrolysis of entrapped organic nitrogen	$\rho_{10}\left(\frac{X_{ND}}{X_I}\right)$

Table 2.4: ASM1-2ND processes

Variable / *Process*	S_I	S_S	X_I	X_S	X_{BH}	X_{NS}	X_{NB}	X_P	S_O	S_{NO2}	S_{NO3}	S_{N2}	S_{NH}	S_{ND}	X_{ND}	S_{alk}
1		Y_H^{-1}			1				$1-(1/Y_H)$							$-(i_{XB}/14)$
2		Y_H^{-1}			1					$-(1-Y_H^{-1})/1.72$		$(1-Y_H^{-1})/1.72$	$-i_{XB}$			$[-i_{XB}-(1-(1/Y_H)/1.72)]/14$
3		Y_H^{-1}			1						$-(1-Y_H^{-1})/2.86$	$(1-Y_H^{-1})/2.86$	$-i_{XB}$			$[-i_{XB}-(1-(1/Y_H)/2.86)]/14$
4				$(1-f_P)$	-1			f_P							$(i_{XB}-f_P i_{XP})$	
5						1			$1-(3.43/Y_{AOB})$	Y_{AOB}^{-1}			$-i_{XB}-Y_{AOB}^{-1}$			$[-1/(1-(7Y_{AOB})]-i_{XB}/14$
6							1		$1-(1.14/Y_{NOB})$	$-Y_{NOB}^{-1}$	Y_{NOB}^{-1}		$-i_{XB}$			$-(i_{XB}/14)$
7				$(1-f_P)$		-1		f_P							$(i_{XB}-f_P i_{XP})$	
8				$(1-f_P)$			-1	f_P							$(i_{XB}-f_P i_{XP})$	
9													1	-1		
10		1		-1										1		-(1/14)
11																

Table 2.5: Stoichiometric matrix of the ASM1-2ND model Ostace et al. (2011)

3 Conclusion

In this chapter we have explored the modelling of wastewater treatment systems, with a particular focus on activated sludge processes for carbon and nitrogen removal. These models are essential tools for understanding, designing and optimising modern wastewater treatment plants, which are evolving into Water Resource Recovery Facilities (WRRFs). By incorporating advanced models such as ASM1 and ASM1-2ND, we can accurately simulate complex biological processes, improve treatment efficiency and meet stringent environmental standards. This shift not only focuses on pollutant removal, but also emphasises water reuse, nutrient recovery and energy generation,. In the end, these models help design smarter, more efficient systems that help conserve resources and protect the environment.

Chapter 3

Design Strategies for ASM1-2nd Simulations

Contents

1 Introduction to Simulation Setup

1.1 Overview of MATLAB Simulink

MATLAB Simulink is a powerful graphical simulation environment that is widely used for modelling, simulating, and analysing dynamic systems. It provides a block diagram-based interface that allows users to represent systems in terms of their components, signals, and interactions. Simulink is particularly effective at handling continuous-time, discrete-time, and hybrid systems, making it well-suited for a variety of engineering applications, including control systems, signal processing, and mechanical and electrical systems.

Simulink integrates seamlessly with MATLAB, allowing users to incorporate custom algorithms, scripts, and functions into their models. It supports both linear and nonlinear systems, provides extensive libraries of predefined blocks, and offers flexibility in simulation settings, making it an ideal tool for dynamic system modelling and simulation.

In all subsequent work, the structure remains the same: we have a folder containing all the code files (.m files) that contain the modelling for the different models used in the simulation. In the same folder we have the Simulink file where the schematic of our platform is built. This platform can include one or more tanks and all the necessary components. The most critical element in all of this is the S-function.

1.2 Overview of S_Function

S-Functions (System Functions) are highly customisable, user-defined blocks in Simulink that are used to model systems that require custom behaviours or algorithms beyond those provided by the standard block library. Written in either MATLAB code (for interpreted S-functions) or C/C++ (for compiled S-functions), S-functions interact with the Simulink engine through a series of callback methods. These callbacks are triggered at various points during the simulation, including initialisation, output computation, state updates, and termination. The Simulink engine controls these callbacks using specific flags that indicate the stage of the simulation. For example, at each time step, the flag might call the function that computes the block's outputs or updates its internal states. This modular approach allows S-Functions to perform complex calculations, simulate non-linear systems and implement control logic not possible with standard blocks. The flexibility of S-Functions makes them essential for simulations that require detailed and dynamic customisation.

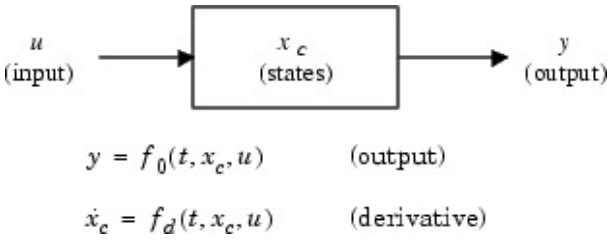

1.3 Some Simulink Blocks Used in Simulations

Mux: The `Mux` (Multiplexer) block combines multiple input signals into a single output signal. This block is used to group signals to streamline the modelling process and simplify signal management within a Simulink model.

Selector: The `Selector` block extracts specific elements from a vector or array of signals. It allows you to select and output specific elements based on index values. This is useful for isolating or manipulating subsets of data in a simulation.

Scope: The `Scope` Block provides a graphical interface for visualising signals during simulation. It displays signal waveforms and helps to analyse the behaviour of the signals in real time or after simulation. This block is essential for debugging and monitoring simulation results.

Demux: The `Demux` (Demultiplexer) block splits a single input signal into multiple output signals. This block is used to break down a composite signal into its individual components, which can then be routed to different parts of the model for further processing.

Manual Switch: The `Manual Switch` block allows manual selection between multiple input signals to be directed to a single output. This block is often used to test different scenarios by switching between different signal paths during simulation. The selection is controlled manually at run time.

2 ASM1-2ND Platform Simulation

2.1 System description and design

The water resources recovery factory(WRRF)(Proposed by Aichouche (2021)) consists of three reactors in series: an anoxic reactor (R1) with a volume of 4000 m^3, followed by an aerobic reactor (R2) with a volume of 6000 m^3 and an aerobic membrane bioreactor (R3) with a volume of 3000 m^3. All reactors are operated as fully mixed systems . The membrane within the bioreactor is ideal, ensuring perfect separation of soluble and particulate matter, without regard to fouling phenomena. The WRRF is equipped with three valves, labelled (A), (B) and (C), each with two operating positions. See Figure 3.1.

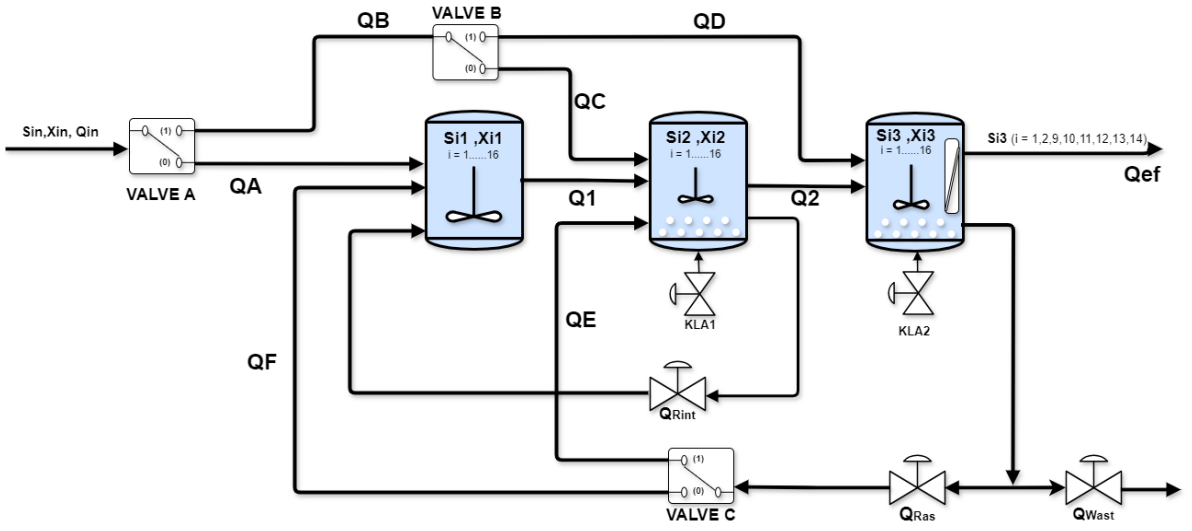

Figure 3.1: Hydraulic process scheme of the proposed flexible platform

The platform design allows six different configurations for nitrogen removal by nitrification and denitrification processes, based on the positions of three valves (Valve A, Valve B and Valve C). These valves control the flow and recirculation between the tanks (R1, R2 and R3) and thus the overall system behaviour. Depending on the valve positions, the system can alternate between pre-denitrification and post-denitrification modes, affecting nitrogen removal efficiency. The table 3.1 lists the six possible configurations, of which we will consider the most important:

Pre-Denitrification System (Configuration C1)

Valve settings:
Valve A = 0, Valve B = 0, Valve C = 0

Flow description:
External recirculation (QRAS) is activated from R3 to the anoxic tank R1, while internal recirculation (Qint) is non-zero.

Process:
External recirculation (QRAS) from reactor R3 (the membrane bioreactor or MBR) to reactor R1 (the anoxic tank) is active, while internal recirculation (Qint) is also running. In this configuration, nitrate is recycled from the aerobic reactors to the anoxic reactor before the effluent undergoes further nitrification.

Control:
The denitrification process can be controlled by adjusting the recirculation rate (QRAS), which controls how much nitrate is returned to R1 for denitrification.

Equivalent process:
This design mirrors the conventional activated sludge process, using a series of fully mixed reactors with continuous recirculation to facilitate nitrogen removal.

Configuration Schema:

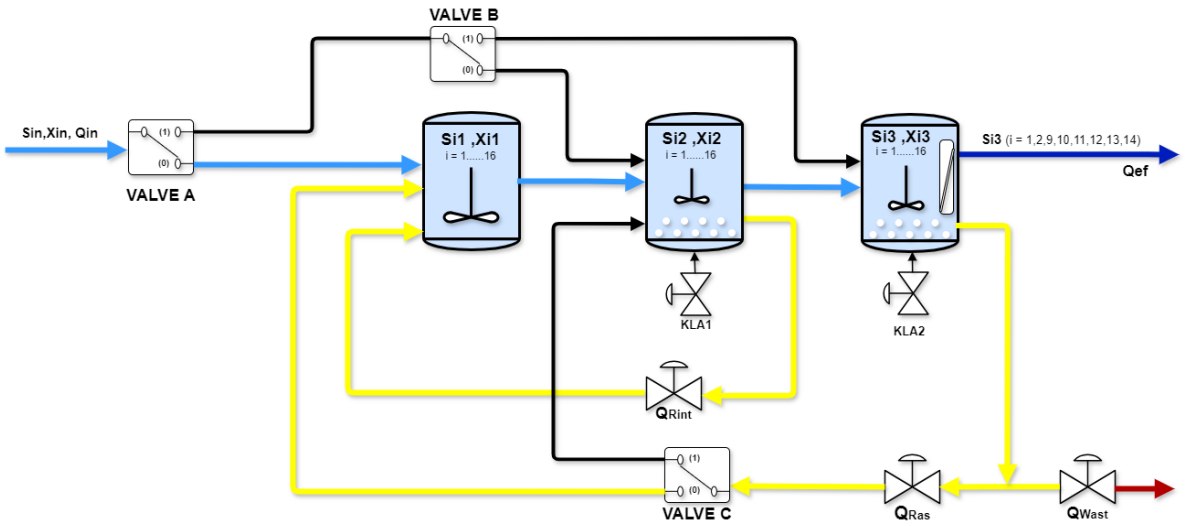

Figure 3.2: Hydraulic process scheme of the Configuration C1

Post-Denitrification System (Configuration C3)

Valve settings:
Valve A = 1, Valve B = 0, Valve C = 0

Flow description:
The input flow is directed to the aerobic tank R2

Process:
The influent flow is directed to reactor R2 (the aerobic tank) where nitrification takes place and recirculation of nitrate to R1 is allowed. After the influent has undergone nitrification in R2, denitrification occurs in R1 as nitrate is recycled back. However, this is referred to as post-denitrification because denitrification happens after nitrification has taken place

Limitation:
The denitrification rate is expected to be low because the carbon source may have already been consumed in R2. However, if the hydraulic retention time (HRT) is sufficiently large and there is adequate oxygen in R2, high-rate nitrification can still occur

Configuration Schema:

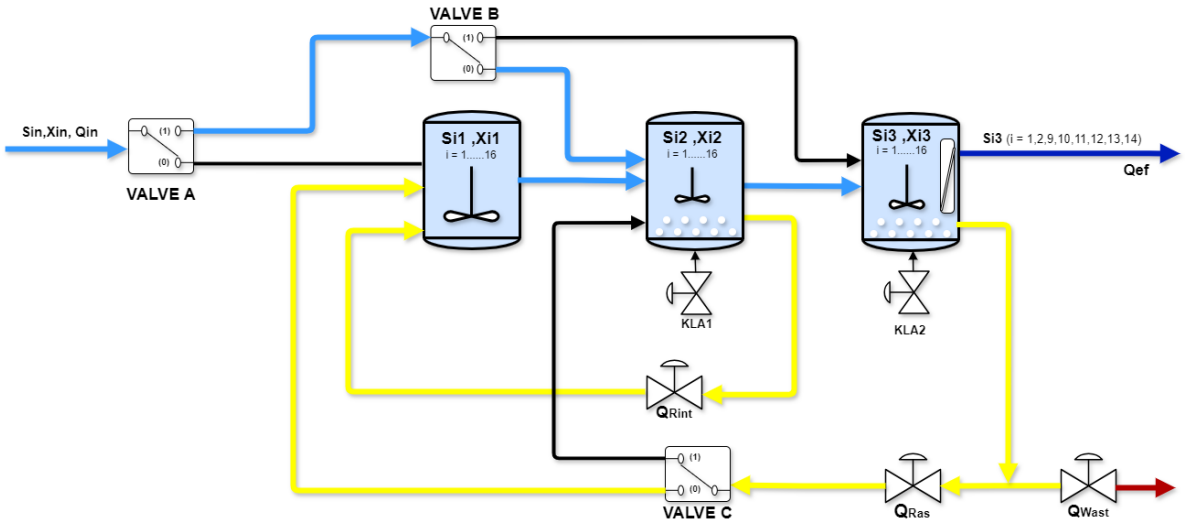

Figure 3.3: Hydraulic process scheme of the Configuration C3

Post-Denitrification with Short HRT (Configuration C5)

Valve settings:
Valve A = 1, Valve B = 1, Valve C = 0

Flow description:
The input flow is directed towards the MBR reactor R3, with some flow going through R2 as well.

Process:
The influent is directed to R3 (the MBR reactor) and R2. This configuration allows simultane-

ous flow through both reactors
Nitrification can occur in R2, but it is limited by a short hydraulic retention time (HRT). A shorter HRT means that the wastewater spends less time in R2, reducing the efficiency of nitrification.

Control:
Nitrification can be adjusted by controlling the sludge retention time (SRT) and the dissolved oxygen (DO) concentration in R3. Maintaining the proper SRT and DO levels is crucial for efficient nitrification, as it directly influences the growth and activity of nitrifying bacteria.
Denitrification occurs in R1, as nitrate is recycled back, but the process may be affected by the shorter HRT in R2, limiting the effectiveness of nitrogen removal

Configuration Schema:

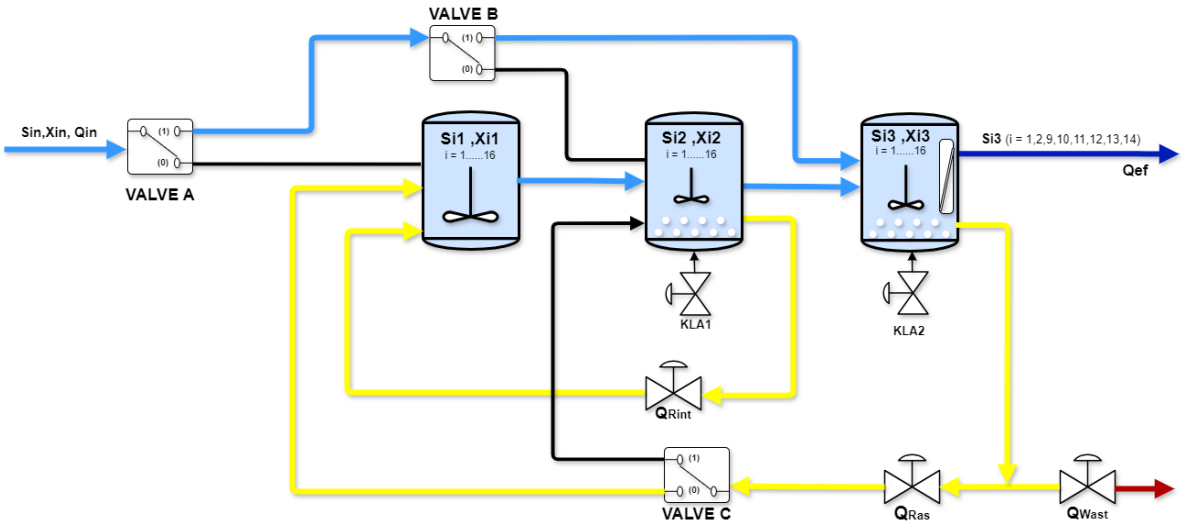

Figure 3.4: Hydraulic process scheme of the Configuration C5

- **Nitrate absence**: It is assumed that no nitrate is present at the process input; instead, all nitrogen is in the ammoniacal form. According to IWA guidelines, the total nitrogen content (TNC) can be calculated using the formula

$$\mathrm{TNC} = \frac{2}{3}\mathrm{NNH_4} + \frac{1}{3}\mathrm{N_{organic}} \tag{3.1}$$

- **Maximum internal recirculation rate**: The maximum mixed liquor recirculation rate (Q_{int}) is set at 100% of the input flow rate, which is 24,000 m³/day.

- **Maximum external recirculation rate**: The maximum sludge recirculation rate (Q_{RAS}) is set at 500% of the input flow rate, which is 120,000 m³/day.

- **Design parameters**: The WRRF is designed for a constant dry weather influent flow of 24,000 m³/day and a constant influent biodegradable COD concentration of 350 g/m³. For dynamic influent scenarios, average values are given in Table 2.2. Additionally, the tank volumes are selected to ensure that the minimum possible hydraulic retention time (HRT) is 3 hours.

The WRRF model is described by equations for both soluble ($S_{i,R}$) and particulate ($X_{i,R}$) components in each reactor. Here, i represents the different components (from 1 to 16, as shown in Table 2.2), and R represents the reactor tanks (from 1 to 3). For the first tank ($R = 1$), the mass balance equation for each component i is:

$$\frac{dS_{i,1}}{dt} = \frac{1}{V_1}\left(Q_{\text{in},1}S_{i,\text{in},1} - Q_1 S_{i,1}\right) + r_j \tag{3.2}$$

$$\frac{dX_{i,1}}{dt} = \frac{1}{V_1}\left(Q_{\text{in},1}X_{i,\text{in},1} - Q_1 X_{i,1}\right) + r_j \tag{3.3}$$

With $Q_{\text{in},1} = QF + QA + Q_{\text{int}}$.
For the second aerobic tank $R = 2$, the mass balance equation is:

$$\frac{dS_{i,2}}{dt} = \frac{1}{V_2}\left(Q_{\text{in},2}S_{i,\text{in},2} - Q_2 S_{i,2} - Q_{\text{int}}S_{i,2}\right) + r_j \tag{3.4}$$

$$\frac{dX_{i,2}}{dt} = \frac{1}{V_2}\left(Q_{\text{in},2}X_{i,\text{in},2} - Q_2 X_{i,2} - Q_{\text{int}}X_{i,2}\right) + r_j \tag{3.5}$$

With $Q_{\text{in},2} = Q_1 + Q_E + Q_C$.
Finally, for the third tank $R = 3$, the mass balance equation for the membrane bioreactor is:

$$\frac{dS_{i,3}}{dt} = \frac{1}{V_3}\left(Q_{\text{in},3}S_{i,\text{in},3} - Q_{\text{RAS}}S_{i,3} - Q_{\text{WAS}}S_{i,3} - Q_{\text{ef}}S_{i,3}\right) + r_j \tag{2.9}$$

$$\frac{dX_{i,3}}{dt} = \frac{1}{V_3}\left(Q_{\text{in},3}X_{i,\text{in},3} - Q_{\text{RAS}}X_{i,3} - Q_{\text{WAS}}X_{i,3}\right) + r_j \tag{2.10}$$

With $Q_{\text{in},3} = Q_D + Q_2$.

All reaction rates r_j are extracted from Table(2.5), and the mass balance equations for all component concentrations $S_{i,R}$ and $X_{i,R}$ share the same structure, except for dissolved oxygen $S_{O,R}$. For dissolved oxygen, the equation follows the same structure but includes an additional term to account for external oxygen input. This term, $(K_L a)(S_{\text{Osat}} - S_{O,R})$, represents the rate of oxygen transfer. It is added to ensure that the dissolved oxygen level is maintained at an optimal level for biological processes, such as aerobic digestion, which require sufficient oxygen.

Valve A	Valve B	Valve C	Description
0	0	0	Configuration C1
0	0	1	Configuration C2
1	0	0	Configuration C3
1	0	1	Configuration C4
1	1	0	Configuration C5
1	1	1	Configuration C6

Table 3.1: Valve Configurations for Nitrogen Removal

2.2 Implementation in SIMULINK

In this simulation, which is the most basic, we will discuss many concepts that will be repeated in other simulations. Therefore, we need to cover them in detail. First, we will introduce the Simulink schema, and we will see that the overall structure in figure 3.5.This simulation has been designed for ease of use. This is because you can easily change all the necessary parameters such as KLa and different flow rates to change the influent concentration (using the constant block). You have the flexibility to adjust each influent parameter and visualise the different concentrations leaving the system in the scope.Additionally, we take the opportunity to point out that there is an extra switch (in red) outside of the platform, allowing you to switch from a constant influent to a dynamic influent. The dynamic input data used corresponds to inputs for dry weather conditions, as utilized in the BSM1LT [BSM]. Note that we have only presented the substrate variables, which makes sense due to the efficient separation of particles in the final membrane reactor as discussed earlier.

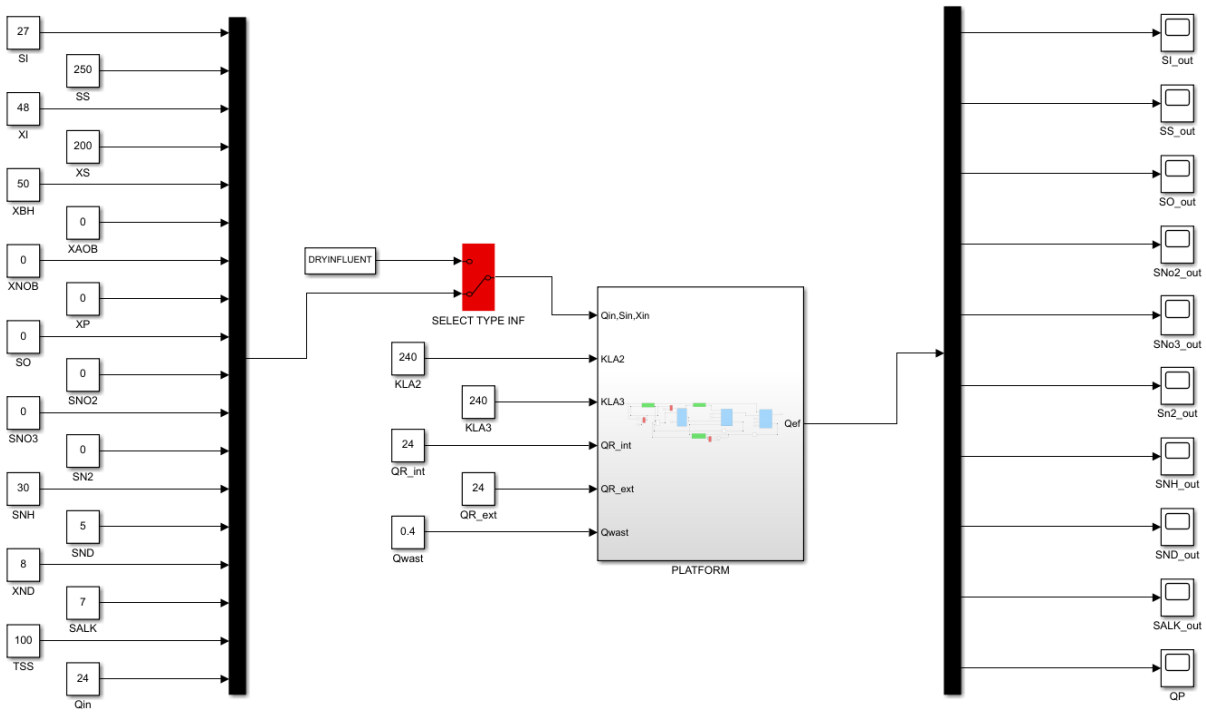

Figure 3.5: Overview of the Simulink Schema

If we go into the subsystem called 'Platform' in Figure 3.6, we find the platform design we discussed earlier in Figure 3.1 The Simulink schematic for this platform is slightly different, so we will explain everything in detail at least once. The first thing to notice are the three valves (represented as red switches in Simulink), which allow us to manipulate and switch between the different configurations mentioned in Table3.1. We can also see the light blue subsystems that model and represent the different tanks in Simulink, along with their respective "inputs".

We can also observe the green subsystems in Figure 2.1, which act as a mechanism for redirecting flows in the valve control system. Originally designed to split the incoming flow, these subsystems are now only used to redirect a specific flow. This is why the constant flows 'Q TO VALVE 1, 2 and 3' are always zero.

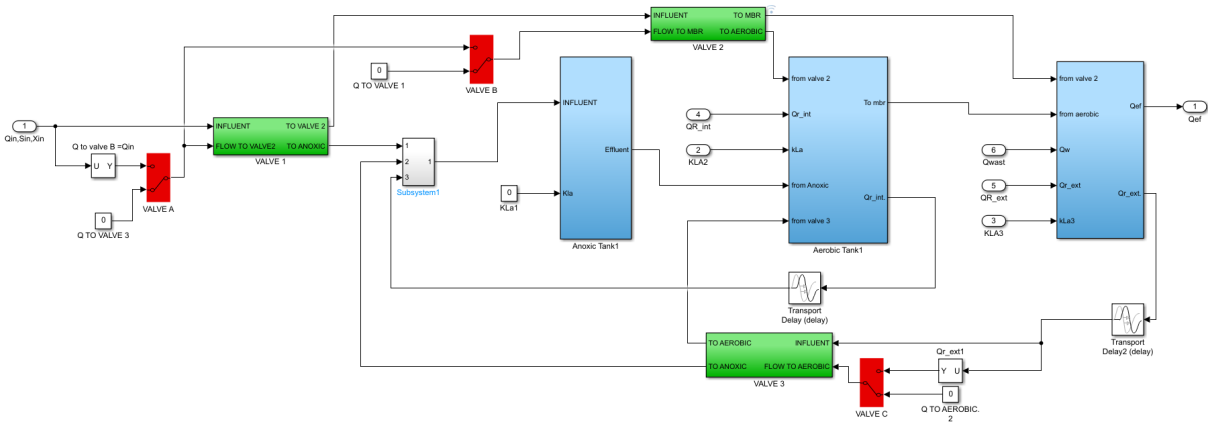

Figure 3.6: Overview of the Platfrom Schema

The operation of the valves is largely dependent on switches **A**, **B**, and **C**. For example, if we look at **Switch A**, the influent remains unchangeable, but the flow to the valve can vary from 0 to Q_{in}. This is illustrated in **Figure 3.7**(case A : valve A=0 and case B : valve A = 1), which shows the behaviour of the system based on the switching logic. The switches control how the flow is directed between different pathways, allowing the system to either send the flow to valve 2 or redirect it elsewhere, such as to an anoxic process, depending on the state of the switches.

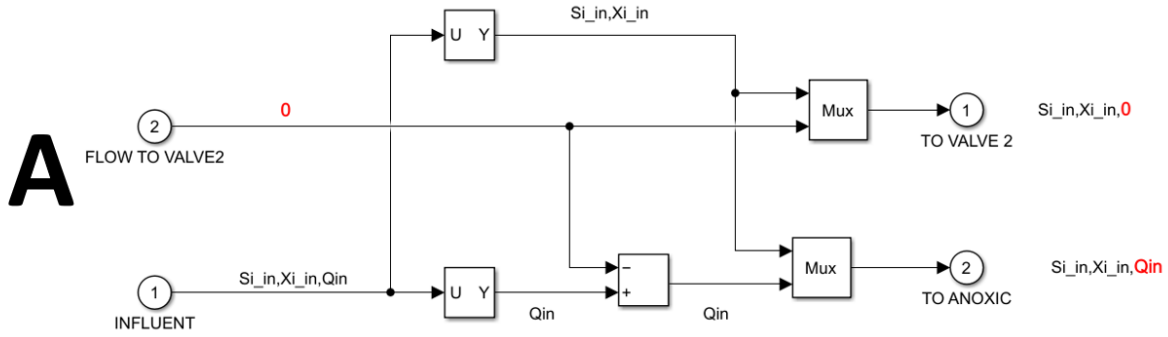

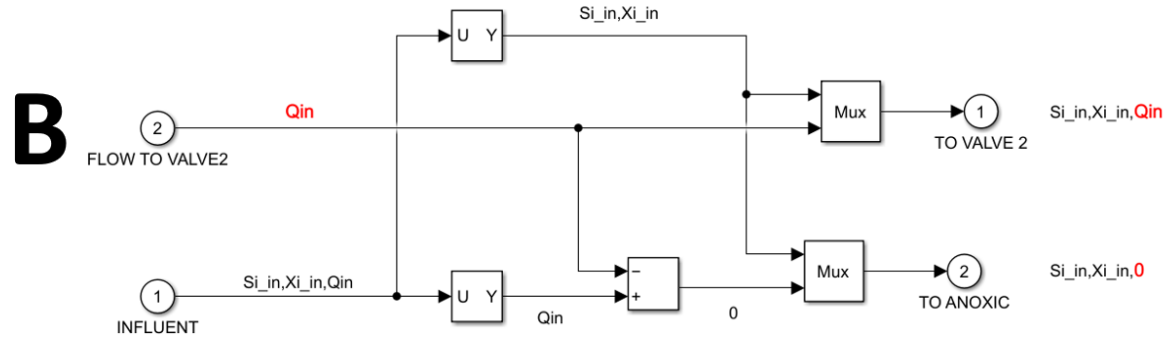

Figure 3.7: Logic of the valve block

We need to maintain the block Transport delay, which is crucial for breaking algebraic loops in closed-loop simulations. Algebraic loops can cause significant problems, especially when different recycling mechanisms are involved. When we first start the simulation, these loops can prevent it from running properly.

We have tried a number of solutions to this problem, including setting the initial conditions to zero and using different types of delay. Of the solutions we tried, the transport delay proved to be the most effective and reliable across all versions of Simulink.

2.2.1 Mathematical Models and Formulations for Multi-Stream Flow System

Since we have discussed all the blocks, we now need to delve deeper into the blocks that model the tanks(figure 3.8). Each tank has at least two different inputs, which requires us to combine these inputs. To address this, we use two additional S-functions (figure 3.9) that handle the addition of the flux. The equations for these functions are as follows:

Model for the ADD_2FLOW Function
Let x be a vector where:

- $x_1(i)$ for $i = 1, 2, \ldots, n$ represent the variables of interest from the first stream.
- $x_2(i)$ for $i = 1, 2, \ldots, n$ represent the variables of interest from the second stream.
- Q_1 and Q_2 represent the flow rates of the two different streams.

Mathematical Equations:
For each output $y(i)$, where i ranges from 1 to n:

$$y(i) = \frac{x_1(i) \cdot Q_1 + x_2(i) \cdot Q_2}{Q_1 + Q_2} \tag{3.6}$$

Total Flow Rate Calculation
The total flow rate $y(n + 1)$ is the sum of the two flow rates:

$$y(n + 1) = Q_1 + Q_2 \tag{3.7}$$

Special Case
If Q_1 or Q_2 is zero, then the function sets all outputs to zero to avoid division by zero:

$$y(i) = 0 \text{ for } i = 1, 2, \ldots, n + 1 \tag{3.8}$$

Model for the ADD_3FLOW Function
Let x be a vector where:

- $x_1(i)$ for $i = 1, 2, \ldots, n$ represent the variables of interest from the first stream.
- $x_2(i)$ for $i = 1, 2, \ldots, n$ represent the variables of interest from the second stream.
- $x_3(i)$ for $i = 1, 2, \ldots, n$ represent the variables of interest from the third stream.
- Q_1, Q_2, and Q_3 represent the flow rates of the three different streams.

Mathematical Equations
For each output $y(i)$, where i ranges from 1 to n:

$$y(i) = \frac{x_1(i) \cdot Q_1 + x_2(i) \cdot Q_2 + x_3(i) \cdot Q_3}{Q_1 + Q_2 + Q_3} \tag{3.9}$$

Total Flow Rate Calculation The total flow rate $y(n + 1)$ is the sum of the three flow rates:

$$y(n + 1) = Q_1 + Q_2 + Q_3 \tag{3.10}$$

Special Case If Q_1, Q_2, or Q_3 is zero, then the function sets all outputs to zero to avoid division by zero:

$$y(i) = 0 \text{ for } i = 1, 2, \ldots, n+1 \tag{3.11}$$

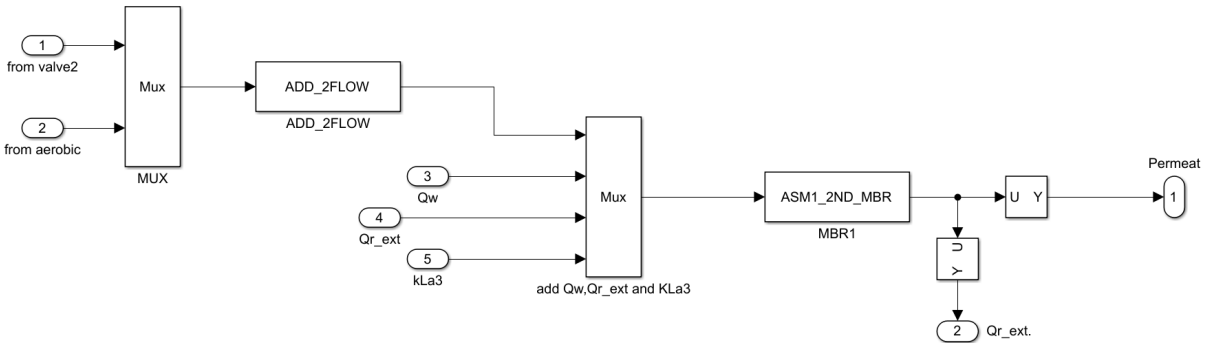

Figure 3.8: Block Diagram of Tank System with Two Flow Inputs

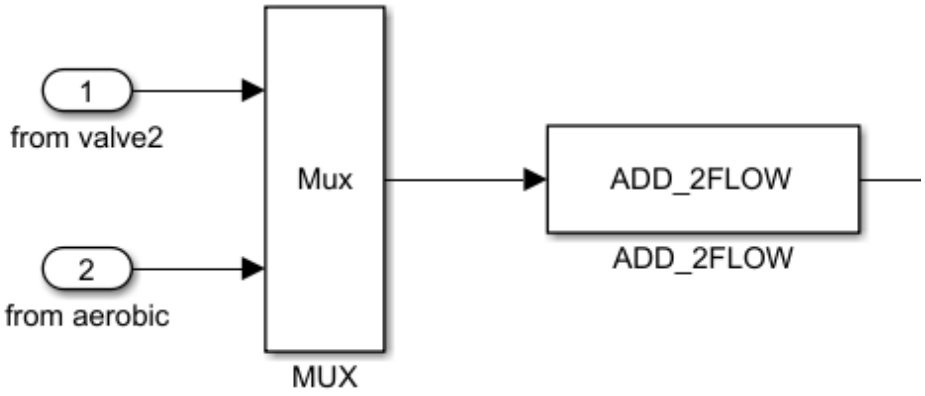

Figure 3.9: $S - function\ ADD\_2FLOW$

Note: We could have used a regular function instead of S-functions for the two blocks that add flux. However, since we are familiar with S-functions and they do not affect the results, we decided to keep them in the implementation.

2.3 Implementation in MATLAB

About the code: Our simulation folder contains five S-functions: three for each tank and two for adding fluxes. None of these functions will work without the main MATLAB file that defines and initialises all the values and parameters. The main file, called asm1_2nd_init, sets initial values for the concentrations of the different substances, which is necessary for the S-functions to work. It also defines the different volumes of each tank, the SOSAT (Saturation of Oxygen or Substrate) for each tank and, most importantly, the stoichiometric and kinetic values. These values, based on a natural pH and 20°C (shown in Table 3.2).

Note: The initial inflow entries are taken from the table proposed by Aichouche (2021), where two columns are provided: one for the constant inflow values and the other for the average data collected under dry conditions(table 3.3).

Parameter	Symbol	Value	Units
Maximum XBH growth rate	μ_H	4	d^{-1}
Half-saturation (hetero. growth)	K_S	10	g COD m^{-3}
Half-saturation (hetero. oxygen)	K_{OH}	0.2	g O_2 m^{-3}
Half-saturation (nitrate and nitrite)	K_{NO}	0.5	g NO_3^--N m^{-3}
Heterotrophic decay rate	b_H	0.3	d^{-1}
Maximum Nitrosomonas growth rate	μ_{AOB}	0.85	d^{-1}
Maximum Nitrobacter growth rate	μ_{NOB}	0.65	d^{-1}
Half-saturation (auto. growth)	K_{NH}	1	g NH_3-N m^{-3}
Half-saturation (auto. oxygen)	K_{OA}	0.4	g O_2 m^{-3}
Nitrosomonas decay rate	b_{AOB}	0.17	d^{-1}
Nitrobacter decay rate	b_{NOB}	0.15	d^{-1}
Anoxic growth rate correction factor	θ_g	0.8	/
Ammonification rate	K_a	0.05	m^3 (g COD d)$^{-1}$
Maximum specific hydrolysis rate	K_h	3	g XS (g XBH COD d)$^{-1}$
Half-saturation (hydrolysis)	K_X	0.1	g XS (g XBH COD)$^{-1}$
Anoxic growth rate correction factor	θ_{NO2}	0.8	/
Anoxic growth rate correction factor	θ_{NO3}	0.38	/
Heterotrophic yield	Y_H	0.45	g COD/g COD
Nitrosomonas yield	Y_{AOB}	0.17	g COD/g N
Nitrobacter yield	Y_{NOB}	0.15	g COD/g N
Fraction of biomass to particulate products	f_p	0.08	/
Fraction nitrogen in biomass	i_{XB}	0.086	g N/g COD
Fraction nitrogen in particulate products	i_{XP}	0.06	g N/g COD
Ammonia inhibition of nitrite oxidation	K_{NH-I}	5	g NH_4-N m^{-3}
Conversion factor for NO_3^- into COD	$i_{COD,NO3}$	1.1414285	g COD g N^{-1}
Conversion factor for NO_2^- into COD	$i_{COD,NO2}$	3.4268028	g COD g N^{-1}
Stoichiometric factor for NO_3^- reduction to N_2	$i_{NO3,N2}$	40/14	g COD g N^{-1}
Stoichiometric factor for NO_2^- reduction to N_2	$i_{NO2,N2}$	1.7242857	g COD g N^{-1}
Conversion factor for NH_4^+ into charge	$i_{Charge,SNHX}$	1/14	Charge g N^{-1}
Conversion factor for NO_3^- into charge	$i_{Charge,SNOX}$	-1/14	Charge g N^{-1}

Table 3.2: Kinetics, parameters and stoichiometric coefficients.
Ostace et al. (2011)

#	Variables	Unit	Constant Influent	Dynamic Influent
1	S_I	g.(COD).m^{-3}	25	27.21
2	S_S	g.(COD).m^{-3}	80	58.15
3	X_I	g.(COD).m^{-3}	40	92.46
4	X_S	g.(COD).m^{-3}	200	363.77
5	X_{BH}	g.(COD).m^{-3}	50	50.66
6	X_{AOB}	g.(COD).m^{-3}	0	0.00
7	X_{NOB}	g.(COD).m^{-3}	0	0.00
8	X_P	g.(COD).m^{-3}	0	0.00
9	S_O	g.(COD).m^{-3}	0	0.00
10	S_{NO2}	g.N.m^{-3}	0	0.00
11	S_{NO3}	g.N.m^{-3}	0	0.00
12	S_{N2}	g.N.m^{-3}	0	0.00
13	S_{NH}	g.N.m^{-3}	30	27.91
14	S_{ND}	g.N.m^{-3}	5	6.66
15	X_{ND}	g.N.m^{-3}	10	19.35
16	SALK	Mole.HCO^{-3}.m^{-3}	7	7.00
	Q_{in}	m^3/d	24000	21590

Table 3.3: Average influent composition for the WRRF simulation model

2.4 Results and Discussion

In wastewater treatment, the management of influent flow is critical to the effective operation of the system. There are two broad types of influent flow patterns: constant influent and dynamic (variable) influent. Constant influent typically reflects stable, controlled flow rates that do not change significantly over time, and is commonly observed in dry weather conditions. In contrast, dynamic influent shows significant variation due to external factors such as industrial discharges or operational changes in the sewer system.

constant influent

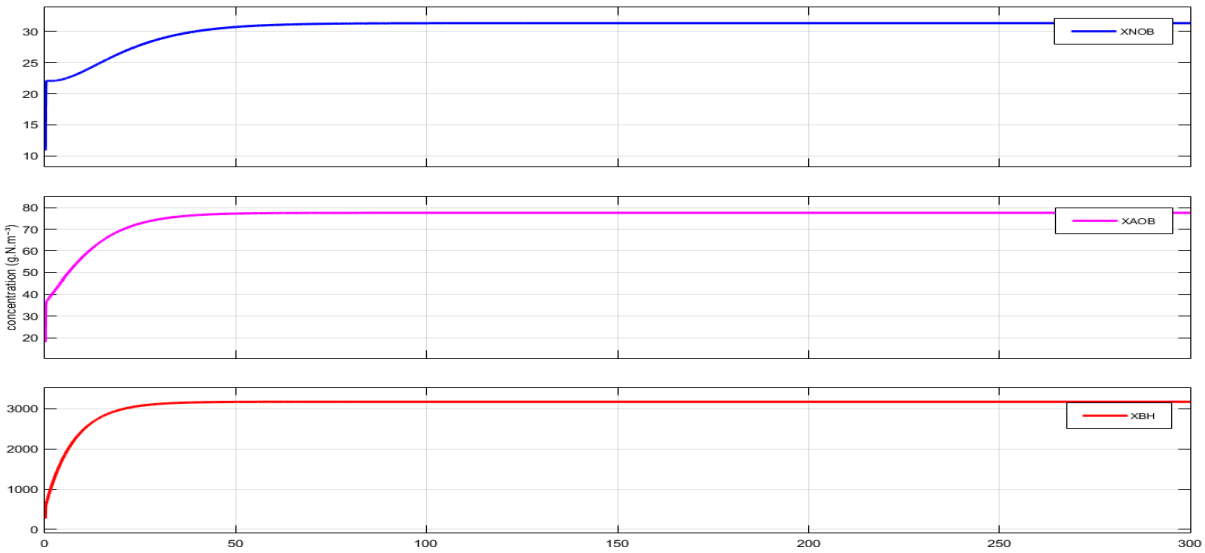

Figure 3.10: The growth of biomass for constant influent.

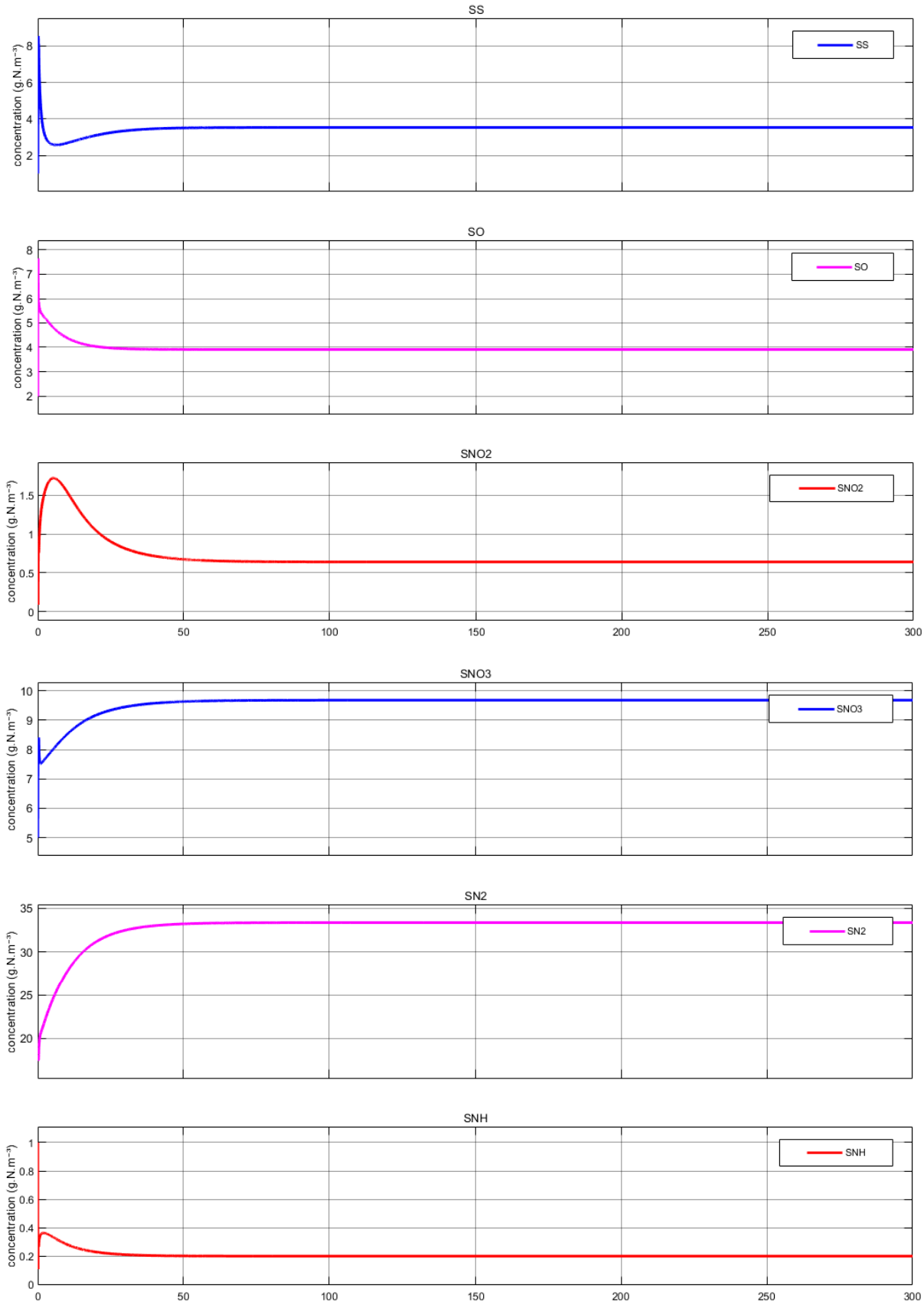

Figure 3.11: observed trends in substrate concentration for constant influent

Remarks Based on Plot of ASM1 Outputs:

- **Ammonia oxidising bacteria (XAOB):**XAOB increased gradually in response to available ammonium (SNH). Due to its slow growth rate, the increase was steady over time, reflecting the ongoing conversion of ammonium to nitrite.
- **Nitrate oxidising bacteria (XNOB):**XNOB followed a similar pattern to XAOB, increasing with the availability of nitrite. As the conversion of nitrite to nitrate progressed, XNOB grew at a slow but steady rate, in line with the behaviour of XAOB
- **Heterotrophic biomass (XBH):**XBH initially increased while sufficient substrate (SS) was available. Over time, as the system reached a steady state and SS was depleted, XBH eventually stabilised, with a slight decrease observed due to the effects of sludge age and biomass decay rates.
- **Soluble Substrate (SS):**The concentration decreases over time as the biomass, mainly heterotrophic bacteria, consume it for growth and energy. In a well-functioning system, this reduction in SS is expected as it is progressively converted to biomass and CO_2.
- **Dissolved Oxygen (SO):** concentrations initially declined sharply, but gradually leveled off and stabilised over time. In the early stages, oxygen was rapidly consumed, probably due to high rates of organic matter decomposition and nitrification. However, as the system approached equilibrium, the oxygen concentration stabilised at around 4 g N.m-^{3}, indicating that oxygen demand and supply were in equilibrium.
- **Nitrite (SNO_2) and nitrate (SNO_3):**

  SNO_2 (nitrite) initially increased when SNH (ammonium) was oxidised by ammonia oxidising bacteria (XAOB). However, the spike was short lived as nitrite was quickly converted to nitrate by nitrate oxidising bacteria (XNAOB).

  SNO_3 (nitrate) levels rose steadily as SNH was progressively converted to nitrate. When denitrification occurred, SNO_3 levels either stabilised or decreased slightly, depending on the effectiveness of the denitrification process.

- **Nitrogen gas (SN_2):** SN_2 increased as denitrification became active, with nitrate and nitrite being reduced to nitrogen gas, which then escaped from the system. In the aerobic zones, however, SN_2 remained low or undetectable.
- **Ammonium (SNH):** SNH decreased steadily over time as nitrification proceeded efficiently. Ammonium was successfully converted to nitrite and then to nitrate by the nitrifying bacteria (XAOB and XNAOB). The steady decrease in SNH indicated that the nitrification process was working effectively.

dry-weather influent

Understanding the difference between Constant inflow and dynamic inflow patterns is important because it directly affects the design, operation and performance of wastewater treatment processes. Constant inflow allows for more predictable treatment processes, while dynamic inflow presents challenges such as the need to adjust treatment operations in real time to accommodate rapid and sometimes extreme changes in flow rates and pollutant loads.

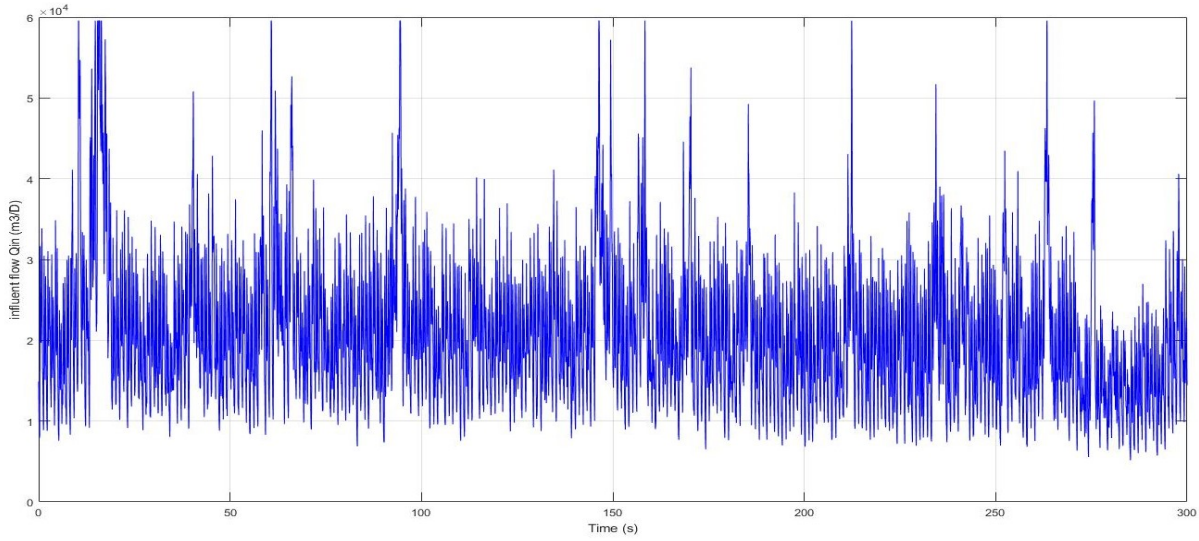

Figure 3.12: Dynamic influent flow (Qin)

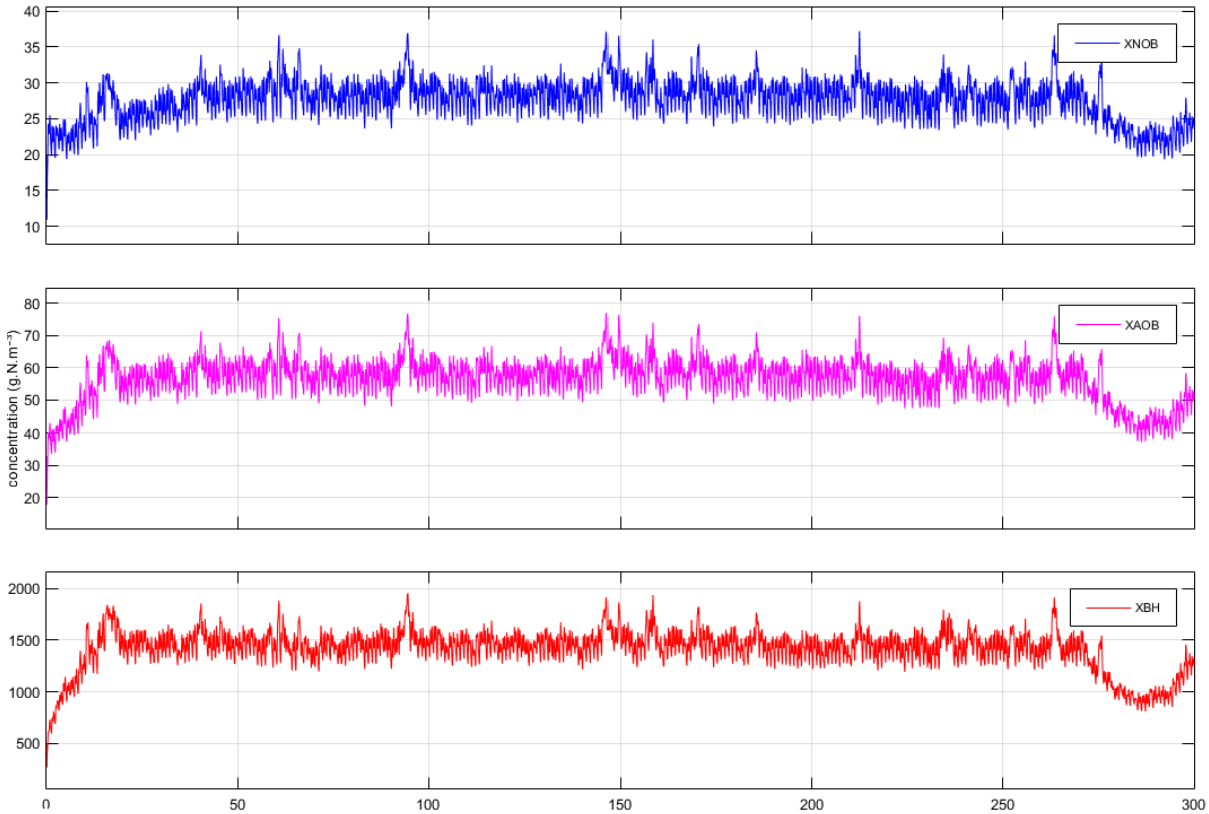

Figure 3.13: The growth of biomass for dry-weather influent

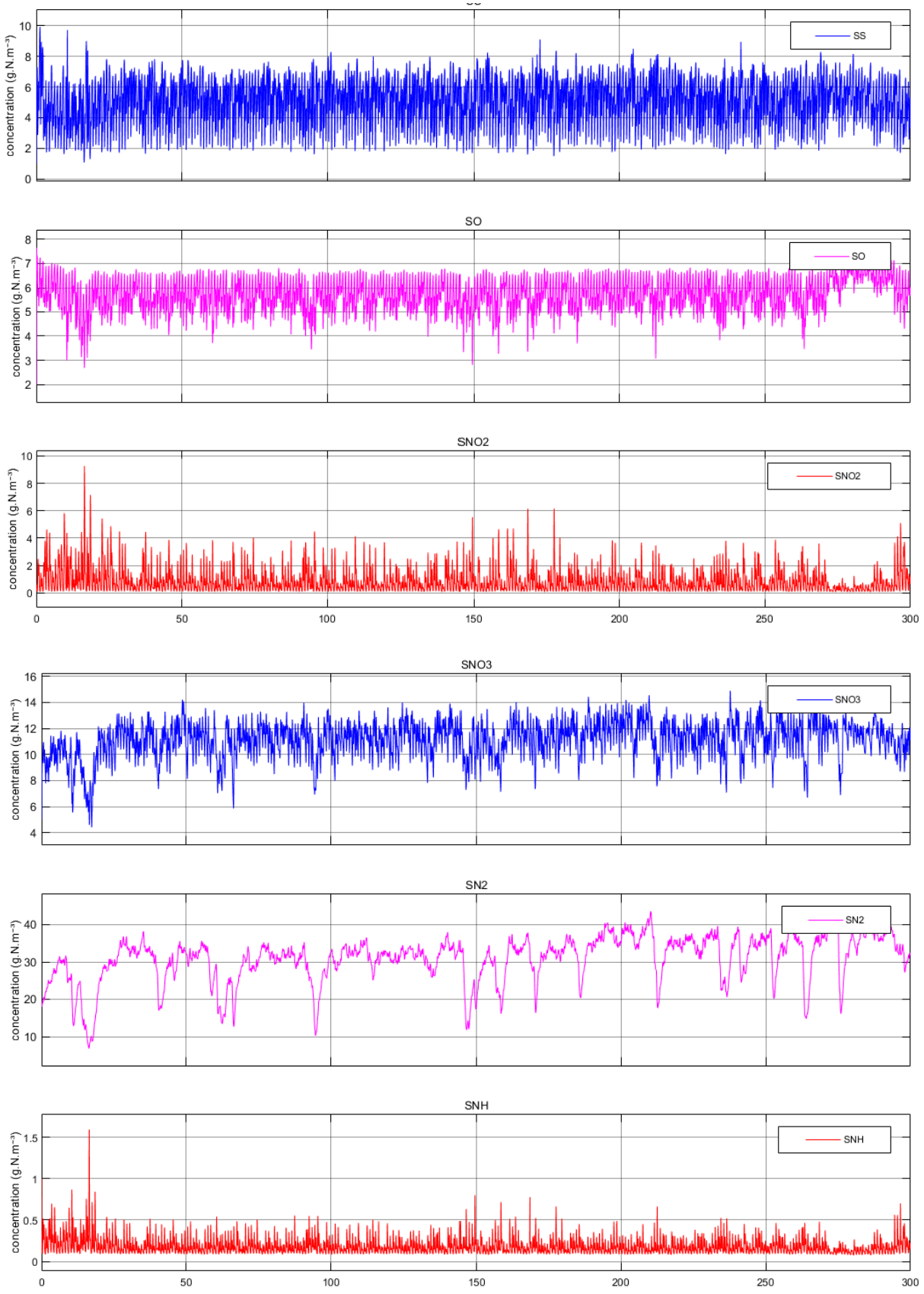

Figure 3.14: observed trends in substrate concentration for dry-weather influent

Remarks Based on Dynamic Inflow:

- **Soluble Substrate (SS):**The concentrations fluctuate significantly over time due to the dynamic nature of the inflow. These fluctuations occur as the availability of substrate rises and falls in response to changes in inflow rate. During periods of increased inflow, the concentration of SS increases as more substrate enters the system. Such fluctuations are to be expected in a dynamic environment, particularly during wet weather conditions when the inflow can vary considerably.

- **Dissolved Oxygen (SO):**The concentration remains relatively stable with only small fluctuations. Under dynamic inflow conditions, oxygen consumption may vary due to changes in biological activity caused by fluctuating substrate availability. Whilst the system will maintain stable oxygen levels through proper aeration, some minor variations can be expected.

- **Nitrite (SNO2):**The concentration peaks intermittently but generally remains low. During periods of high inflow, more ammonia (SNH) is converted to nitrite by ammonia oxidising bacteria (XAOB). However, this nitrite is quickly converted to nitrate, resulting in transient spikes in SNO_2 levels.

- **Nitrate (SNO3):**The concentration remains relatively stable with only small fluctuations. This stability reflects the ongoing nitrification process. Although the dynamic inflow causes some variation in nitrate levels, the system as a whole maintains a constant rate of nitrate accumulation.

- **Nitrogen Gas (SN2):**The concentration of nitrogen gas (SN_2) fluctuates but generally follows a stable trend. This is due to active denitrification, where nitrate is converted to nitrogen gas, causing an increase in SN_2 levels. Dynamic inflows cause some variability in denitrification rates and contribute to the observed variations.

- **Ammonium (SNH):**The concentration spikes at certain points but remains low overall. Dynamic inflow conditions introduce varying amounts of ammonia into the system. However, the nitrification process efficiently converts ammonia to nitrite and nitrate, resulting in generally low steady-state levels, with occasional spikes during inflow surges.

- **Ammonia Oxidizing Bacteria (XAOB) and Nitrate Oxidizing Bacteria (XNOB):**Both ammonia oxidising bacteria (XAOB) and nitrite oxidising bacteria (XNOB) show a steady increase in concentration, with slight fluctuations due to dynamic conditions. These bacteria respond to the availability of their respective substrates - ammonium for XAOB and nitrite for XNOB. Their growth remains steady as they carry out the nitrification process, although variations in the influent cause occasional fluctuations in their growth rates.

- **Heterotrophic Biomass (XBH):**The concentration increases and then stabilises, with occasional fluctuations. These bacteria respond to the availability of organic substrate (SS) and grow during periods of high substrate availability. Their concentration stabilises as the system approaches a quasi-steady state, while fluctuations occur due to the dynamic inflow conditions.

conclusion

In summary, the ASM1-2ND simulation produced reliable and consistent results under both constant and dynamic influent conditions. In the case of constant influent, the system achieved steady state performance with stable concentrations of key variables such as ammonia (SNH), nitrite (SNO_2) and nitrate (SNO_3). The microbial populations, including ammonia-oxidising bacteria (XAOB), nitrite-oxidising bacteria (XNOB) and heterotrophic bacteria (XBH), showed predictable growth trends in line with substrate availability.

Under dynamic influent conditions, the system responded effectively to fluctuations in influent, demonstrating the robustness of the nitrification and denitrification processes. Despite periodic spikes in ammonia and nitrite levels, the overall system remained stable with efficient conversion of ammonia to nitrate and nitrogen gas. This performance highlights the adaptability of the ASM1-2ND model to simulate wastewater treatment processes in different operational scenarios, providing valuable insights for real-world applications.

3 Simulation of the ASM1-2ND/Carbamazépine

Pharmaceuticals are common contaminants in aquatic environments, with carbamazepine and diclofenac being among the most commonly detected. Elimination of these xenobiotic pharmaceuticals, along with other trace chemicals (commonly referred to as micropollutants), in wastewater treatment plants (WWTPs) is often inefficient.As a result, many wastewater treatment plants (WWTPs) will need to be upgraded in the near future to reduce the potential environmental risks posed by their effluent.We have focused our attention on carbamazepine.

3.1 Understanding Carbamazepine and Its Modeling Approaches

Carbamazépine is a pharmaceutical micropollutant commonly found in wastewater. In the activated sludge model (ASM), it is treated as a trace organic compound with potential implications for modelling pollutant removal in wastewater treatment plants (WWTPs). Carbamazépine is persistent and can be difficult to remove by conventional treatment processes, which can affect the effectiveness of wastewater treatment and the quality of the effluent. Its presence and removal are important considerations in advanced wastewater treatment strategies aimed at mitigating environmental risks.

Adding xenobiotic organic micropollutants to an ASM1-based simulation provides valuable insight into how these emerging contaminants interact with biological treatment processes. It allows WWTP operations to be optimised, removal efficiencies and microbial community impacts to be assessed, and advanced treatment solutions to be designed, all in line with regulatory requirements. This second simulation step is essential for modernising WWTPs to meet the growing challenge of micropollutants in wastewater systems.

Using the article An activated sludge modeling framework for xenobiotic trace chemicals (ASM-X): Assessment of diclofenac and carbamazepine by Plósz et al. (2012) We were able to obtain the Gujer matrix associated with carbamazepine. This provided us with a description of this molecule in wastewater treatment plant sludge(table 3.4).And Table 3.5 explains the significance of each variable from Table 3.4.

Component → i	1 C_{LI}	2 C_{CJ}	3 C_{SL}	4 $C_{SL,I}$	**Process rate**
j Process ↓					
De-sorption	1		−1		$k_{\text{Des}} C_{SL}$
Aerobic processes					
Sorption	−1		1		$k_{\text{Des}} K_{\text{D,Ox}} C_{LI} \frac{S_O}{K_O+S_O} X_{SS}$
Parent compound retransformation	1	−1			$k_{\text{Dec,Ox}} f(S_S) \times C_{CJ} \frac{S_O}{K_O+S_O} X_{SS}$
Biotransformation	−1				$[q_{\text{C,Ox}} f(S_S) + k_{\text{Bio,Ox}}] C_{LI} \frac{S_O}{K_O+S_O} X_{SS}$
Anoxic processes					
Sorption	−1		1		$k_{\text{Des}} K_{\text{D,Ax}} C_{LI} \frac{K_O}{K_O+S_O} X_{SS}$
Parent compound retransformation	1	−1			$k_{\text{Dec,Ax}} f(S_S) C_{CJ} \frac{K_O}{K_O+S_O} X_{SS}$
Biotransformation	−1				$[q_{\text{C,Ax}} f(S_S) + k_{\text{Bio,Ax}}] C_{LI} \frac{K_O}{K_O+S_O} X_{SS}$

Table 3.4: Stoichiometric matrix for the ASM for xenobiotic organic micropollutants.

Component	**Description**
C_{LI}	Sorption: Pollutant in sorbed phase (attached to sludge).
C_{CJ}	Aqueous Phase: Pollutant in dissolved phase (free in water).
C_{SL}	Sorption: Substrate (organic matter or biomass) that sorbs micropollutants.
$C_{SL,I}$	Sorption Interface: Represents the interface between the sorbed pollutant and the substrate or sludge.

Table 3.5: Description of components involved in the activated sludge model for micropollutants.

Since we have the stoichiometric matrix for the ASM of xenobiotic organic micropollutants, we need to add it to the stoichiometric matrix table of the ASM1-2ND model, as shown in Figure 3.16.

In this simulation we use the same platform design but with three additional variables. The good thing is that the previous processes remain unchanged, so we only need to add the new processes - from 7 to 18 processes and from 16 reactions to 19. It's important to note that the mass balance remains the same for all the tanks. However, we must consider that in the membrane reactor two variables, Cli and Ccj, are treated as soluble due to their physical form, so they follow equation (2.9). As Csl is in solid form, it follows equation (2.10).

In the simulation view(figure 3.15 we see that three more entries have been added due to the three new variables, which also required three new initial conditions to be added to the init file.Of course, we have also updated the necessary blocks as well, such as making changes to the flux adders and selectors, along with other adjustments.

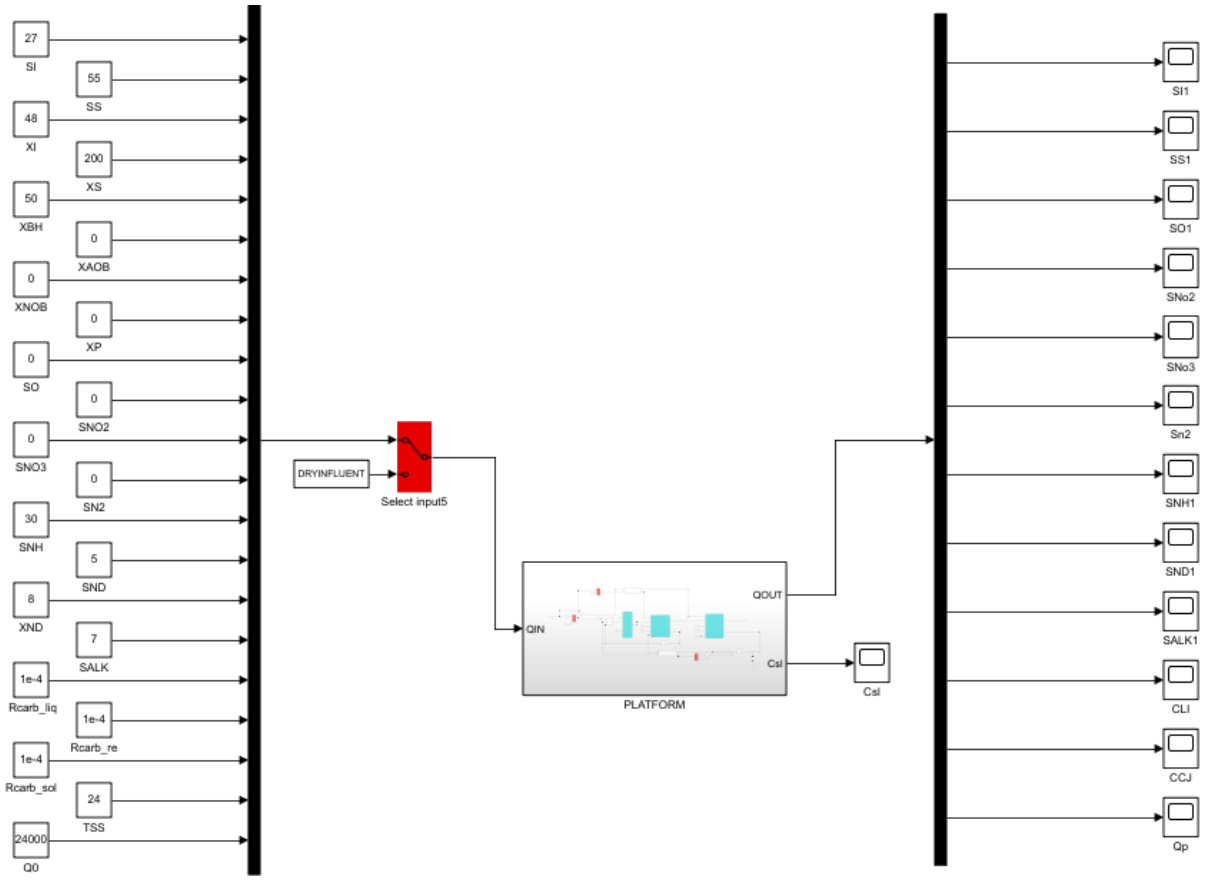

Figure 3.15: simulink platfrom overview Carbamazepine

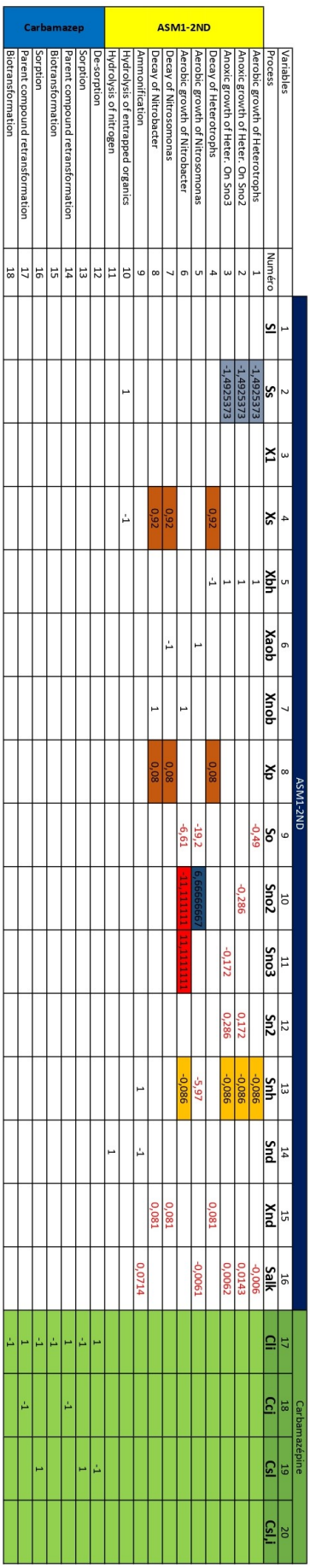

		ASM1-2ND																Carbamazépine			
	Variables																				
	Process																				
	Numéro	1	2	3	4	5	6	7	8	9	10	11	12	13	14	15	16	17	18	19	20
ASM1-2ND	Aerobic growth of Heterotrophs	Sl	Ss	X1	Xs	Xbh	Xaob	Xnob	Xp	So	Sno2	Sno3	Sn2	Snh	Snd	Xnd	Salk	Cli	Cci	Csl	Csl.i
	1		-1,4925373			1				-0,49				-0,086			-0,006				
	Anoxic growth of Heter. On Sno2		-1,4925373			1					-0,286		0,172	-0,086			0,0143				
	2		-1,4925373			1						-0,172	0,286	-0,086		0,081	0,0062				
	Anoxic growth of Heter. On Sno3				0,92	-1			0,08		6,6666667			-5,97			-0,0061				
	3						1			-19,2											
	Decay of Heterotrophs									-6,61	-11,111111	11,111111		-0,086		0,081					
	4				-0,92			1	-0,68												
	Aerobic growth of Nitrosomonas						-1								-1	0,081					
	5				-0,92				-0,08					1			0,0714				
	Aerobic growth of Nitrobacter							1							1			1		-1	
	6																	-1		1	
	Decay of Nitrosomonas																	1	-1		
	7																	-1	1		
	Decay of Nitrobacter																	1	-1		
	8																	-1	1		
	Ammonification																				
	9																				
	Hydrolysis of entrapped organics		1		-1																
	10																				
	Hydrolysis of nitrogen																				
	11																				
	De-sorption																				
	12																				
	Sorption																				
	13																				
	Parent compound retransformation																				
	14																				
Carbamazep	Biotransformation																				
	15																				
	Sorption																				
	16																				
	Parent compound retransformation																				
	17																				
	Biotransformation																				
	18																				

Figure 3.16: Matrice de Gujer ASM1-2ND + Carbamazep

3.2 Results and Discussion

Always keeping the first configuration in mind, we noticed that adding carbamazepine didn't affect the other results. This is logical, because in the equations, these three new variables don't add any new terms to the original 16. Therefore, we have introduced only the three new variables

3.2.1 constant influent

Liquid-Phase Carbonates:

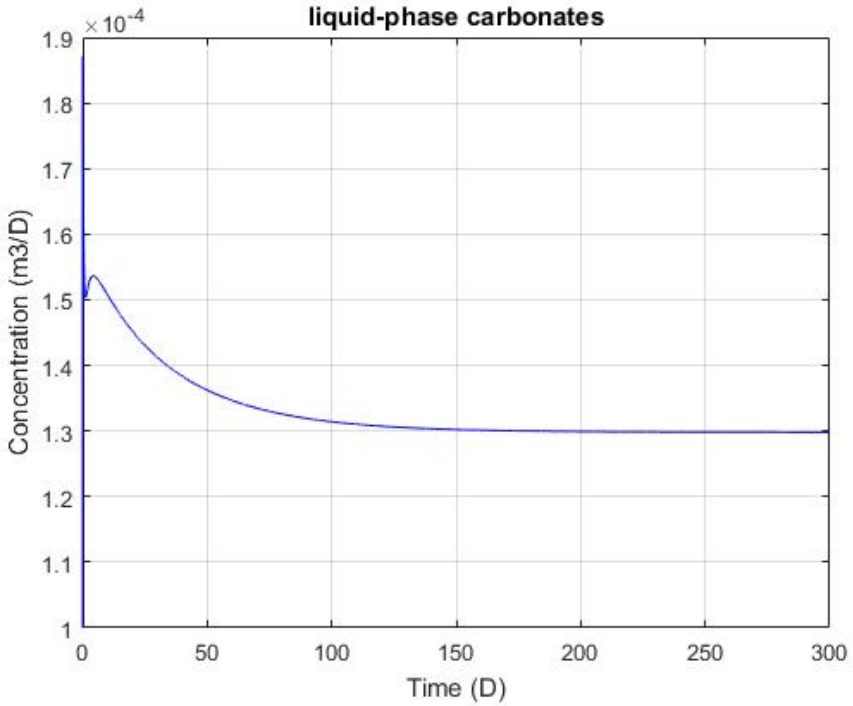

Figure 3.17: Liquid-Phase Carbonates

- In the early phase of the simulation, the concentration of liquid phase carbonates increases to approximately 1.55×10^{-4} m³/D within the first 10 days, reflecting the adaptation period during which crabzipamine begins to interact with the components of the system, particularly the carbonates. This initial increase is attributed to rapid reactions such as sorption to biomass and other solids, as well as potential dissolution processes affecting carbonate dynamics in the liquid phase. Following this initial increase, the concentration of liquid phase carbonates gradually decreases and stabilises at around 1.3×10^{-4} m³/D by day 100. This stabilisation means that the system has reached an equilibrium where sorption, desorption and biotransformation processes are balanced, resulting in a stable concentration with no significant changes thereafter.

- The transient increase in liquid phase carbonates indicates active early stage reactions between crabzipamine and carbonates. This increase is likely due to sorption of crabzipamine onto biomass or other suspended solids, as governed by reactions such as 'proc12' and 'proc15'. In addition, interactions leading to the reformation or retransformation of carbonates, as described by 'proc13' and 'proc16', also contribute to this increase. The subsequent stabilisation phase suggests that the system undergoes a period of adjustment before reaching equilibrium.

- The main biochemical processes involved are :

  Sorption and desorption: Early sorption of crabzipamine onto the biomass drives the initial increase in liquid phase carbonates, while desorption (e.g. ‘proc18‘) and retransformation processes (e.g. ‘proc16‘) gradually reduce these carbonates, leading to stabilisation.

  Biotransformation: The biotransformation of crabzipamine (e.g. processes ‘proc14‘ and ‘proc17‘) converts or consumes liquid phase carbonates into other forms such as reactive or solid phase carbonates, contributing to the equilibrium of the system.

  The rate constants for sorption, desorption and biotransformation (e.g. ‘K_Des‘, ‘K_Dox‘, ‘K_bioOx‘) are crucial in determining the rate and extent of these reactions and thus influence the stabilisation time scale.

Reactive and Solid-Phase Carbonates:

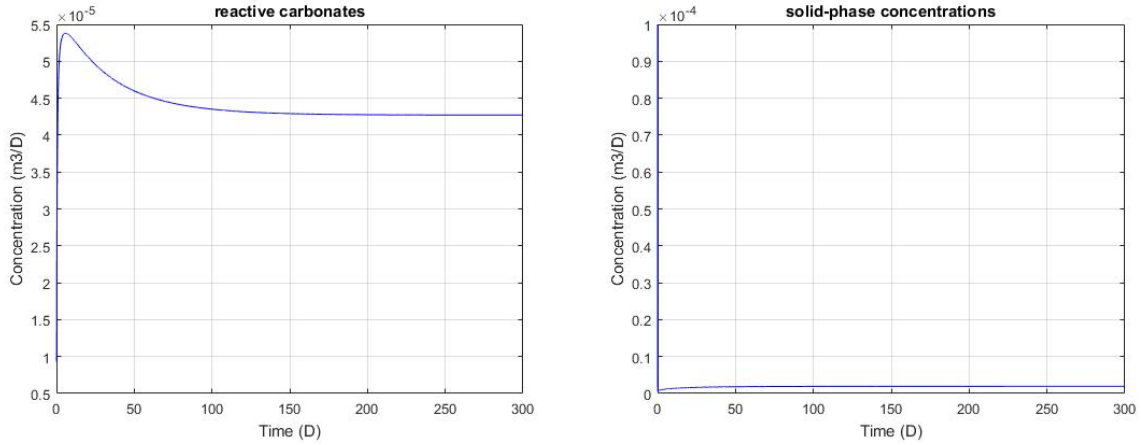

Figure 3.18: Reactive and Solid-Phase Carbonates:

It is important to consider the interactions of liquid phase carbonates with reactive carbamazepine (Ccj) and solid phase carbamazepine (Csl). Processes such as retransformation (proc16) and biotransformation (proc17) indicate that carbamazepine also affects these phases.Specifically:

- **Reactive Carbonates:** Over time, reactive carbonates decrease due to biotransformation and retransformation processes. These processes convert crabzipamine and carbonates into more stable forms, thereby reducing the concentration of reactive carbonates.

- **Solid-Phase Carbonates:** There may be a slight increase in solid-phase carbonates as liquid-phase carbonates transition into solid forms through desorption processes (‘proc18‘). This transition contributes to the observed dynamics in solid-phase concentrations.

In summary, the interplay between these carbonate phases is influenced by the presence of crabzipamine, affecting their concentrations and transformation over time.

3.2.2 Dynamic influent

Liquid-Phase Carbonates (Dynamic Input)

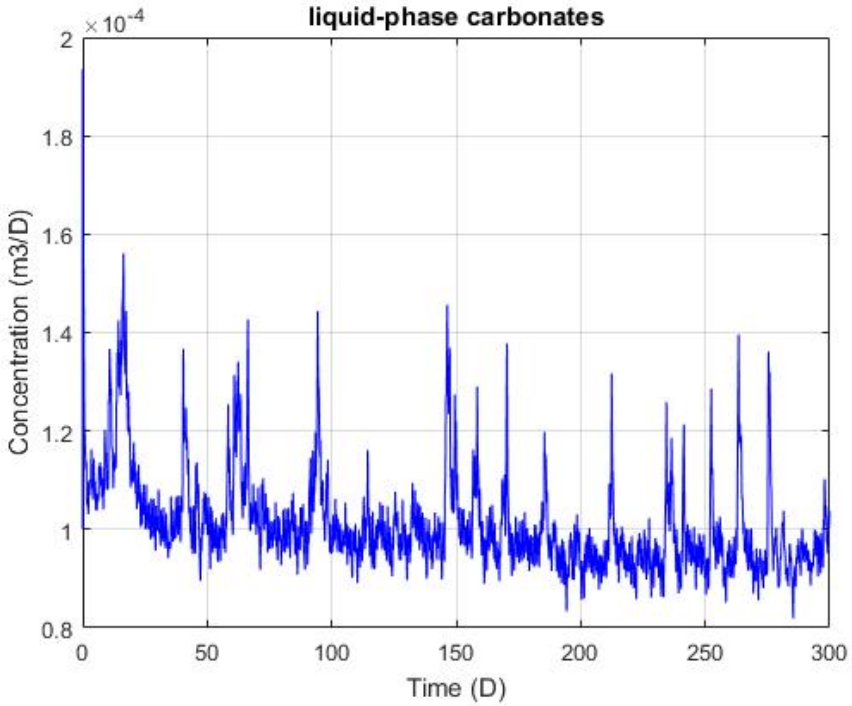

Figure 3.19: Liquid-Phase Carbonates Dynamic input

In the figure (3.19) representing liquid phase carbamazepine under dynamic input conditions, the most striking feature is the presence of significant fluctuations throughout the simulation. The concentration fluctuates between a lower limit of about $0.8 \times 10^{-4}\,m^3/D$ and an upper bound of about $1.5 \times 10^{-4}\,m^3/D$, with no clear stabilisation. This suggests that the system is continuously responding to changing inputs, with carbamazepine driving dynamic processes such as sorption, desorption and biotransformation in the liquid phase.

In contrast to a steady-state scenario, the absence of a stabilisation phase indicates that the liquid-phase carbamazepine is highly sensitive to the dynamic changes in the system. Each fluctuation corresponds to new interactions, likely triggered by periodic changes in input levels or other external factors that keep the system from reaching equilibrium.

Reactive Carbonates (Dynamic Input)

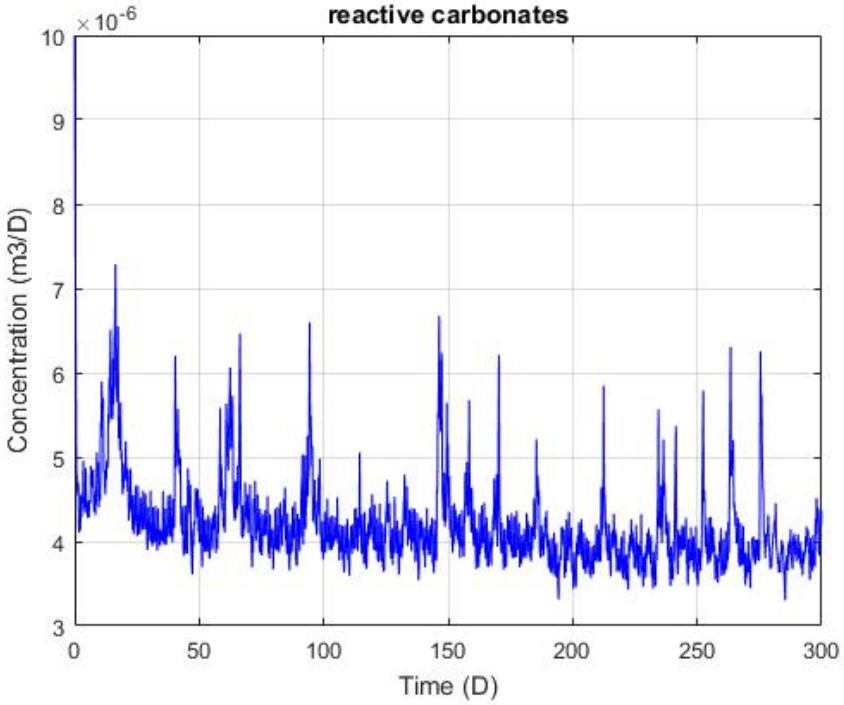

Figure 3.20: Reactive Carbonates Dynamic input

The reactive carbamazepine curve (figure 3.20) also shows fluctuations, although the concentration is much lower than that of liquid phase carbamazepine, ranging from 3×10^{-6} m^3/D and 7×10^{-6} m^3/D. The oscillatory pattern suggests that reactive carbamazepine is continuously formed and consumed, probably as intermediates in reactions involving carbamazepine.

The smaller magnitude of the fluctuations compared to liquid phase carbamazepine suggests that reactive carbamazepine is less sensitive to dynamic changes. However, it still plays a critical role as an intermediate in processes such as biotransformation (e.g. `proc17`), retransformation and possibly sorption/desorption cycles. The periodic rises and falls in concentration are indicative of continuous reformation and retransformation processes driven by dynamic input conditions.

Solid-Phase Carbonates (Dynamic Input)

The solid phase carbamazepine plot(figure 3.21) shows much smaller fluctuations in concentration, remaining consistently around the 1×10^{-5} m^3/D mark. The minimal changes in solid phase concentrations suggest that although some of the liquid phase carbamazepine is transferred to the solid phase (by sorption processes such as `proc18`), the extent of this transfer is limited.

Solid-phase carbamazepine is likely to be a more stable endpoint in the system. Its relatively small fluctuations compared to the liquid and reactive phases suggest that solid-phase carbamazepine is less affected by dynamic inputs. This form of carbamazepine is likely to accumulate slowly over time as liquid phase and reactive carbamazepine are converted to more stable solid forms. The small peaks may correspond to periodic peaks in sorption, but overall solid-phase carbamazepine remains largely stable despite dynamic input conditions.

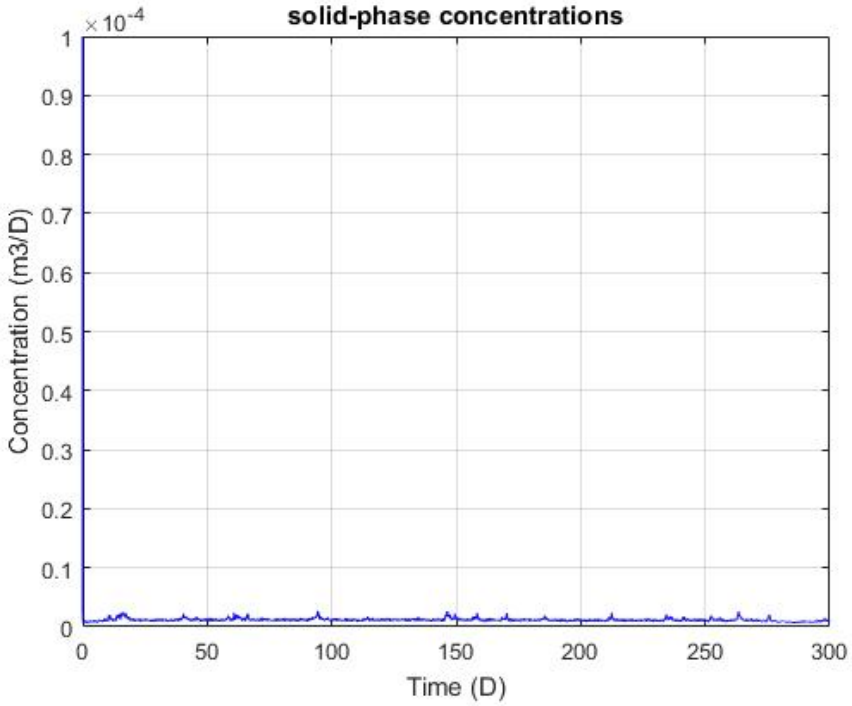

Figure 3.21: Solid-Phase Carbonates Dynamic input

Important note about the two simulations we have discussed: If you use transport delay with constant inputs, it can cause small oscillations in the results. Therefore, it's generally better to use unit delay. Although this approach takes longer to calculate, it produces smoother results. However, when dealing with dynamic inputs or more complex simulations (such as SNO3 control), we can use transport delay for faster simulations without significantly affecting the results.

In summary, the simulation of carbamazepine in wastewater treatment plants provides valuable insights into the behaviour of persistent pharmaceutical micropollutants. By integrating the ASM-X model with ASM1-2ND, the researchers were able to follow the distribution of carbamazepine in the liquid, reactive and solid phases under both constant and dynamic influent conditions. The results show that carbamazepine undergoes complex interactions involving sorption, desorption, biotransformation and retransformation processes. While carbamazepine in the liquid phase shows significant sensitivity to dynamic inputs, carbamazepine in the solid phase remains relatively stable. This modelling approach provides a useful tool for optimising treatment processes and designing advanced solutions to address the growing challenge of micropollutants in wastewater systems, ultimately contributing to improved environmental protection.

4 Coupling the ASM1-2ND simulation with a membrane fouling model

The anaerobic membrane bioreactor (AnMBR) is an innovative wastewater treatment technology that combines anaerobic digestion, which breaks down organic pollutants, with a physical separation process between sludge and liquid, resulting in enhanced purification of the treated effluent Benyahia et al. (2024).

One of the major challenges limiting the wider use of membrane technology is the inevitable decline in performance over time. This is due to membrane fouling, where particles and compounds block the tiny pores in the membrane. As a result, less filtered water or liquid passes through, making the process harder to manage. Preventing fouling is key to improving and expanding the use of membrane technologies.

Permeate flux and transmembrane pressure (TMP) are the best indicators of membrane fouling. Fouling increases resistance, which either reduces the flow of filtered liquid (permeate flux) or raises the pressure needed to maintain flow (TMP). In systems where flow is maintained by increasing TMP, more energy is required, leading to higher costs. Over time, membrane fouling becomes harder to reverse with backwashing alone, and with repeated filtration cycles, fouling becomes more permanent. Chemical cleaning is often necessary to restore performance, but it adds costs and can shorten the membrane's lifespan due to repeated chemical exposure Abdelrasoul et al. (2013).

Fouling can generally be classified as backwashable or non-backwashable, and reversible or irreversible, depending on how strongly particles attach to the membrane surface. Backwashable fouling can be removed by reversing the liquid flow through the membrane at the end of each filtration cycle. Non-backwashable fouling, however, cannot be removed by normal backwashing but can be addressed through chemical cleaning. Irreversible fouling cannot be removed by any means, including backwashing, flushing, or chemical cleaning, and the membrane cannot be restored to its original flow capacity.

Several models have been developed to better understand membrane fouling, such as the resistance-in-series model, which incorporates the kinetics of soluble microbial products (SMP) and extracellular polymeric substances (EPS). Other approaches include data-driven fouling control methods, machine learning techniques, and models based on fractal geometry and sectional approaches to describe fouling cake permeability. Simple models focus on cake formation and pore plugging, while newer models integrate biological dynamics. Advances in computer science have also introduced alternatives like artificial neural networks, which are used to predict fouling in membrane bioreactors and help extend membrane life through intelligent control systems.

In the simulation, the aim was to build on the study of our supervisor, as presented in his article Benyahia et al. (2024), which attempts to describe the dynamics of the entire MBR process by coupling biological process dynamics with membrane fouling models. In this study, the AM2b model, which has been proposed specifically for control purposes, was used. This simple model describes only the two main biological processes of anaerobic digestion, while including SMP dynamics. Our aim was to achieve a similar integration with the ASM1 2ND model.

4.1 Fouling Mechanisms and Membrane Dynamics Model

The simplified model uses feedback to adjust the output flow rate (Q_{out}) based on the mass of solids attached to the membrane and solute deposited in the pores.

4.1.1 Fouling Mechanisms

Fouling mechanisms vary, but this model focuses on two main types:

- **Cake Formation (Surface Fouling figure:** Solids attach to the membrane surface, decreasing the effective filtration area ($m_c(t)$) as shown in figure 3.22 (a).
- **Pore Constriction (Pore Fouling):** Solutes, smaller than the pore sizes, clog the membrane pores, reducing the porous area ($m_p(t)$) as shown in figure 3.22 (b).

This model simplifies the complexity of fouling mechanisms by separating the effects of surface fouling and pore fouling.

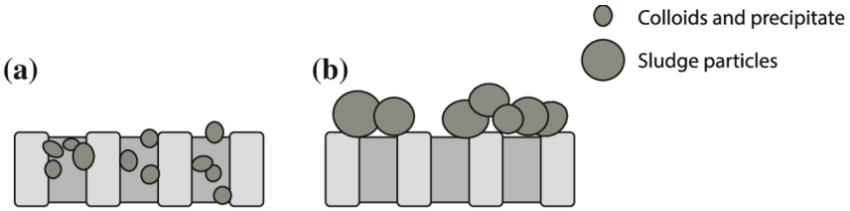

Figure 3.22: Membrane fouling by cake formation and pores clogging

4.1.2 Model Equation

Models of Permeate flux and membrane resistance
Using a resistance-in-series approach based on Darcy's Law, the membrane fouling model for constant transmembrane pressure (TMP) is expressed as 3.12:

$$J(t) = \frac{Q_{\text{out}}(t)}{A(t)} = \frac{\Delta P}{\mu(R_m + R_f)} \tag{3.12}$$

where:

- $J(t)$ = Membrane flux at time t
- $Q_{\text{out}}(t)$ = Output flow rate at time t
- $A(t)$ = Membrane area at time t
- ΔP = Transmembrane pressure
- μ = Viscosity of the fluid
- R_0 = Clean membrane resistance
- $R(t)$ = Fouling resistance includes contributions from cake formation ($R_c(t)$) and pore constriction ($R_p(t)$) given by 3.13

$$R(t) = R_c(t) + R_p(t) \tag{3.13}$$

where $R(t)$ and $R_p(t)$ are typically dependent on the masses $m_c(t)$ and $m_p(t)$, respectively. Both $R_c(t)$ and $R_p(t)$ are modeled by equations 3.14 and 3.15:

$$R_c(t) = \alpha_c \, m_c(t) \, A(t), \tag{3.14}$$

$$R_p(t) = \alpha'_p \, m_p(t) \, \epsilon \, A(t), \tag{3.15}$$

where α_c and α'_p are the specific resistances, and ϵA (with $0 < \epsilon < 1$) is the porous area, which is a fraction of the total useful surface area A. See Figure 3.23 for an example with a flat sheet membrane.

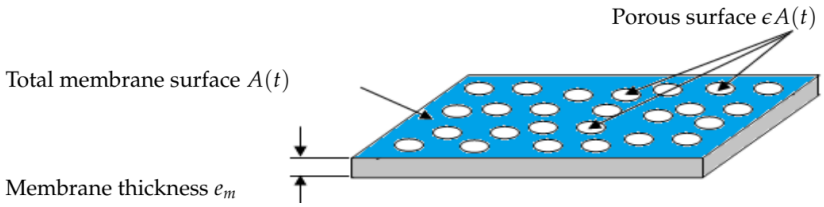

Figure 3.23: Schematic representation of the total membrane surface A
Benyahia et al. (2024)

Models of membrane area

In contrast to many fouling modelling studies, it is proposed that the total filtration membrane surface area, $A(t)$, varies over the course of a filtration period and between multiple filtration and cleaning cycles. It is described in a general way by Equation 3.16 (Benyahia et al. (2024)) as a decreasing function of $m_c(t)$ and $m_p(t)$:

$$A = \frac{A_0}{1 + \frac{m_c}{\sigma} + \frac{m_p}{\sigma'}} \tag{3.16}$$

The initial membrane area, A_0, is modelled together with the parameters σ and σ', which take into account the influence of m_c and m_p on surface reduction. This model assumes that the total filtration area is divided into a filter area and a porous area. As $m_p(t)$ increases, the porous surface is reduced, contributing to the overall loss of $A(t)$, even if cake fouling remains minimal. Similarly, an increase in $m_c(t)$ reduces the filter surface area, as attached particles can obstruct the flow, even though the pore-clogging fouling is stable or insignificant.

In summary, the membrane surface $A(t)$ decreases when $m_c(t)$ and/or $m_p(t)$ increase, mathematically tending to zero as $m_c(t)$ and/or $m_p(t)$ approach infinity.

Models of attached solids on the membrane surface and blocked into pores

Both compounds, $m_c(t)$ and $m_p(t)$, show distinct dynamics, with their concentrations increasing during the filtration phase and decreasing during the relaxation or backwash phase. An important difference was observed when comparing the ASM1 2ND and AM2b models: the absence of SMPs (soluble microbial products) in our model. Consequently, it is assumed that all soluble components are represented by

$$S_T = \sum S_i \quad (i = 1, 2, \dots)$$

and all particulate components are represented by:

$$X_T = \sum X_i \quad (i = 1, 2, \dots)$$

As a result, these dynamics can be represented using Equation 3.17 instead of Equation 3.18 from Benyahia et al. (2024).

$$\dot{m_c} = Q_{out}(C_S S_T + C_X X_T) \tag{3.17}$$

$$\dot{m_c} = Q_{out}(C_S S_T + C_X X_T + C_{SMP} SMP) \tag{3.18}$$

C_S and C_X are weighting parameters used to represent the contribution and rate of each variable in the cake formation process.

The membrane effectively rejects particulate matter, such as biomass, and large soluble compounds because their size exceeds the pore diameter. In contrast, smaller soluble compounds are able to pass through the membrane. A dynamic model (6) is proposed to describe the pore clogging caused by $m_p(t)$:

$$\dot{m}_p = Q_{out}\,(\beta_2\, S_T)\,, \tag{3.19}$$

Note: SMP-related terms have been removed, so this model replaces Equation 3.20 from the original reference, where β_2 is used to model the contribution of solute substrates to the pores clogging..

$$\dot{m}_p = Q_{out}\,(\beta_1\, S_{\mathrm{MP}} + \beta_2\, S_T)\,, \tag{3.20}$$

Additional Hypothesis: Following the same hypothesis from the article, there is no biomass growth on the membrane surface, detached solids do not impact bulk liquid concentration, and both fouling mechanisms are partially irreversible, with pore clogging being more irreversible than cake formation.

4.1.3 Fouling Models for Filtration and Backwashing Phases

This section explores the fouling model during the filtration phase, focusing on cake formation and pore constriction, and introduces the model for the backwashing phase to assess cleaning effectiveness and membrane recovery, as our simulation will concentrate on these two distinct fouling models.

- **Fouling Model for the Filtration Phase:**Based on the previous equations and hypotheses, the complete fouling model for the filtration phase ($\Delta P > 0$) is described by Equations (3.21)–(3.25). The output flow rate Q_{out} decreases over time, requiring membrane cleaning after a significant reduction in permeate flux.

$$\dot{m}_c = Q_{\text{out}}(C_s S_T + C_x X_T) \tag{3.21}$$

$$\dot{m}_p = Q_{\text{out}}\,(\beta_2 S_T) \tag{3.22}$$

$$R = \alpha_c m_c A + \alpha'_p m_p \epsilon A \tag{3.23}$$

$$A = \frac{A_0}{1 + \frac{m_c}{\sigma} + \frac{m_p}{\sigma'}} \tag{3.24}$$

$$Q_{\text{out}} = J \cdot A = \frac{\Delta P \cdot A}{\mu(R_0 + R)} \tag{3.25}$$

- **Fouling Model for the Backwashing Phase:**To clean the membrane by backwashing, the feed to the MBR is stopped and the transmembrane pressure is reversed ($\Delta P < 0$). This reversal causes the permeate flow to move back into the feed, effectively lifting the fouling layer from the pores and surface of the membrane. In some cases, MBR systems implement a relaxation period as an alternative to backwashing, during which the flow is

simply stopped for a short period of time ($\Delta P = 0$), allowing the natural removal of matter and particles. This process can be modelled using equations (3.26) and (3.27), where ω and ω' are positive constants calibrated on the basis of experimental data, and $m_{\mathrm{c,\,irr}}$ and $m_{\mathrm{p,\,irr}}$ are the amounts of irreversible fouling after cleaning.

$$\dot{m}_c = -\omega m_c + m_{\mathrm{c,\,irr}} \tag{3.26}$$

$$\dot{m}_p = -\omega' m_p + m_{\mathrm{p,\,irr}} \tag{3.27}$$

4.2 Implementation in MATLAB for a Single Membrane Bioreactor (MBR)

4.2.1 Introducion

In this simulation we only consider the third reactor of our platform, since it has the membrane model we used. Previously we considered it as an ideal separation without considering the fouling phenomenon, but now we try to integrate the ASM1 model with the fouling. The simulation is shown in Figure 3.24, where you can see a new block, which is a pulse generator linked to a switch that allows us to switch from -1 to 1. We also have a manual switch that switches from the alternation of -1 and 1 to 0. We chose this mechanism to make it easy to switch between the different modes. The manual switch allows us to switch from filtration/backwash to simple filtration without membrane fouling, and the other switch allows us to switch between filtration and backwash, taking into account the fouling phenomena. The pulse generator gives us the ability to generate the command signal to make the switch. In Figure 3.25 we can see the period; for example, we're doing 1/2, which means that every 30 minutes we switch to backwashing, which takes 4.5 minutes (controlled by pulse width (% of period)).

That was the view from Simulink. In the code part, we have made many changes. The first change is that now we have three different cases based on the entries of the command, and those cases are:

coupled model for the filtration phase(when Command = 1):

Input Variables

- Q_{in}: Inflow rate
- Q_w: Waste flow rate
- K_{LA}: Oxygen transfer coefficient
- Command: Control signal (1 for filtration -1 for back-washing)

Membrane Fouling and Flux

$$A = \frac{A_0}{1 + (M_C/\gamma_1) + (M_P/\gamma_2)} \tag{3.28}$$

$$R = \alpha_1 \cdot (M_C/A) + \alpha_2 \cdot (M_P/A \cdot \varepsilon) \tag{3.29}$$

$$J = \frac{P}{\mu \cdot (R_0 + R)} \tag{3.30}$$

$$Q_{out} = J \cdot A \tag{3.31}$$

Mass Balance Equation

$$Q_{in} = Q_w + Q_{out} \tag{3.32}$$

General Differential Equation for Components:

$$\frac{dS_i}{dt} = \frac{1}{V}\left(Q_{\text{in}} \cdot S_{i,\text{in}} - Q_{\text{out}} \cdot S_i - Q_w \cdot S_i - (S_i \cdot C_s \cdot Q_{\text{out}})\right) + r_i \tag{3.33}$$

with $i = [1, 2, 10, 11, 12, 13, 14, 16]$.

$$\frac{dX_i}{dt} = \frac{1}{V}\left(Q_{\text{in}} \cdot X_{i,\text{in}} - Q_w \cdot X_i - (X_i \cdot C_x \cdot Q_{\text{out}})\right) + r_i \tag{3.34}$$

with $i = [3, 4, 5, 6, 7, 8, 15]$.
Where:

- S_i: Substrate concentration of component i
- X_i: Biomass concentration of component i
- V: Reactor volume
- $S_{i,\text{in}}$: Input substrate concentration of component i
- $X_{i,\text{in}}$: Input biomass concentration of component i
- r_i: Reaction rate for component i
- C_s: fraction of S_T attached onto the membrane
- C_x: fraction of X_T attached onto the membrane

Oxygen Dynamics

$$\frac{dS_O}{dt} = \frac{1}{V} \cdot (Q_{in} \cdot S_{O,in} - Q_{out} \cdot S_O - Q_w \cdot S_O - (S_i \cdot C_s \cdot Q_{\text{out}})) + r_9 + K_{LA} \cdot (S_{O,sat} - S_O) \tag{3.35}$$

Fouling Dynamics

$$\frac{dM_C}{dt} = Q_{out} \cdot (C_s \cdot \sum S_i + C_x \cdot \sum X_i) \quad \text{(Cake layer formation)} \tag{3.36}$$

$$\frac{dM_P}{dt} = Q_{out} \cdot \beta \cdot \sum S_i \quad \text{(Pore blocking)} \tag{3.37}$$

Simplified Backwash Phase Model (when Command $= -1$)

Flux and Outflow

$$J = \frac{P}{\mu \cdot (R_0 + R)} \tag{3.38}$$

$$Q_{out} = J \cdot A \tag{3.39}$$

$$Q_{in} = 0 \tag{3.40}$$

Resistance

$$R = \alpha_1 \cdot (M_C/A) + \alpha_2 \cdot (M_P/A \cdot \varepsilon) \tag{3.41}$$

General Component Equation For each component i:

$$\frac{dS_i}{dt} = \frac{1}{V} \cdot (-S_i \cdot Q_w) + react_i + S_i \cdot C_{sp} \tag{3.42}$$

and

$$\frac{dX_i}{dt} = \frac{1}{V} \cdot (-X_i \cdot Q_w) + react_i + X_i \cdot C_{xp} \tag{3.43}$$

Where C_{sp} is fraction of S_i reinjected into the bulk during cleaning operation and C_{xp} fraction of X_i reinjected into the bulk during cleaning operation.

Oxygen Dynamics

$$\frac{dSo}{dt} = \frac{1}{V} \cdot (-So \cdot Q_w) + react_9 + K_{LA} \cdot (SOSAT1 - So) + (So \cdot C_{sp}) \tag{3.44}$$

Fouling Dynamics

$$\frac{dMC}{dt} = -W \cdot MC \tag{3.45}$$

$$\frac{dMP}{dt} = -W \cdot MP \tag{3.46}$$

Where:

- P: Transmembrane pressure
- μ: Dynamic viscosity
- R_0: Intrinsic membrane resistance
- A: Membrane area
- M_C: Mass of cake layer
- M_P: Mass of pore blocking
- ε: Membrane porosity
- W: detachment rate during relaxation phase

Simplified Relaxation Phase Model (when Command = 0)

Outflow

$$Q_{out} = Q_{in} - Q_w \tag{3.47}$$

General Component Equation For each component i:

$$\frac{dx_i}{dt} = \frac{1}{V} \cdot (Q_{in} \cdot C_{i,in} - C_i \cdot Q_w) - \delta_i \cdot C_i \cdot Q_{out} + react_i \tag{3.48}$$

Where:

- $\delta_i = 1$ for soluble components and $\delta_i = 0$ for particulate components
- $C_{i,in}$ is the influent concentration of component i

Oxygen Dynamics

$$\frac{dSo}{dt} = \frac{1}{V} \cdot (Q_{in} \cdot So_{in} - So \cdot Q_w) - So \cdot Q_{out} + react_9 + K_{LA} \cdot (SOSAT1 - So) \tag{3.49}$$

Fouling Dynamics

$$\frac{dMC}{dt} = 0 \tag{3.50}$$

$$\frac{dMP}{dt} = 0 \tag{3.51}$$

Note: As the reactor is assumed to be well mixed, the substrate and biomass concentrations are uniform throughout. Consequently, the internal recycling flow Q_r does not affect these concentrations, as they are already uniformly distributed, and is therefore not included in the previous equations.

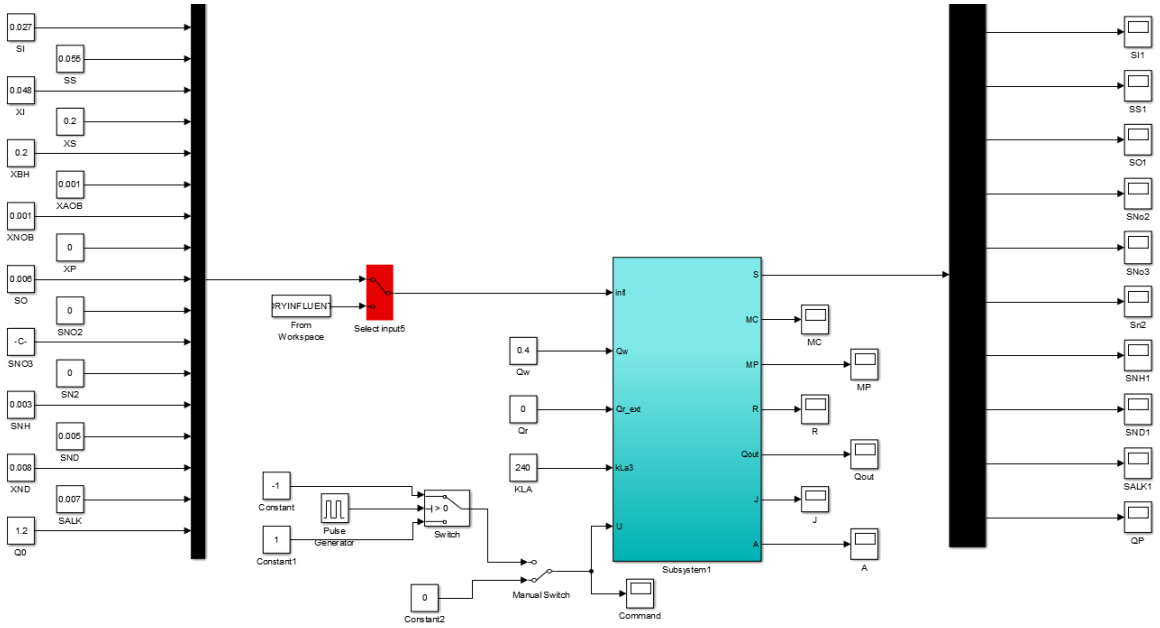

Figure 3.24: Simulink Model with Fouling in a Single Reactor

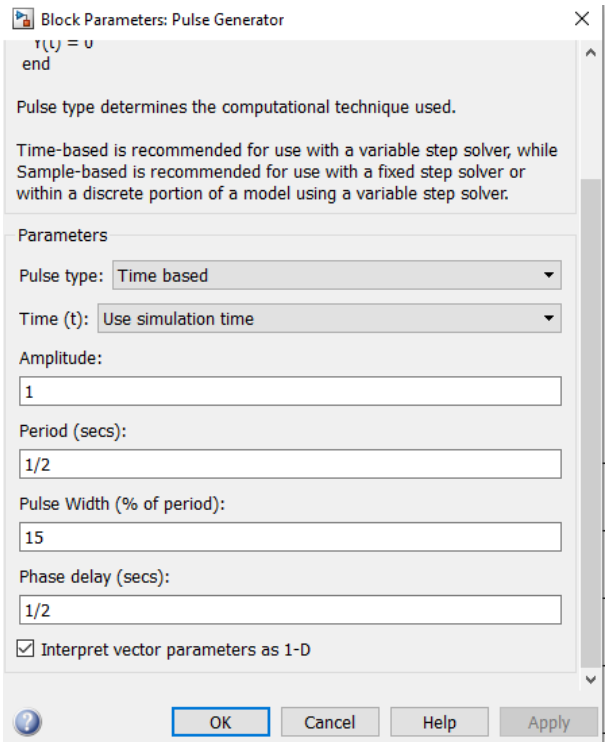

Figure 3.25: pulse generator

Time Unit Adjustment in Simulation

In our single bioreactor simulation, we made an important change to the time units. We converted all the original daily values to hourly values by dividing them by 24. For example, the maximum growth rate (μ_H) changed from 4.0 per day to $4.0/24 = 0.1667$ per hour. We did this to make it easier to work with and understand the results, since our system switches phases every 30 minutes. This change in time units doesn't affect how the system actually behaves; it just lets us see what's happening more clearly over shorter periods. By using hours instead of days, we can better observe and analyze the quick changes that occur in our bioreactor.

4.2.2 Challenges in our simulation

Our main problem was the differences between the models and working conditions in our case compared to our supervisor's article. This made it impossible to use the same parameter values, such as how much the clean membrane resists the flow of water (R_0) and how quickly we can clean off the dirt (W), and other parameters, and we were not satisfied with the result.

To solve this, we had to use a 'guess and check' method. We tried different values until we got results that made sense. It's not perfect, but it was the best we could do with what we had.

We looked at a lot of scientific papers and other sources to find better values, but none of them fit our exact situation. This means that there's still a lot of work to be done in this area.

It's important to remember that even if our simulation isn't perfect, it still gives us useful information. It helps us understand how these systems might work, and gives other researchers a place to start when they do more studies in the future.

4.2.3 Results and Discussion

All results presented below are combined data: results from fouling and backwash simulations are highlighted in red, while results from standard operation using the ASM1 2ND model are shown in blue. The estimated values give the Q_{out} (as shown in Figure 3.29) in red. To facilitate comparison with the standard operating phase, Q_{in} has been adjusted to 2.4 to better match the flow rates observed during filtration and backwashing. In addition, the low values of Q_{in} and Q_{out} increase the Solids Retention Time (SRT), which promotes biomass growth while preventing excessive biomass leaching into the effluent.

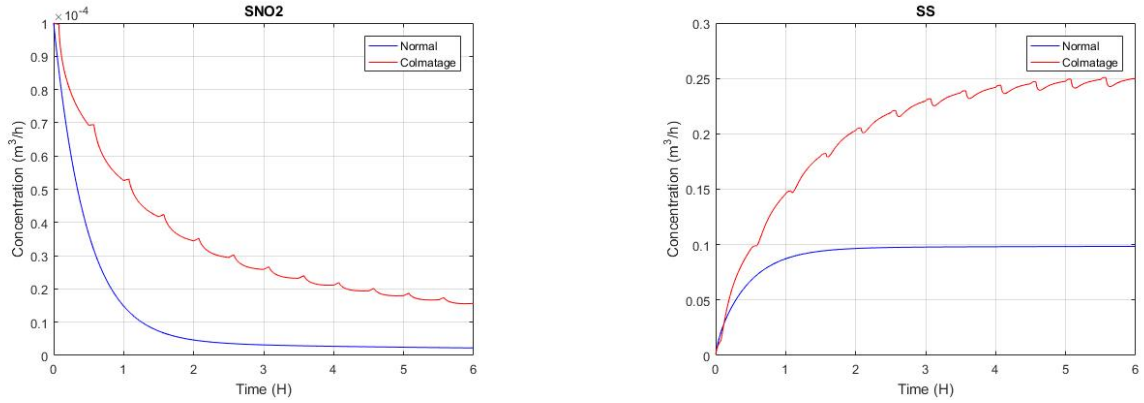

Figure 3.26: Comparison of SNO_2 (left) and SS (right) concentrations for normal and fouling conditions.

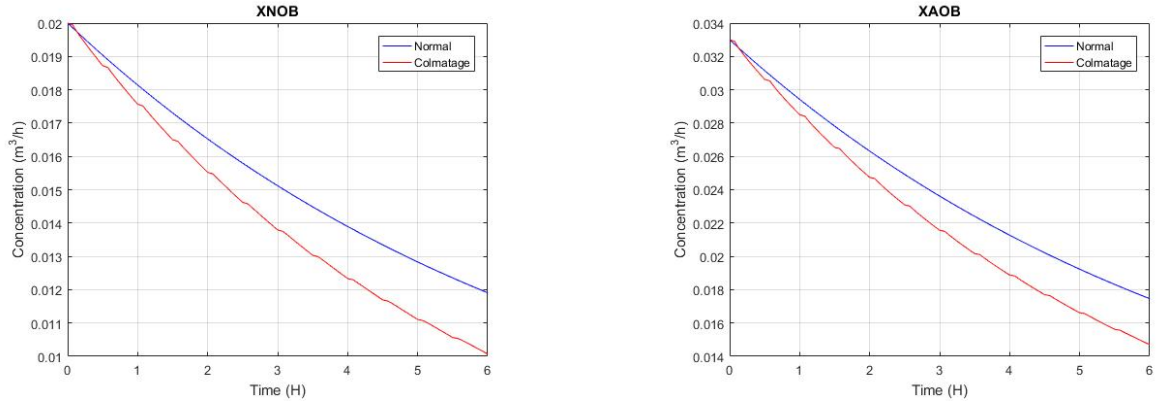

Figure 3.27: Comparison of X_{NOB} (left) and X_{AOB} (right) concentrations for normal and fouling conditions.

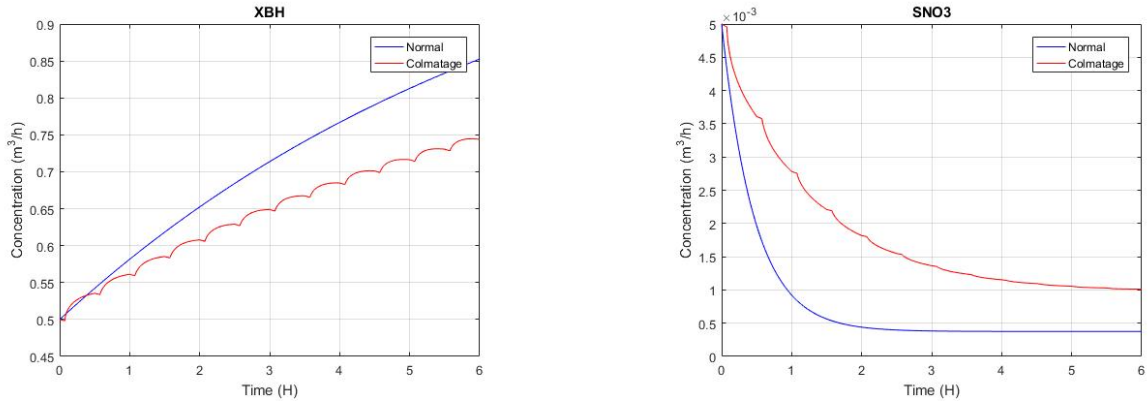

Figure 3.28: Comparison of X_{BH} (left) and SNO_3 (right) concentrations for normal and fouling conditions.

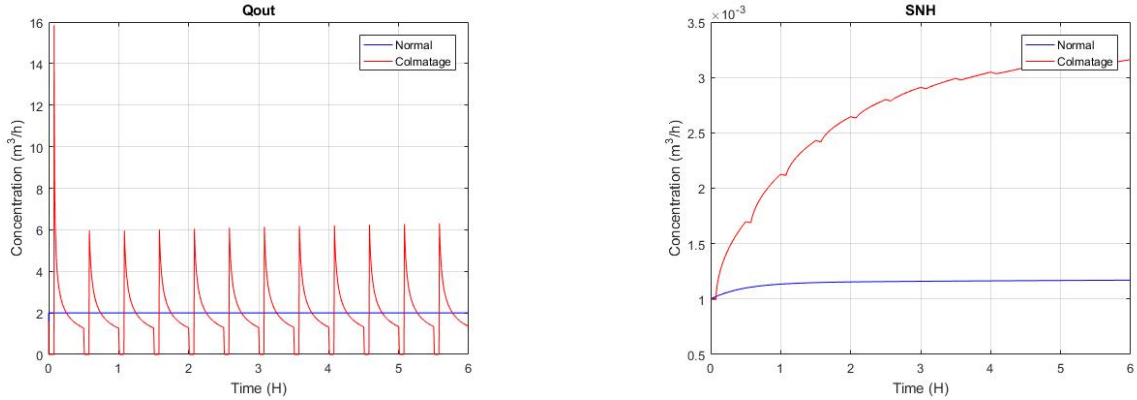

Figure 3.29: Comparison of Q_{out} (left) and SNH (right) concentrations for normal and fouling conditions.

- **SNO_2 (Nitrite Concentration):**
  Normal Operation: The nitrite concentration decreases rapidly and stabilises at a very low level within the first hour, indicating efficient conversion of nitrite to nitrate (NO_3^-) or nitrogen gas (N_2) by nitrification and denitrification processes. (Figure 3.26, left).

  Fouling (Colmatage): The nitrite concentration decreases more slowly, with noticeable steps. This suggests that fouling reduces the efficiency of the process, preventing the system from removing nitrite as effectively as during normal operation.

  Conclusion:Fouling reduces the efficiency of nitrite removal. The result is a slower conversion rate and higher residual nitrite concentrations

- **SS (Soluble Substrate):**
  Normal Operation: The soluble substrate concentration increases gradually and stabilises at around 0.1 m^3/h after two hours, demonstrating efficient substrate consumption by the microorganisms. (Figure 3.26, right).

  Fouling (Colmatage): The concentration increases more rapidly and reaches a higher level (around 0.25 m^3/h), with noticeable oscillations. This indicates that fouling reduces the ability of microorganisms to consume the substrate, leading to its accumulation.

Conclusion: Fouling inhibits the decomposition of organic matter and results in higher substrate accumulation in the system.

- **X_{NOB} (Nitrite Oxidizing Bacteria):**
  Normal Operation: Reflecting stable system operation, the concentration of nitrite oxidising bacteria (NOB) is steadily decreasing as expected. (Figure 3.27, left).

  Fouling (Colmatage): The concentration of NOB decreases more rapidly under fouling conditions, indicating that fouling limits the availability of critical resources such as oxygen and nitrite.

  Conclusion: Fouling negatively affects the growth of NOB. This reduces the system's ability to oxidise nitrite to nitrate.

- **X_{AOB} (Ammonia Oxidizing Bacteria):**
  Normal Operation: The concentration of ammonia oxidising bacteria (AOB) decreases steadily over time. This indicates stable nitrification (Figure 3.27, right).

  Fouling (Colmatage): The concentration decreases more rapidly under fouling conditions. This suggests that fouling affects the activity and growth of AOB.

  Conclusion: Fouling has a significant impact on AOB. It slows the nitrification process and reduces the conversion of ammonia to nitrite.

- **X_{BH} (Heterotrophic Bacteria):**
  Normal Operation: The concentration of heterotrophic bacteria increases steadily and stabilises at 0.85 m^3/h after five hours, reflecting effective degradation of organic matter. (Figure 3.28, left).

  Fouling (Colmatage): The concentration is lower and increases more slowly, with noticeable oscillations. Fouling is likely to limit the growth of heterotrophic bacteria due to reduced substrate availability.

  Conclusion: Fouling slows down the growth of heterotrophic bacteria and hinders the breakdown of organic matter.

- **SNO_3 (Nitrate Concentration):**
  Normal Operation: The nitrate concentration drops rapidly and stabilises at a low level, an indication of efficient denitrification (Figure 3.28, right).

  Fouling (Colmatage): The nitrate concentration decreases more slowly and remains higher than under normal conditions, indicating reduced denitrification efficiency.

  Conclusion: Fouling, probably due to reduced availability of denitrifying bacteria or unfavourable process conditions, reduces the efficiency of nitrate removal.

- **Q_{out} (Outflow Rate):**
  Normal Operation: Indicating consistent filtration, the effluent rate remains stable at approximately 2 m^3/h. (Figure 3.29, left).

  Fouling (Colmatage): The discharge rate is highly variable, with large peaks (up to 16 m^3/h) and rapid declines. These fluctuations indicate system instability caused by blockages and intermittent backwashing.

  Conclusion: Fouling causes instability in the system's flow rate, requiring more frequent backwashing to maintain performance.

- **SNH (Ammonium Concentration):**
  Normal Operation: Stable and low ammonium concentration, an indication of effective nitrification. (Figure 3.29, right).

  Fouling (Colmatage): The ammonium concentration rises steadily to a higher level. This indicates reduced ammonium removal efficiency due to fouling.

  Conclusion: Fouling will reduce the rate of nitrification, causing ammonium to build up in the system.

.

4.2.4 Overall Conclusion

Fouling reduces the overall efficiency of the system in the key processes of nitrification, denitrification and organic matter decomposition. It leads to higher concentrations of substrates and nitrogen compounds (e.g. SNO_2, SNO_3, SNH) while reducing the concentrations of essential bacteria (e.g. X_{NOB}, X_{AOB}, X_{BH}). In addition, fouling causes instability in the effluent flow rate, requiring more frequent or increased backwash cycles to restore system performance.

5 Conclusion

In this chapter, we explored the setup of the simulation platform using the ASM1-2ND model in MATLAB Simulink, along with key components such as S-functions and membrane bioreactor (MBR) configurations. We investigated different scenarios for controlling nitrogen removal and incorporating membrane fouling dynamics, highlighting the challenges faced during implementation. The results indicate that fouling has a significant impact on system performance, leading to reduced nitrogen removal efficiency and biomass growth. This chapter lays the foundation for further research into optimising control strategies to improve wastewater treatment processes.

Chapter 4

Simulation Control for Wastewater Quality

Contents

1 Introduction

Activated sludge treatment is a common method of treating industrial and domestic wastewater. It is a secondary (biological) treatment. The process involves microorganisms that break down pollutants, but their behaviour is complex, making the process non-linear and difficult to manage. The main aim of wastewater treatment is to reduce harmful substances in the water before it is released back into the environment. However, the process doesn't remove all pollutants and can only reduce some of them to acceptable levels.

In addition, the treatment plant faces challenges such as fluctuating water flows and varying concentrations of pollutants in the incoming wastewater. Despite these variations, the plant must always operate to meet strict water quality standards. As the process consumes a lot of energy, it's important to run the plant efficiently. These factors make controlling the plant a difficult task, requiring an effective control strategy to ensure smooth and efficient operation Tejaswini et al. (2020).

Different types of control systems, from basic PI control to more advanced methods like MPC, are used in wastewater treatment plants around the world. The **Proportional-Integral (PI) control** is one of the most widely used controllers in the industry because of its simplicity and ease of tuning Aichouche (2021).

In activated sludge plants, it's important to maintain the right level of dissolved oxygen (DO) in the tanks where the sludge is treated. Sufficient oxygen helps the microorganisms to break down pollutants more effectively. But if there's too much oxygen, it requires more airflow, which uses more energy and can also reduce the quality of the sludge.

Finding the right balance is key to making the treatment process efficient and keeping energy costs low, while ensuring that the sludge works properly.

2 PI Control and Tuning Method

A **PI controller** (Proportional-Integral controller) combines two control actions: **Proportional** and **Integral**. Its main function is to control a process by adjusting a specific variable (the process variable) based on the target value (the setpoint) and the difference between the two (the error). The **proportional** part reacts quickly to changes, while the **integral** part helps to eliminate long-term errors.

The PI controller is widely used in industrial automation because it can automatically adjust the process to achieve the desired objectives. It's a closed-loop system, which means it constantly checks and adjusts the process to stay on track. By tuning the PI controller, it can be adapted to the specific process, ensuring that the system responds quickly and accurately to changes, minimising errors over time.

Mathematical Expression of PI Controller

$$u(t) = K_p \cdot e(t) + K_i \cdot \int e(t)\, dt$$

PI Tuning

In the two control strategies we implemented, which we will discuss next in this chapter, we observe the presence of 4 or 5 PI controllers in each strategy. One of the biggest challenges we faced was tuning these controllers. Luckily, we had two advantages:

First, each PI controller acted as a perturbation to the others, but was quickly rejected by the system. Second, Simulink provided a tuning tool that was quite effective for the second strategy,

where the 4 PI controllers were different. With some additional trial and error, we were able to achieve excellent results.

In the first strategy, however, we had two PI controllers in cascade, which even Simulink struggled with. As our model is non-linear, we had no choice but to tune each controller manually by trial and error, which took a lot of time. In the process, we made an important discovery, which is discussed in the following section.

3 First Control Strategy: Controlling SNO_3

3.1 Why Control SNO_3 (Nitrate) in Wastewater Treatment?

Controlling nitrate (SNO_3) levels in wastewater treatment is important to protect the environment and ensure safe water reuse. High levels of nitrate can cause pollution when released into water bodies, leading to algae growth and oxygen depletion, which can harm fish and other aquatic life. If treated water is used for agriculture, too much nitrate can be harmful to plants. While nitrate is useful as a nutrient, excessive amounts can cause soil imbalance and damage crops. In wastewater treatment, particularly with activated sludge, nitrates are removed through a process called denitrification, where they are converted to nitrogen gas. This step is crucial to meeting regulations on nitrogen levels in treated water, ensuring that harmful nitrogen compounds are removed before the water is reused or discharged.

3.2 Overview of the First Control Strategy

The first control strategy is designed to track and control the nitrate concentration in the effluent. This strategy uses a set of PI controllers cascaded as shown in Figures 4.1 and 4.2. The system controls the oxygen levels in the aerobic reactors, which then control the ammonium concentration (SNH4) based on the desired setpoint. The ammonium setpoint is itself determined by a controller that controls the nitrate concentration (SNO3).

As the nitrate concentration is also influenced by the denitrification process, three additional PI controllers have been added to manage the internal and external recirculation loops (Qint, QRAS and QWAS). These controllers help to maintain the solids retention time (SRT) of the system. Although each controller may slightly affect the others, the system remains stable and overall performance is not affected.

The design is robust because even if one loop fails, the others continue to regulate nitrate levels effectively. The control system relies on only two measurements, the ammonium and nitrate concentrations in the final reactor, making it simple but efficient.

The PI controller parameters were fine-tuned by trial and error, using dynamic input and setpoint data. In addition, the QWAS flow rate was limited to a range of 0 to 1300 m^3/day to ensure safe operation,and the oxygen transfer coefficient (KLA) has been limited to 300 in order to stay within its physical limits and not to exceed the operational limits.

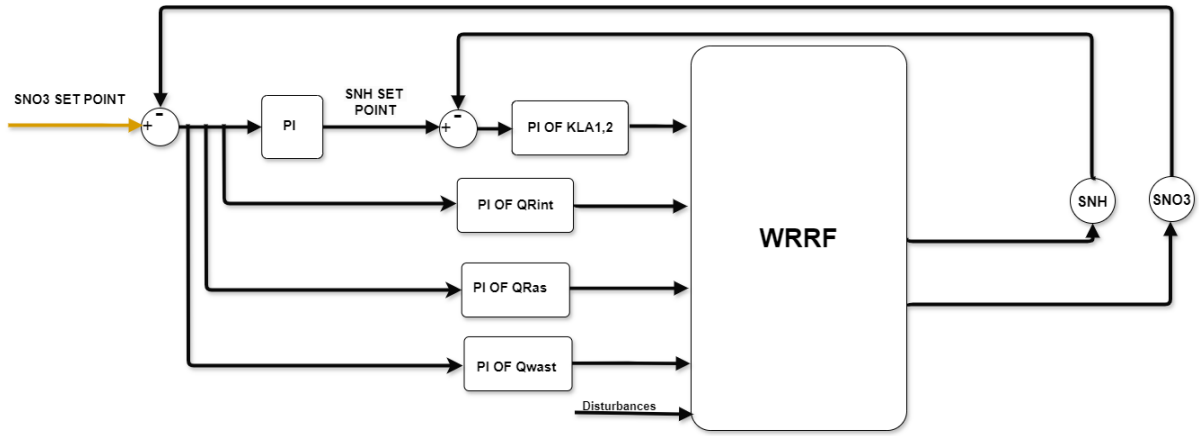

Figure 4.1: Diagram of nitrate control

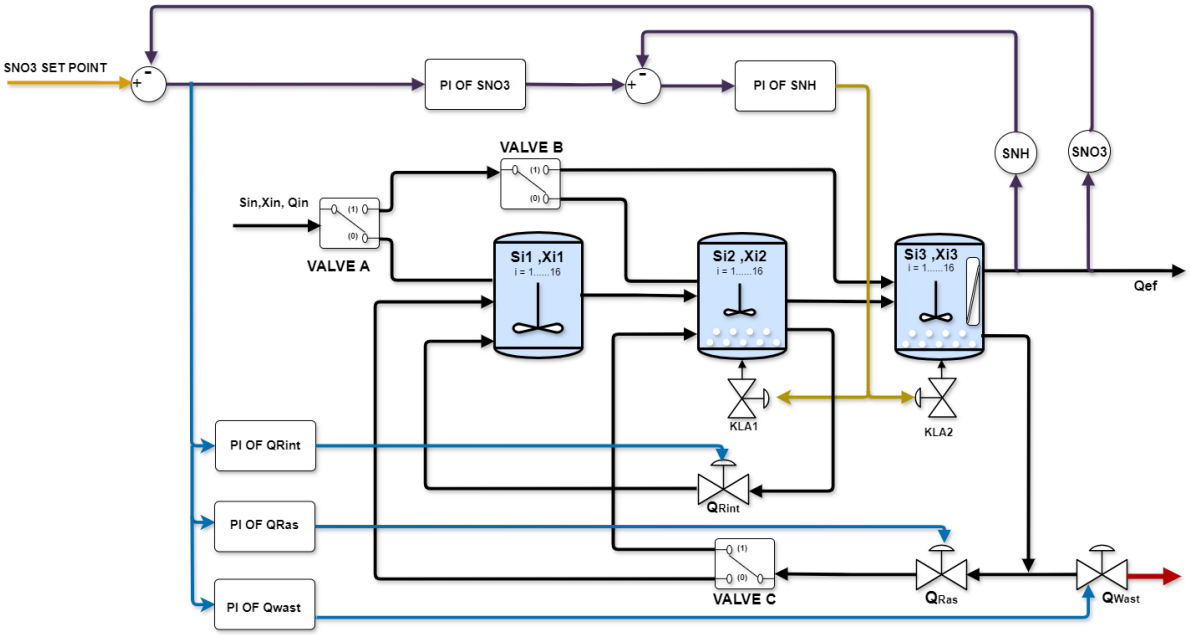

Figure 4.2: Nitrate Control Loop Scheme

The configuration was chosen for its ability to maintain stable and efficient operation, with a focus on controlling the main nitrogen compounds (nitrate and ammonium) in the wastewater treatment process. The cascaded PI controllers and additional controls for oxygen transfer and recirculation flows work together to ensure consistent effluent quality while optimising energy use and minimising disturbance.

3.3 Results and Discussion

Constant inflow

Here we present the results for the control of SNO_3 using a constant inflow.

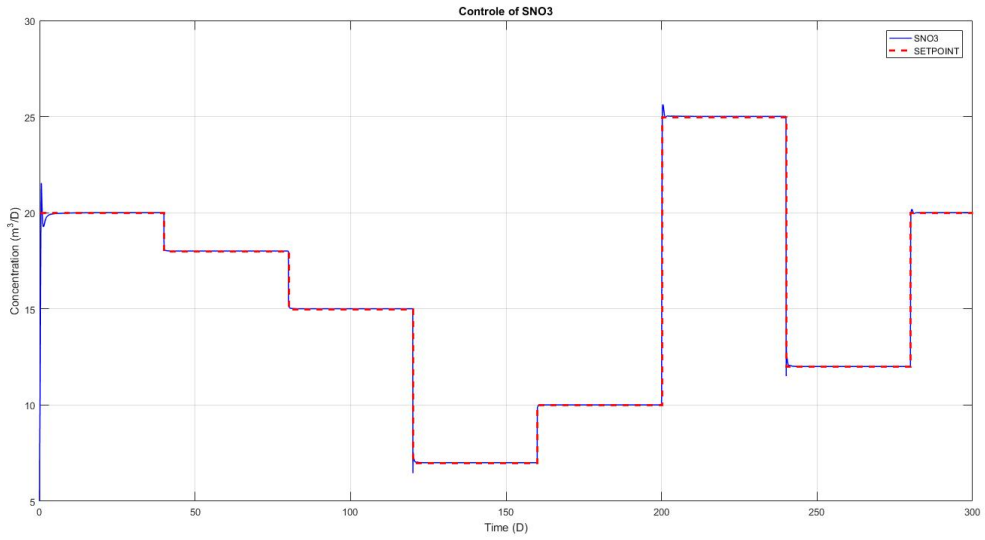

Figure 4.3: Nitrate Concentration Control (SNO3)

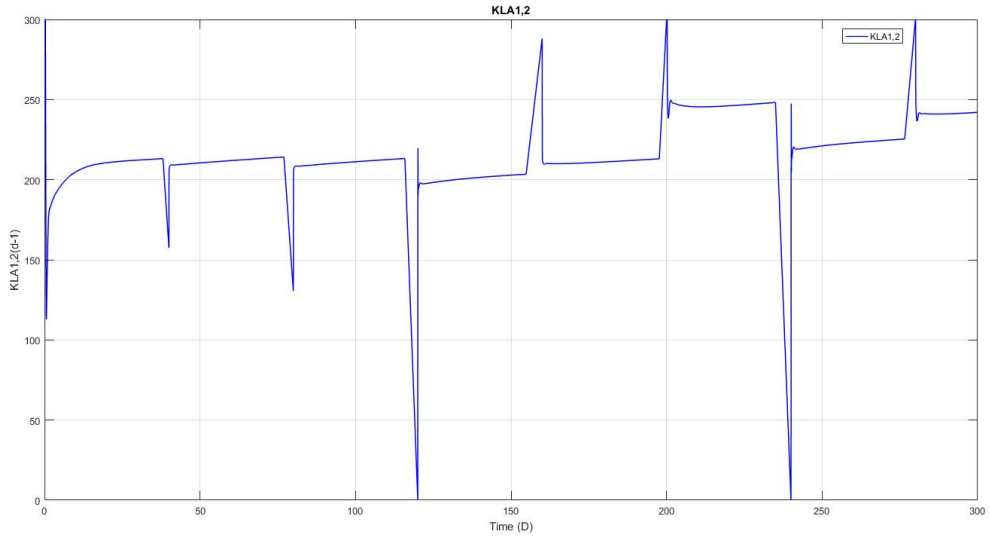

Figure 4.4: Oxygen Transfer Coefficient Control (KLA1,2)

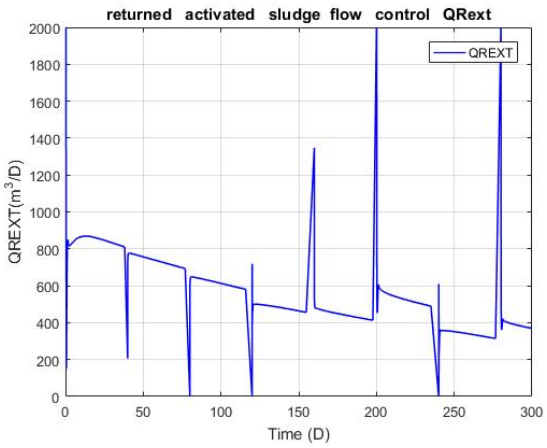

Figure 4.5: Returned Activated Sludge Flow Control (QRext)

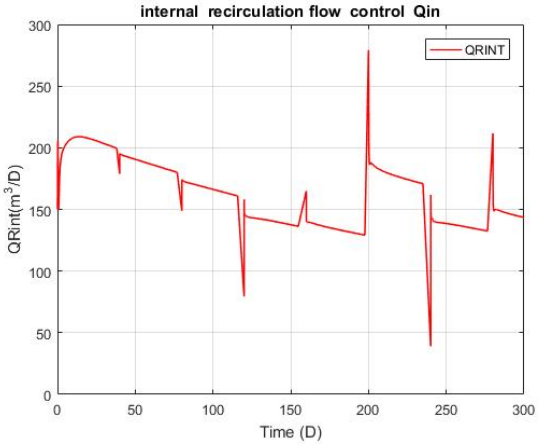

Figure 4.6: Internal Recirculation Flow Control (QRint)

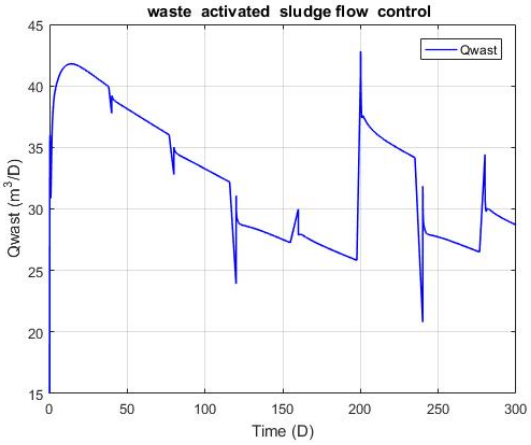

Figure 4.7: Waste Activated Sludge Flow Control (Qwast)

Nitrate Concentration Control (SNO3):

The Nitrate Concentration (SNO3) graph shows the control of nitrate levels in the effluent. The red dashed line represents the desired setpoint, while the blue line shows the actual nitrate con-

centration. The system closely follows the setpoint, with only minor deviations, indicating that it effectively manages nitrate levels to meet discharge or reuse standards, even under varying conditions..

Oxygen Transfer Coefficient Control (KLA1,2):

The KLA graph shows the control of the oxygen transfer coefficient, which is crucial for maintaining the correct oxygen levels in the aerobic reactors. The KLA remains fairly constant, with sharp drops at certain intervals. These dips are likely to correspond to periods when oxygen demand decreases, causing the system to adjust the KLA to conserve energy and avoid over-oxygenation.

Returned Activated Sludge Flow Control (QRext):

The graph shows the variation of the flow of recycled activated sludge (QRext) over time. Initially the flow remains relatively stable, but over time there are significant peaks and troughs. The aim of controlling QRext is to ensure that the correct amount of sludge is returned to maintain optimum treatment efficiency..

Internal Recirculation Flow Control (QRint):

The graph illustrates the control of the internal recirculation flow (QRint). The steady decline, followed by occasional spikes, indicates that the system is optimising the internal flow to manage the treatment process. These spikes are likely to be in response to changes in effluent load where adjustments are required to keep the system in balance and operating efficiently.

Waste Activated Sludge Flow Control (Qwast):

The graph tracks the waste activated sludge flow rate (Qwast), which shows periodic adjustments. A steady decline is followed by significant increases at certain points, indicating that the system removes sludge regularly to prevent excess accumulation. Controlling Qwast helps maintain a healthy sludge concentration in the treatment process, ensuring efficient operation.

Optimising PI Controllers for System Efficiency

Important note: During the tuning process we discovered that using just two PI controllers in cascade and setting Q_{wast} to 300, Q_{rext} to 1100 and Q_{rint} to 800 worked just as well as having all three controllers. These fixed values were the average of what the PI controllers produced, and the system became faster and more efficient. So we decided to remove the three controllers that were controlling the flow rates, especially during the dynamic inflow phase. This was a good solution because controlling flow rates in real industrial environments is more difficult than in simulations.

dynamic inflow

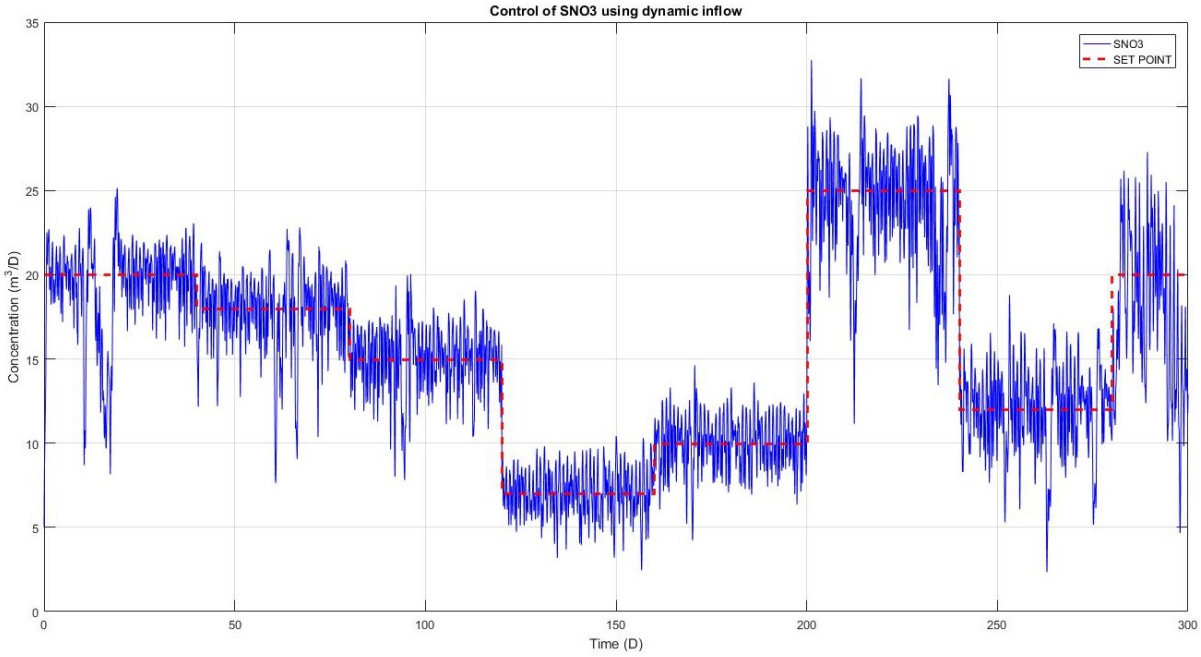

Figure 4.8: Control of Nitrate Concentration (SNO_3) using Dynamic Inflow

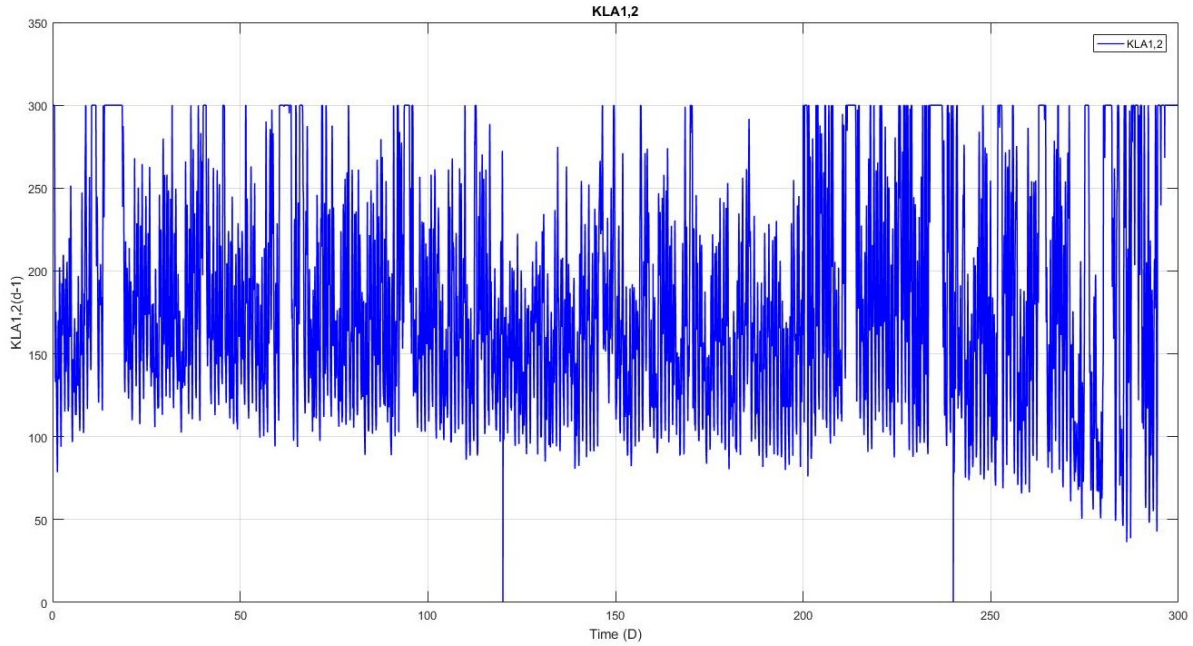

Figure 4.9: Oxygen Transfer Coefficient (KLA1,2) Variation under Dynamic Inflow

Oxygen transfer coefficient (KLA1,2) using dynamic inflow

The first plot shows the variation of the oxygen transfer coefficient, KLA1,2, over time under dynamic inflow conditions. As can be seen, the oxygen transfer rate fluctuates significantly, oscillating between approximately 50 and 300 d^{-1}. This dynamic behaviour reflects the response of the system to variations in inflow, with higher inflow leading to increased aeration

demand. Despite the oscillations, the system maintains a stable operating range, indicating that the aeration process is able to adapt to changes in inflow rates. This is critical for maintaining an efficient oxygen supply for biological processes, especially under fluctuating conditions that mimic real industrial scenarios.

Control of SNO_3 using dynamic inflow

The second graph shows the control of the nitrate concentration (SNO_3) under dynamic inflow conditions. Here the system aims to follow the setpoint (represented by the red dashed line) despite inflow fluctuations. The nitrate concentration shows several shifts reflecting the transitions in the inflow. In particular, the system experiences an increase in SNO_3 between 150 and 200 days, which is quickly corrected. The PI controllers effectively bring the system back to the setpoint, but with some delay, demonstrating the ability of the controllers to deal effectively with changing inflow conditions.

4 Second Control Strategy: Controlling the Ratio of SNO_3/SNH

4.1 Why Control SNO_3/SNH in Wastewater Treatment?

Controlling the SNO_3/SNH (nitrate to ammonium) ratio is crucial to maintaining a balance between two key nitrogen removal processes: nitrification, where ammonium is converted to nitrate, and denitrification, where nitrate is reduced to nitrogen gas. This balance ensures that both processes work properly. If ammonium levels are too high, this signals incomplete nitrification, which can lead to ammonia pollution. Conversely, if nitrate levels are too high in relation to ammonium, this indicates inadequate denitrification, leading to nitrate accumulation in the effluent. When wastewater is reused for irrigation, nitrogen management is essential. Plants need nitrogen, but both its form (nitrate vs. ammonium) and its concentration are important. Nitrate is readily absorbed by many crops, but high levels can be toxic, while excessive ammonium can harm plants by affecting soil pH and nutrient uptake. Controlling the SNO_3/SNH ratio ensures that the nitrogen content in the treated water benefits the crop without causing nutrient imbalances or toxicity. This helps to tailor the nutrient composition to the specific needs of the crop and ensures that the treated water is safe and effective for irrigation, promoting healthy plant growth.

4.2 Overview of the Secound Control Strategy

The second control strategy, shown in Figure 4.10 (or Figure 4.11 for further illustration), focuses on controlling the ratio between nitrate (SNO_3) and ammonia (SNH_4). This strategy uses a combination of PI controllers to achieve this. The closed loop configuration consists of four independent PI controllers, all working to maintain the SNO_3/SNH_4 ratio measured during the process.

The four PI controllers each control a different part of the system:

1. **KLA**: Controls the oxygen concentration in the last reactor to ensure complete nitrification.

2. **Three pumps**: These control the internal recirculation (Q_{INT}), the return activated sludge flow (Q_{RAS}) and the waste sludge flow (Q_{WAS}).

Limits are applied to ensure safe operation:

- The oxygen transfer rate (K_{LA}) is limited to a range of 0 to 300 per day.
- The Q_{RAS} flow rate is limited to between 0 and 5 times the input flow (Q_{in}), and Q_{int} is limited to Q_{in}.

The initial gains for the controllers (K_P and K_I, $i = 1..4$) were first tuned using Matlab's linearisation tool and then refined by trial and error for optimal performance. This strategy is particularly robust because if one loop fails, the other controllers can compensate, ensuring effective system operation.

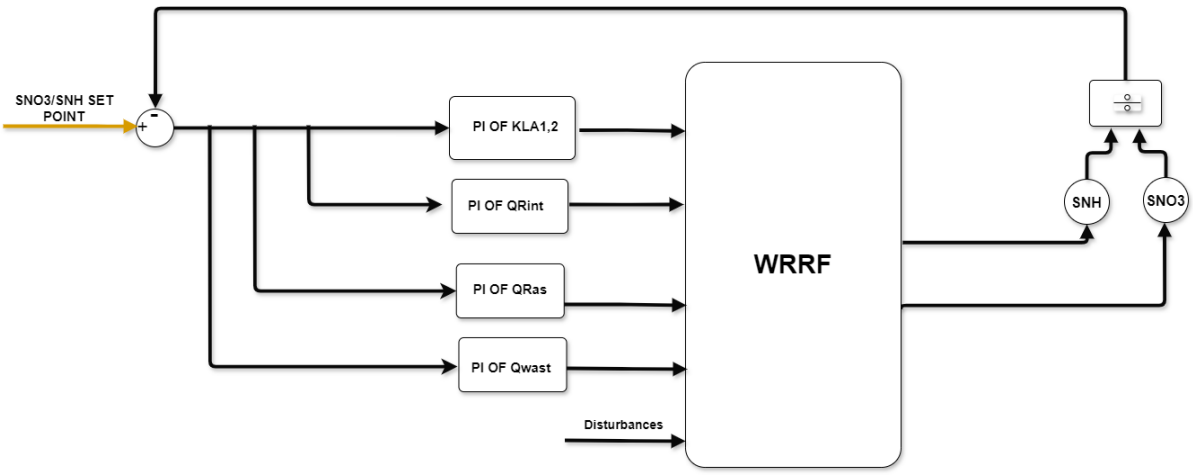

Figure 4.10: Diagram of SNO3/SNH ratio control

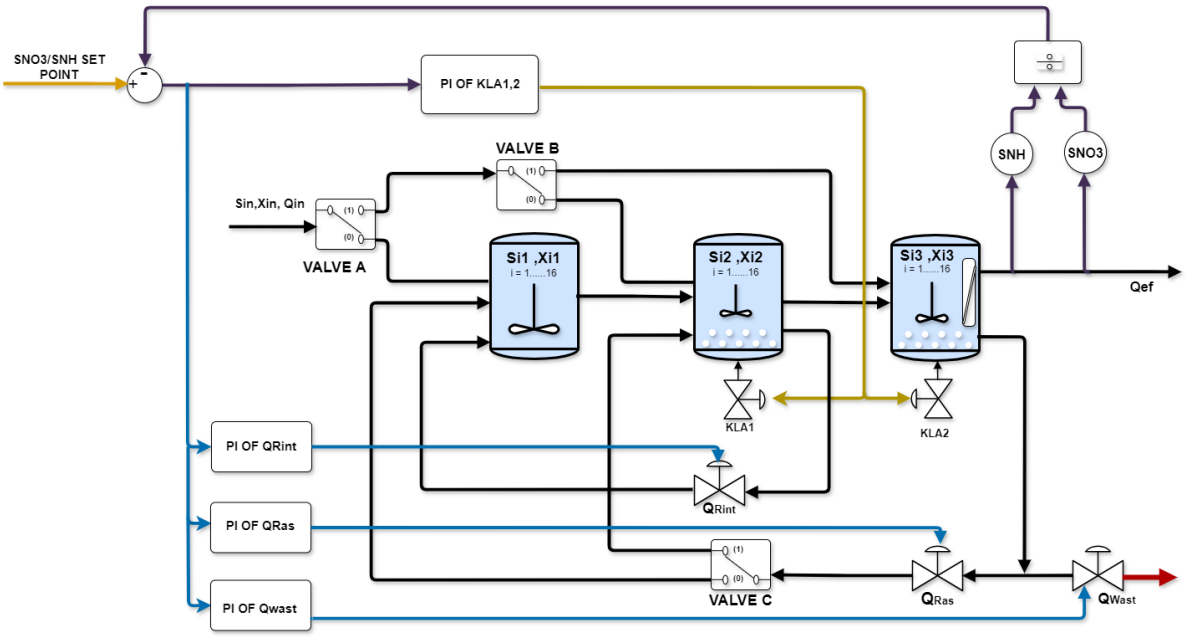

Figure 4.11: SNO3/SNH ratio Control Loop Scheme

We chose this specific configuration with PI controllers to control the SNO_3/SNH ratio because it helps to balance the key processes of nitrification and denitrification in the wastewater

treatment system. By using PI controllers to manage oxygen levels (KLA), internal recirculation (Qint), return sludge (QRAS) and waste sludge (Qwast), we can control the conversion of ammonium to nitrate and ensure that the system remains stable. This setup allows us to respond quickly to changes or disturbances in the system. The PI controllers work together to keep the nitrogen balance right, and because they adjust automatically, the system stays efficient without requiring a lot of complex measurements. The configuration is also robust, meaning that even if one part fails or fluctuates, the other controllers can adjust to maintain stability. This makes the control system reliable and effective in maintaining the correct nitrate/ammonium ratio.

4.3 Control of SNO_3/SNH (Constant Inflow)

The control of SNO_3/SNH in the system under constant inflow conditions is illustrated in the following figures.

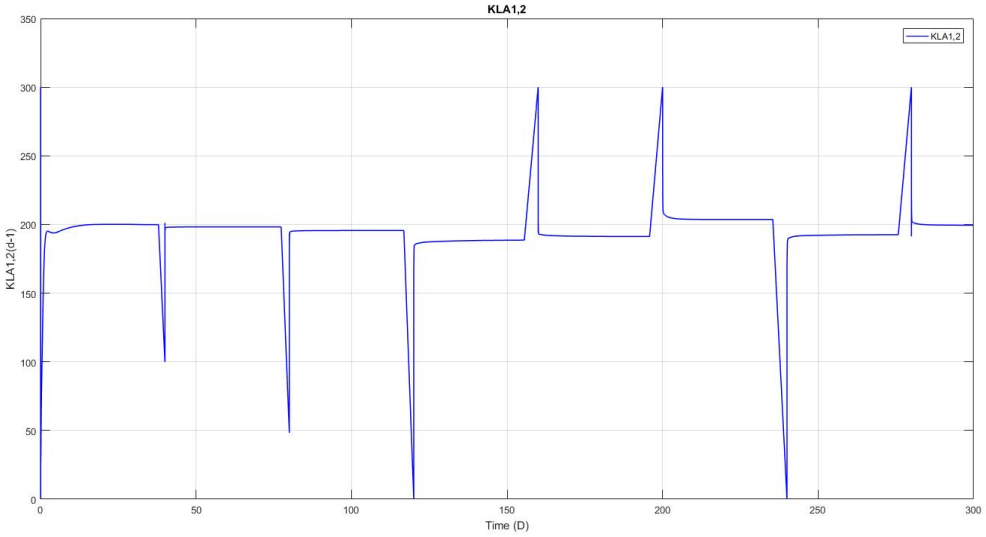

Figure 4.12: Control of SNO_3/SNH Ratio

Figure 4.12: Control of SNO_3/SNH Ratio
This graph shows how well the system is able to follow the set target (shown by the red dashed line) for the SNO_3/SNH ratio. The blue line shows the actual performance. The system follows the target closely and when the target changes (around days 40, 80, 120 and 200) the system takes a little time to adjust but eventually reaches the desired level. This shows that the controllers are doing a good job in keeping the balance between nitrate and ammonium stable.

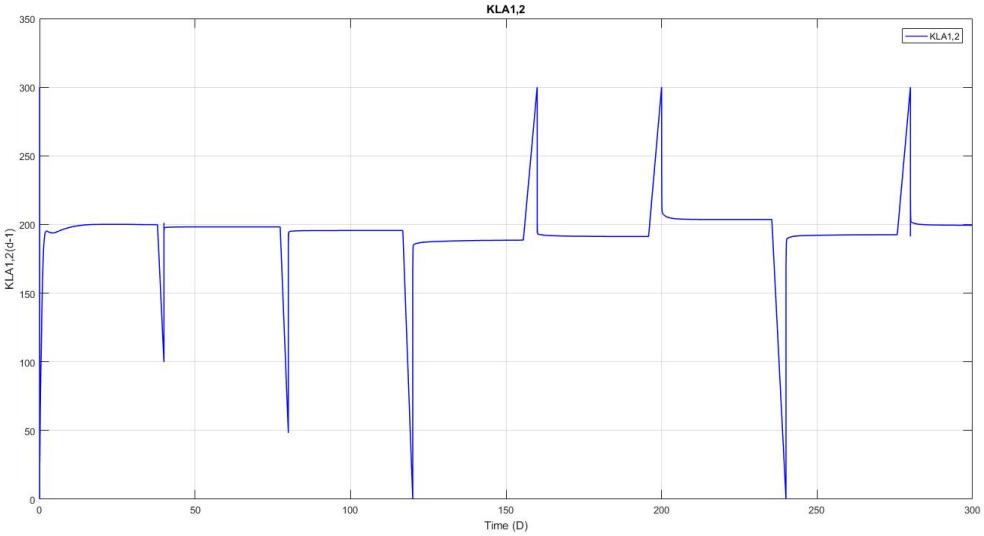

Figure 4.13: Oxygen Transfer Coefficient (KLA1,2)

Figure 4.13: Oxygen Transfer Coefficient (KLA1,2)
This graph shows how oxygen is added to the system. The oxygen transfer rate is mostly constant, but there are occasional spikes, especially after day 150. These spikes indicate that the system needs more oxygen to convert ammonium (SNH) to nitrate (SNO_3), helping to maintain the correct balance between the two.

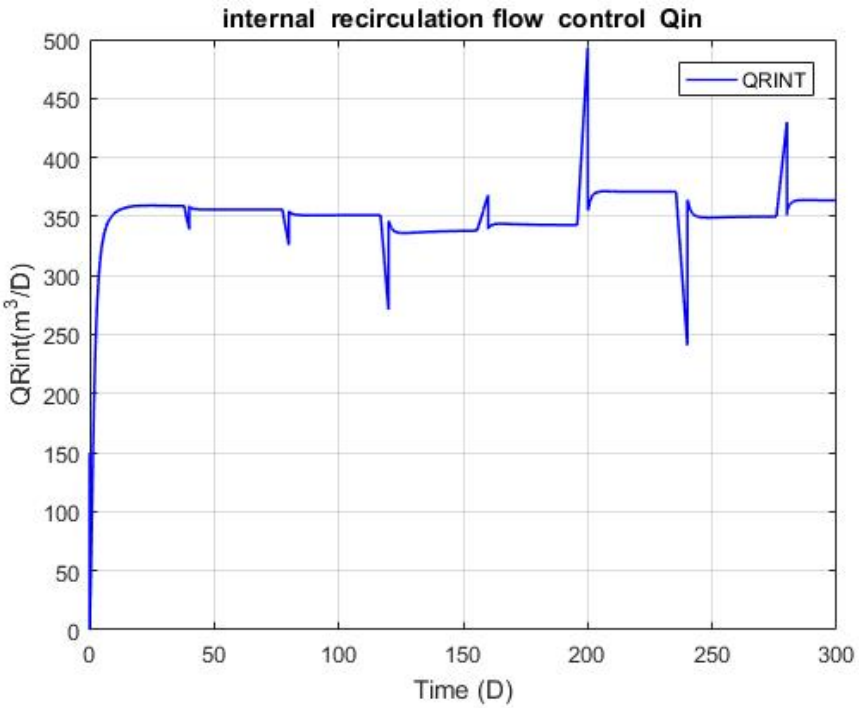

Figure 4.14: Internal Recirculation Flow (QRINT)

Figure 4.14: Internal Recirculation Flow (QRINT)

This graph shows how the system controls the internal recirculation flow, which helps to bring nitrate-rich water back into the process. The flow remains mostly around 350 m^3/day, but makes some adjustments between days 150 and 250 to maintain the balance of nitrate (SNO_3) and ammonium (SNH). These adjustments are small but important to keep the system stable.

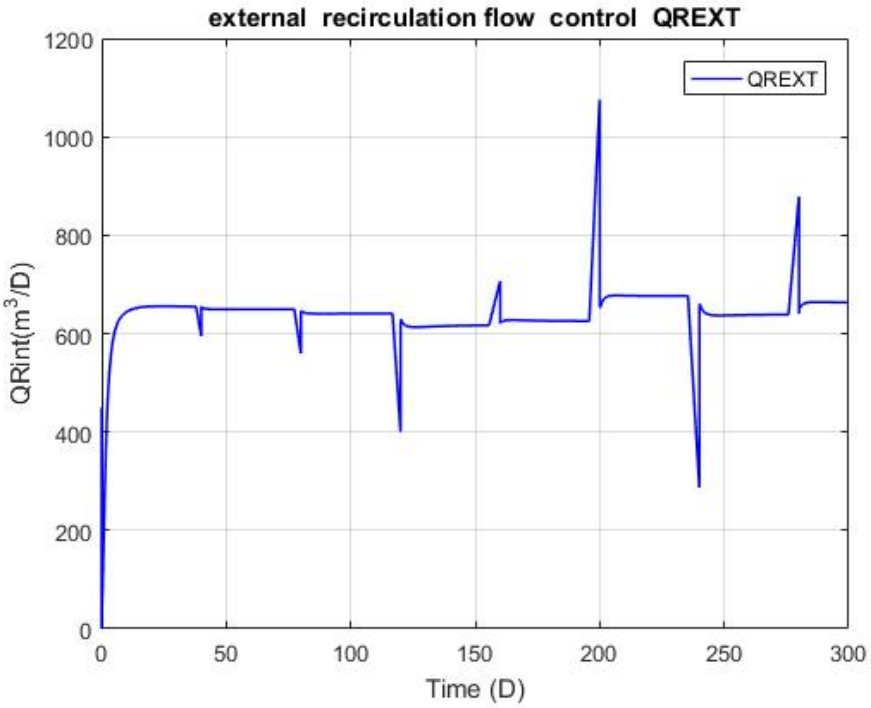

Figure 4.15: External Recirculation Flow (QREXT)

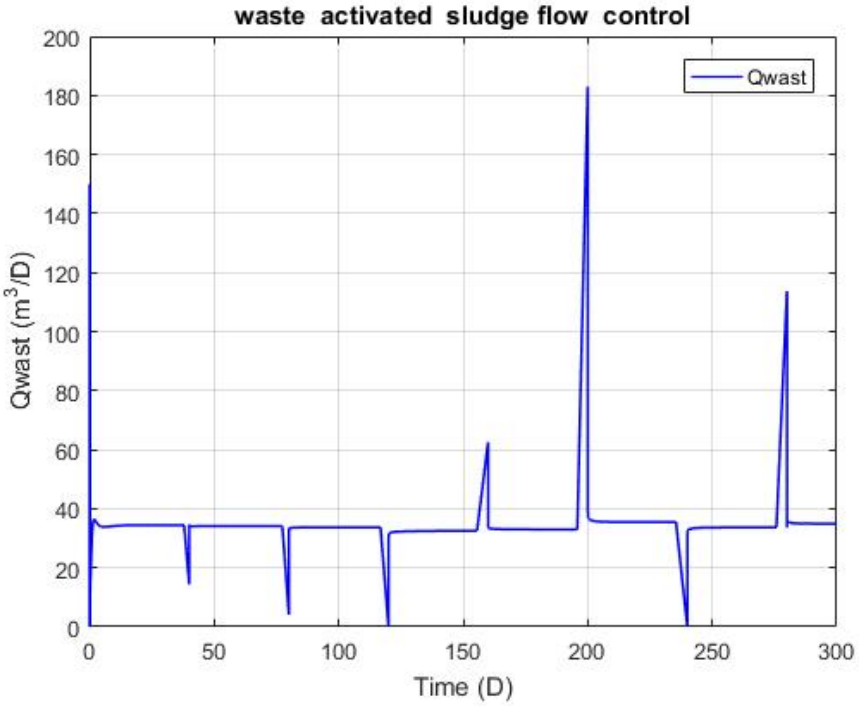

Figure 4.16: Waste Activated Sludge Flow (QWast)

Figure 4.15: External Recirculation Flow (QREXT)
This graph shows how the external recirculation flow (which returns treated water to the biological process) is controlled. The flow fluctuates between 600 and 800 m^3/day. There's a spike around day 200, which probably means the system needs more nitrate recirculation to cope with rising ammonium levels. This helps to keep the SNO_3/SNH ratio in balance.

Figure 4.16: Waste Activated Sludge Flow (QWast)
This diagram shows how the sludge flow is controlled. The system removes excess biomass (sludge) to prevent overloading. There are peaks in sludge removal around days 150 and 200, which help the system cope with high biomass levels and keep the SNO_3/SNH ratio under control.

Recap

These figures show how the system manages to maintain the right balance between nitrate and ammonium (SNO_3/SNH) even when things change slightly in the system. It does this by adjusting recirculation rates, oxygen levels and sludge removal. At the moment the system handles constant inflow, but once we introduce dynamic inflow (changing input) we expect to see more variation as the system adapts to these changes.

4.4 Control of SNO_3/SNH (Dynamic Inflow)

Control of SNO_3/SNH using Dynamic Inflow

This graph shows how the system controls the ratio of nitrate (SNO_3) and ammonia (SNH) over time, even when the influent changes. The red dashed line represents the target. The system tries to follow this target and, after some initial changes, it successfully corrects itself, bringing the values back to the setpoint..

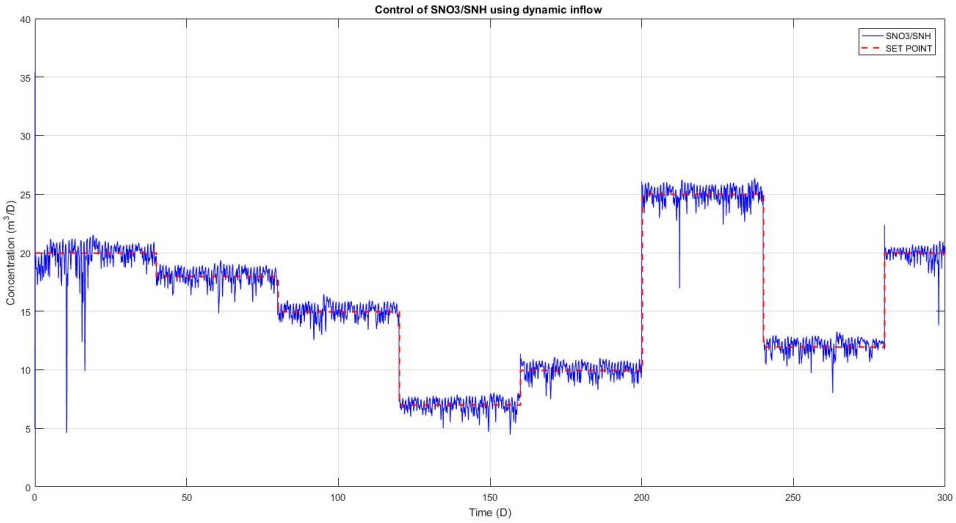

Figure 4.17: Control of SNO_3/SNH using Dynamic Inflow

Oxygen Transfer Coefficient (KLA1,2) under Dynamic Inflow

This graph shows how the oxygen transfer rate (KLA1,2) changes over time with varying inflows. The oxygen transfer rate varies between 50 and 300 units per day. These changes occur because

as more water flows in, the system needs more air to treat it. Despite the fluctuations, the system works efficiently and easily adjusts to the different inflows..

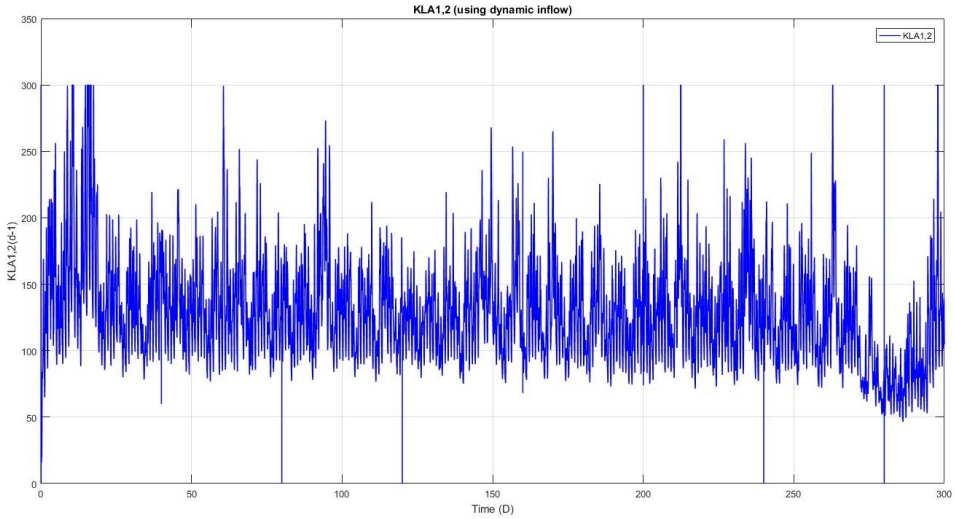

Figure 4.18: Oxygen Transfer Coefficient (KLA1,2) under Dynamic Inflow

Development of Three Fluxes under Dynamic Influent Conditions

The external recirculation flow (Qrext) is the largest as it plays a key role in maintaining the efficiency of the biological treatment, particularly for processes such as nitrogen removal where treated water is recirculated to assist denitrification. It fluctuates around 1200 m^3 per day to adapt to varying influent flows and ensure stable performance. The internal recirculation flow (Qrint) remains constant at around 600 m^3 per day, adjusting slightly as required to balance oxygen levels and mixing in the reactor. Waste flow (Qwast) remains low as only small amounts of excess sludge are periodically removed from the system to maintain optimum sludge levels..

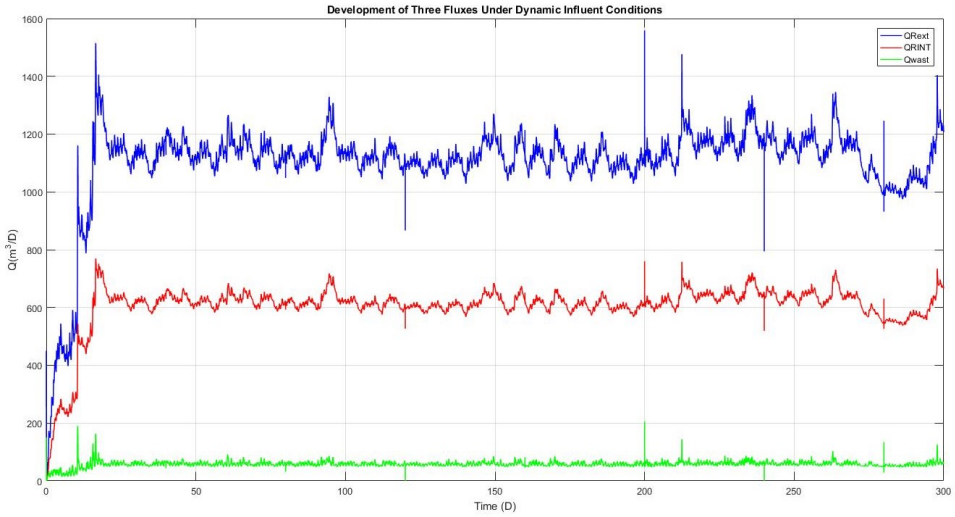

Figure 4.19: Development of Three Fluxes under Dynamic Influent Conditions

Recap

In these dynamic inflow simulations, the system effectively adapts to varying flow rates, both for oxygen transfer and for control of key flow parameters (Qrext, Qrint, Qwast). Although the system experiences fluctuations, it is able to self-correct and stabilise around the set targets, ensuring efficient performance under changing conditions..

4.5 Control Strategy Limitations

In both strategies, we encountered a limitation in the last two configurations. Their primary function is to direct the influent directly to the third reactor, where the first reactor is anoxic and the second and third are aerobic. This configuration limits the system's ability to achieve high SNO_3 levels due to several factors.

Firstly, bypassing the anoxic first reactor disrupts the **denitrification process**, where nitrate (SNO_3) is typically reduced to nitrogen gas. This step is crucial for nitrogen removal, and by skipping it, the system misses an important opportunity to remove nitrate upfront. As a result, ammonium (SNH_4^+) enters the aerobic reactors without proper treatment in the anoxic zone, making it harder for the system to balance nitrogen removal effectively.

Secondly, the **nitrification process** in the aerobic reactors is compromised. Since the influent bypasses the second reactor, which is also aerobic, the third reactor must handle all the ammonium. This reduces the time and capacity available for nitrifying bacteria to convert ammonium to nitrate. The third reactor alone cannot provide sufficient processing time for complete nitrification, limiting the production of nitrate (SNO_3). Consequently, achieving high SNO_3 levels becomes difficult.

In addition, the system faces **oxygen supply limitations**. Bypassing the second reactor increases the **oxygen demand** in the third reactor, which tries to compensate by increasing the oxygen transfer coefficient (kLa). However, this results in **unrealistically high kLa values**, beyond what is physically possible. The system cannot achieve the necessary oxygen levels to support efficient nitrification, further limiting nitrate production. At the same time, the **solids retention time (SRT)** in the third reactor is reduced, giving nitrifying bacteria less time to convert ammonium to nitrate, making high SNO_3 levels nearly impossible to achieve.

In conclusion, the inability to achieve high SNO_3 levels in this configuration is due to the bypassing of the critical denitrification step, reduced nitrification capacity, and the system's attempt to compensate for oxygen limitations by pushing kLa to unrealistic levels, which is not physically feasible.

5 Conclusion

In this chapter we have examined two control strategies for managing nitrate levels and the nitrate/ammonium ratio in wastewater treatment. Both strategies effectively used PI controllers to maintain stable operation under constant and dynamic influent conditions. The system was able to adapt to changes in influent rates, ensuring efficient oxygen transfer and proper control of key flows such as recirculation and sludge removal. However, we also identified limitations when certain reactors were bypassed, making it more difficult to achieve high nitrate levels. Overall, the control strategies were successful, but further optimisation could improve system performance under more challenging conditions.

General Conclusion

This thesis aimed to address key challenges in wastewater treatment, with a focus on controlling nitrogen levels and optimising the treatment process using a flexible simulation platform based on the ASM1 2ND model. The platform developed included three reactors - one anoxic and two aerobic - and incorporated two control strategies designed to improve wastewater treatment, particularly for agricultural reuse.

Principal Contributions:

- **Simulation of Crabmezapamine Treatment:** One of the unique aspects of this work was the inclusion of *crabmezapamine*, a challenging compound for wastewater treatment. Our simulations demonstrated the difficulty of the system in dealing with crabmezapamine and highlighted the limitations of traditional treatment methods in degrading this compound.
- **Addressing Membrane Fouling:** Although not the primary focus, membrane fouling became a notable challenge throughout the study. Fouling can significantly reduce the efficiency of membrane filtration, requiring more frequent backwash cycles and increasing operating costs. Our simulations demonstrated the impact of fouling on system performance and highlighted the need for effective strategies to mitigate its effects. Although fouling management was not directly optimised, its role in limiting the efficiency of the treatment process was recognised, particularly in systems using membrane bioreactors.
- **Control Strategies:**
  - The **first control strategy** A key focus of this study was the control of nitrate (SNO_3) levels to ensure both efficient nitrogen removal and safe reuse of treated effluent. Control strategies were developed to maintain an optimal balance between nitrification and denitrification, ensuring that nitrate concentrations were within desired limits for both environmental discharge and agricultural reuse. By optimising key parameters such as solids retention time (SRT) and oxygen transfer, the system effectively managed nitrate levels under different operating conditions. This precise control is essential not only for nitrogen removal, but also for producing treated water that meets the quality standards required for agricultural reuse. .
  - The **second control strategy** aimed to control the ratio of nitrate to ammonium (SNO_3/SNH). This approach was critical for maintaining a balanced nutrient profile in the effluent, particularly for agricultural applications, where excessive nitrogen compounds could harm crops. The strategy also ensured effective nutrient removal, even under fluctuating load conditions.

- **Challenges and Limitations:**
  - *Influent Bypass:* Directing the influent to the third reactor resulted in low solids retention time (SRT) and oxygen supply issues, which hindered the nitrification process. Attempts to compensate for this by increasing the oxygen transfer coefficient (kLa) led to values that were physically unattainable.
  - *Membrane Fouling:* Simulations showed that fouling significantly reduced treatment efficiency, requiring more frequent backwashing cycles and increasing operational costs. Our control strategies helped to mitigate these effects but revealed the need for more advanced control techniques to handle such operational challenges.
  - *Crabmezapamine Treatment:* The presence of crabmezapamine in the influent posed additional challenges, as it resisted traditional biological treatment processes, further complicating nutrient removal and requiring more complex control solutions.

Future Work: To further improve system performance, future research could explore more *advanced control algorithms*, such as model predictive control (MPC), to dynamically adjust to the presence of challenging compounds like crabmezapamine. Additional strategies to better manage fouling, perhaps through *real-time monitoring* and automated control of backwashing cycles, could enhance the efficiency of membrane systems.

Conclusion: This thesis contributed valuable insights into the control of wastewater treatment systems, particularly under challenging conditions like the presence of *crabmezapamine* and *membrane fouling*. The two developed control strategies provided a strong foundation for managing nitrogen levels and optimizing treatment processes, but they also revealed the system's physical and operational limits. Future work should focus on refining control approaches and integrating advanced monitoring technologies to ensure the system remains robust and efficient in the face of operational challenges.

References

Abdelrasoul, A., Doan, H., and Lohi, A. (2013). Fouling in membrane filtration and remediation methods. In Nakajima, H., editor, *Mass Transfer*, chapter 8. IntechOpen, Rijeka.

Aichouche, F. (2021). Contribution of modelling and control approaches to improve the flexibility of treatment systems for reuse of wastewater treated in agriculture. Environmental Engineering NNT : 2021NSAM0009, Montpellier SupAgro. English.

Bastin, G. and Dochain, D. (1990). *On-line Estimation and Adaptive Control of Bioreactors*, volume 1 of *Process Measurement and Control*. Elsevier Science.

Benyahia, B., Charfi, A., Lesage, G., Heran, M., Cherki, B., and Harmand, J. (2024). Coupling a simple and generic membrane fouling model with biological dynamics: Application to the modeling of an anaerobic membrane bioreactor (anmbr). *Membranes*, 14:69. Received: 31 December 2023; Revised: 2 March 2024; Accepted: 14 March 2024; Published: 20 March 2024.

Candela, L., Fabregat, S., Josa, A., Suriol, J., Vigués, N., and Mas, J. (2007). Assessment of soil and groundwater impacts by treated urban wastewater reuse: A case study of a golf course in girona. *Environmental Monitoring and Assessment*, 135(1-3):145–158.

de Gooijer, C., Bakker, W., Beeftink, H., and Tramper, J. (1996). Bioreactors in series: an overview of design procedures and practical applications. *Enzyme and Microbial Technology*, 18:202–219.

Hajaya, M. (2019). Identifying the effect of non-ideal mixing on a pre-denitrification activated sludge system performance through model based simulations. *Jordanian Journal of Engineering and Chemical Industries*, 2(1).

Helmecke, M., Fries, E., and Schulte, C. (2020). Regulating water reuse for agricultural irrigation: risks related to organic micro-contaminants. *Environmental Sciences Europe*, 32:4.

Henze, M., Grady, C., Gujer, W., Marais, G., and Matsuo, T. (1987). *Activated Sludge Model No.1*. IAWPRC Scientific and Technical Report No.1, London (GB).

Henze, M., Gujer, W., Mino, T., Matsuo, T., Wentzel, M. C., Marais, G. v. R., and Van Loosdrecht, M. C. M. (1999). Activated sludge model no. 2d, asm2d. *Water Science and Technology*, 39(1):165–182.

Henze, M., Gujer, W., Mino, T., and van Loosdrecht, M. (2000). *Activated Sludge Models ASM1, ASM2, ASM2d and ASM3*. Scientific and Technical Report No.9. IWA Publishing, London (GB).

Jaramillo, M. F. and Restrepo, I. (2017). Wastewater reuse in agriculture: A review about its limitations and benefits. *Sustainability*, 9(10):8–9.

Jr, W. W. E. and Porges, N. (1957). Activity of microorganisms in organic waste disposal: Iv. bio-calculations. *Applied Microbiology*, 5(3):180. Cited on page 25.

OpenWA (2023). Introduction to human geography. https://openwa.pressbooks.pub/geog101human/chapter/6-3/. Accessed: October 16, 2024.

Ostace, G. S., Cristea, V. M., and Şerban Agachi, P. (2011). Cost reduction of the wastewater treatment plant operation by mpc based on modified asm1 with two-step nitrification/denitrification model. *Computers & Chemical Engineering*, 35(11):2469–2479.

Plósz, B. G., Langford, K. H., and Thomas, K. V. (2012). An activated sludge modeling framework for xenobiotic trace chemicals (asm-x): Assessment of diclofenac and carbamazepine. *Biotechnology and Bioengineering*, 109(11):2757–2769.

Scuras, S. E., Jobbagy, A., and Jr., C. L. G. (2001). Optimization of activated sludge reactor configuration: kinetic considerations. *Water Research*, 35(18):4277–4284.

Sfez, S., De Meester, S., Vlaeminck, S. E., and Dewulf, J. (2019). Improving the resource footprint evaluation of products recovered from wastewater: A discussion on appropriate allocation in the context of circular economy. *Resources, Conservation and Recycling*, 148:132–144. Cited on page 10.

Shakir, E., Zahraw, Z., and Al-Obaidy, A. H. M. (2017). Environmental and health risks associated with reuse of wastewater for irrigation. *Egyptian Journal of Petroleum*, 26(1):95–102. Cited on page 12.

Tejaswini, E., Panjwani, S., and Seshagiri Rao, A. (2020). Design of hierarchical control strategies for biological wastewater treatment plants to reduce operational costs. *Chemical Engineering Research and Design*, 161:197–205.

UN-Water (2021). Summary progress update 2021: Sdg 6 - water and sanitation for all. https://www.unwater.org/publications/summary-progress-update-2021-sdg-6-water-and-sanitation-all. Accessed: 2024-08-06.

World Health Organization (2023). Drinking water.

World Wildlife Fund (2024). Water scarcity. Accessed: 2024-08-06.

Abstract

In response to the growing scarcity of water resources, reusing treated wastewater is emerging as a sustainable solution. This thesis develops and tests simulation models, including a standard activated sludge system and one addressing the treatment of carbamazepine.

The models assess system performance under conditions like membrane fouling and explore how different compounds impact the process. A key focus is on optimizing treatment efficiency, especially for challenging contaminants.

The work also integrates control systems to ensure treated effluent consistently meets standards, supporting improved wastewater reuse in agriculture.

Keywords: Flexibility, Modelling, Control, Reuse, Optimization, Wastewater treatment, Observation.

Résumé

En réponse à la raréfaction croissante des ressources en eau, la réutilisation des eaux usées traitées émerge comme une solution durable. Cette thèse développe et teste des modèles de simulation, incluant un système standard à boues activées et un modèle traitant spécifiquement la carbamazépine.

Les modèles évaluent les performances du système dans des conditions telles que l'encrassement des membranes et analysent l'impact de différents composés sur le processus. L'accent est mis sur l'optimisation de l'efficacité du traitement, en particulier pour les contaminants difficiles.

Le travail intègre également des systèmes de contrôle afin de garantir que les effluents traités respectent constamment les normes, contribuant ainsi à l'amélioration de la réutilisation des eaux usées en agriculture.

Mots clés: Flexibilité, Modélisation, Contrôle, Réutilisation, Optimisation, Traitement des eaux usées, Observation.

ملخص

استجابةً لتزايد ندرة موارد المياه، تبرز إعادة استخدام مياه الصرف الصحي المعالجة كحل مستدام. تطور هذه الأطروحة وتختبر نماذج محاكاة، بما في ذلك نظام الحمأة المنشطة القياسي ونموذج يعالج مركب الكاربامازيبين.

تقوم النماذج بتقييم أداء النظام في ظل ظروف مثل انسداد الأغشية، وتستكشف كيفية تأثير المركبات المختلفة على العملية. ينصب التركيز على تحسين كفاءة المعالجة، خصوصاً مع الملوثات الصعبة.

كما يتضمن العمل أنظمة تحكم لضمان أن المياه المعالجة تفي باستمرار بالمعايير المطلوبة، مما يدعم تحسين إعادة استخدام مياه الصرف الصحي في الزراعة

الكلمات المفتاحية: المرونة، النمذجة، التحكم، إعادة الاستخدام، التحسين، معالجة المياه العادمة، المراقبة